Prediction and Prevention of Downhole Complications in Real-time Oil Well Drilling

A thesis submitted in fulfilment of the requirements for the degree of

Doctor of Philosophy

by

Viswanth Ramba

(Regd No. 156151010)

School of Energy Science and Engineering

Indian Institute of Technology Guwahati

Guwahati – 781039, India

September 2021

Thesis is dedicated to

My beloved family and friends

for their unconditional love, support and encouragement

"నేనొక దుర్గమ్!
నాదొక స్వర్గమ్!
అనర్గళమ్, అనితర సాధ్యమ్, నా మార్గమ్"
-శ్రీరంగం శ్రీనివాసరావు (శ్రీ శ్రీ)
మహాప్రస్థానం – (01-06-1934)

"The path that I take is like a mountain,
blissful heaven,
unceasing and well-articulated, which is possible for everyone"
-Srirangam Srinivasa Rao (Sri Sri)
Maha prasthanam – (01-06-1934)

"मैं जो रास्ता अपनाता हूं वह पहाड़ की तरह है
आनंदमय स्वर्ग,
निरंतर और अच्छी तरह से व्यक्त, जो सभी के लिए
संभव है"
-श्रीरंगम श्रीनिवास राव (श्री श्री)
महा प्रस्थानम – (01-06-1934)

School of Energy Science and Engineering

Indian Institute of Technology Guwahati

Guwahati-781039

INDIA

STATEMENT

This is to certify that I have carried out the research work in this thesis entitled "**Prediction and Prevention of Downhole Complications in Real-time Oil Well Drilling**", at the School of Energy Science and Engineering, Indian Institute of Technology Guwahati, under the supervision of **Prof. P. Muthukumar** and **Prof. Senthilmurugan Subbiah**. The results documented in this thesis are achieved by me and have not been submitted to any other university or institute for the award of any degree or diploma.

In keeping with the general practice of reporting scientific observation, due acknowledgement has been made wherever the work described is based on the findings of other investigations.

Viswanth Ramba

Regd.No.156151010

School of Energy Science and Engineering

Indian Institute of Technology Guwahati

Guwahati-781039, Assam, India

September 2021

School of Energy Science and Engineering

Indian Institute of Technology Guwahati

Guwahati-781039

INDIA

CERTIFICATE

This is to certify that the work contained in this thesis entitled "**Prediction and Prevention of Downhole Complications in Real-time Oil Well Drilling**", being submitted by **Viswanth Ramba** (**Regd.No.156151010**), for the award of Ph.D. degree, is a record of bona fide research carried out by him at the School of Energy Science and Engineering, Indian Institute of Technology Guwahati, under our guidance and supervision. The work embodied in this thesis has not been submitted to any other University or Institute for the award of any other degree or diploma.

Prof. P. Muthukumar
Professor
Department of Mechanical Engineering
Indian Institute of Technology Guwahati
Guwahati-781039, Assam, India
September 2021

Prof. Senthilmurugan Subbiah
Professor
Department of Chemical Engineering
Indian Institute of Technology Guwahati
Guwahati-781039, Assam, India
September 2021

Acknowledgments

I want to convey my profound sense of gratitude to my supervisors, Prof. P. Muthukumar and Prof. Senthilmurugan Subbiah, for the opportunity, support, guidance, and trust they have bestowed upon me to pursue research in this exciting field. Their advice and help have been of high value throughout the whole Ph.D. program. During my research, both the supervisors provided me with the most precious ideas and resources that played a vital role in successfully completing the thesis. I enjoyed working under their supervision every moment and learned many things from them, which will be an asset for my future research.

I want to thank my doctoral committee members, Prof. Amaresh Dalal, Prof. Anugrah Singh, and Prof. Sukhomay Pal, for their encouragement, help, and insightful comments. I also thank Prof. K.Mohanty, Head of School of Energy Science and Engineering, for providing all the facilities needed for my research work. I take this opportunity to thank all the faculty and staff members of the institute for their valuable suggestions and cooperation during this Ph.D. program.

I want to express my sincere gratefulness to all the Taxpayers of the Government of India.

I am grateful for the funding sources that allowed me to pursue my doctoral studies: Ministry of Human Resource Development, Government of India, and Oil and Natural gas Corporation Limited (ONGC), India. I would like to extend my gratitude to ONGC for technical and financial assistance. And this work has been done as a part of the Make-in-India initiative and PAN-IIT-ONGC program (Project. No. xCEESPNONGC00985xxSS004). I would like to extend my gratitude to the senior management of ONGC, Sanjay Kumar Gauba (DGM), Amol Musale (SE), and Lekkala Ravi (SE).

Finally, I would like to acknowledge friends who supported me during my time here. I wanted to express my gratitude to my colleagues at Prof. P. Muthukumar's research group and Prof. S. Senthilmurugan’s research group, School of Energy Science and Engineering, Department of Mechanical, Chemical, and Civil Engineering, for making my stay livelier and more meaningful. I want to express special gratitude to Mr. Senthil Selva and Mr. Bala Kumara Vignesh for their stupendous support throughout the project's

tenure. Working in a team with this set of people has always pushed me forward to aspire for learning.

I want to extend my warm regards to Mr. Aman Srivastava, Well Construction Engineer, Halliburton, for all the technical discussions through the SPE portal.

The occasion to express gratefulness to one's family on text does not present itself often, and I genuinely appreciate their eternal love. Finally, yet importantly, I want to thank my parents and siblings for their help and encouragement, especially for believing in me and supporting me in times of adversity. I also thank the rest of my family and friends outside IIT Guwahati.

Sincerely,

Viswanth Ramba

September 2021

ABSTRACT

The global economic growth is closely related to its energy demand; therefore, with the growing global economy, the need for oil and gas is projected to grow more, making the sector conducive for investment (Commodity Markets Outlook, 2021). The global crude oil demand is expected to exceed global supply by year 2022 (Short-Term Energy Outlook - U.S. Energy Information Administration (EIA), 2021). To bridge this market gap, the Oil and Gas (O&G) companies are exploring new oilfields in both offshore and onshore. While drilling, the operators are expected to have downhole complications such as stuck pipe, string washout, kick, loss circulation, and other drilling-related problems. And such problems are expected to be more for high angled wells. These wellbore complications during drilling activities would lead to unwanted incidents, indirectly increasing overall drilling costs and non-productive time (NPT). The detection of some of these downhole complications well in advance would help to reduce the drilling cost. Hence, there is an apparent requirement for developing new drilling technologies to detect the upcoming wellbore and drill string complications. This thesis work aims to develop an innovative method to help drilling engineers detect abnormal drilling conditions in real-time. In this work, three approaches are presented to detect the wellbore complications in real-time.

The drilling industry is forced to drill high angled and extended-reach wells both offshore and onshore to explore the deeper origins of hydrocarbons to meet the requirements. While drilling high-angle wells, the operators are expected to have downhole complications such as stuck pipe, string washout, kick, loss circulation, and other drilling-related problems at a higher rate. These wellbore complications during drilling activities would lead to unwanted incidents, which indirectly increases the overall drilling costs and non-productive time (NPT). The detection of some of the downhole complications well advance may help to reduce the drilling cost. Hence, there is an apparent requirement for developing new drilling technologies to detect the upcoming wellbore and drill string complications. This thesis work aims to develop an innovative method to help drilling engineers detect abnormal drilling conditions in real-time. In this work, three approaches are presented to detect the wellbore complications in real-time.

The first approach of this work is focused on developing a robust drag model that would determine the hookload acting on the deadline. And this is achieved by utilizing Aadnoy's

3-Dimensional frictional model, where bottom-up approach calculations are performed. The real-time measured weight on bit (WOB) is used to estimate the position of the neutral point, and the neutral point is utilized to estimate the load acting at the surface and deadline. To improve the model prediction ability, the factors affecting the position of hookload measurement at the deadline and throughout the rig structure are grouped to form a new metric termed “Rig Uncertainty Compensation” (RUC) factor. The analysis of actual drilling data and model output revealed that the hookload mainly depends on the direction of block movement, global friction factor, sheave efficiency, weight parameter, and RUC factor of rig structure. Therefore, the above-mentioned model parameters are tuned to improve the accuracy of the hookload prediction at the deadline. The methodology will minimize the potential downhole drilling hazards by dynamic predictions of hookload and neutral point. The proposed hookload model is validated for vertical and directional wells during the rotary drilling operation using standard drilling data obtained from ONGC Ltd.

The modified Aadnoy’s model doesn’t consider the impact of the mud effects on the drill string. To incorporate the same, in second approach, the true tension and effective tensional model was utilized to evaluate the structural integrity of the tubular in directional wellbores. While drilling, the drill string is subjected to internal and external pressures, and it can be well explained in terms of true tension and effective tension. Estimating these tensional forces and other load forces acting on the drill string is important for efficient drilling operation and selecting optimum operational parameters. In addition, these forces are further utilized to estimate the neutral point and load acting at the deadline. To consider the factors affecting the accuracy of the hookload at the deadline, the aforementioned RUC factor is utilized.

Further, the estimated hookload is compared with the actual hookload to detect the upcoming complications and prevent aggravation. Also, the predicted anomaly is verified by monitoring the wellbore secondary drilling parameters such as hookload, mud flow rate (strokes per minute - SPM), stand pipe pressure (SPP), torque, and rate of penetration (ROP). Additionally, all the forces acting along the drill string were also determined and monitored dynamically such that stress exposure in all the sections of the drill string is below a threshold value. The efficacy of the developed model is determined by implementing it on a directional wellbore, and a case study is presented in brief.

The third approach presented in the thesis mainly focuses on minimizing the NPT and overall drilling costs by reducing the total expended specific energy by improved play-back methodology. And this was achieved by optimizing the rate of penetration (ROP) and the drilling efficiency. The improved play-back methodology is formulated to provide optimum drilling parameters for the development wells based on real-time optimization of drilling rates, drilling efficiency, and bit hydraulics of exploratory well data analysis. The drilling parameters such as drilling specific energy (DSE) and mechanical specific energy (MSE) were estimated to determine the inefficient drilling zones for different lithologies. The result shows that utilization of optimal drilling parameters estimated by play-back methodology reduces input power by nearly 75%. Also, a new metric termed hydraulic drilling impact (HDI) is introduced to optimize the drilling performance during real-time rotary drilling operations. Monitoring the HDI in actual field conditions can help the operator evaluate the ongoing drilling operation's reliability. Fallouts from the comparison disclose that the excessive energy spent for the low ROP was due to inappropriate drilling parameters chosen for a particular formation. In this approach, data derived from surface sensors and lab is utilized, and downhole sensors were not used. The efficacy of the proposed model was validated and tested in a development well drilled in the north-eastern parts of India.

All the above-developed models were integrated with the Decision Support System (DSS) to have dynamic predictions of anomalies by calculating hookload at the surface and neutral point. The DSS would provide optimum drilling parameters to achieve the best performance in real-time drilling activity. The outcomes from the studies conclude that timely detection of the upcoming wellbore and drilling complications could minimize the overall rig time and cost of drilling. Further, optimal selection of operating drilling parameters would aid in a reduction in overall specific energy utilization.

NOMENCLATURE

A_B	drill bit area, in^2
A_e	external cross-sectional area, in^2
A_i	internal cross-sectional area, in^2
D_b	drill bit diameter, *in*
ΔD	difference in diameter of tool joint and drill pipe
E	well path energy
E_s	sheave efficiency
F	force in the drill string, *lb.-f*
F_{apa}	axial force in pressure-area method, *lb.-f*
F_{bottom}	bottom force, *lb.-f*
$F_{buc.stab}$	buckling stability force, *lb.-f*
F_c	critical buckling force, *lb.-f*
F_{eff}	effective force, *lb.-f*
F_{side}	side force/ normal force, *lb.-f*
F_{true}	true tensional force, *lb.-f*
ΔF_{area}	change in force due to change in cross-sectional area, in^2
L	drill string component length, *m*
L_{tj}	separation of tool joints, *m*
w	unit weight, *lb./ft*
h_b	block position, *m*
HP_b	bit hydraulic horsepower, *psi*
n	no of drilling lines
P_e	external pressure, *psi*
P_{hyd_sta}	hydrostatic pressure, *psi*
P_i	internal pressure, *psi*
P_{sa}	surface pressure on annulus section side, *psi*
P_{sp}	surface pressure on drill pipe side, *psi*
W_{air}	unit weight/foot of drill string in air, *lb./ft*
W_{block}	block weight, *tonne*
W_{hl}	weight acting at the top of the drill string during lowering, *tonne*
W_{hr}	weight acting at the top of the drill string during raising, *tonne*

x	block position, *m*

Greek symbols

α	wellbore inclination
β	buoyancy factor
λ	dimensionless bit hydraulic factor
λ_{bp}	weight parameter, tonne/m
μ	coefficient of friction
Φ	wellbore azimuth angle
Ψ	angle between axial and tangential velocity
ρ_{gp}	pressure gradient on drill pipe side, *psi/ft*
ρ_{ga}	pressure gradient on annulus side, *psi/ft*
θ	dogleg angle, °

Acronyms

AI	artificial Intelligence
BCS	borehole compensated sonic tool
BHA	bottom hole assembly
BHHP	bit hydraulic horse power
BIT-DEP	bit depth (actual drill bit location), *m*
BSMF	bending stress magnification factor
CAL	caliper log
DSE	drilling specific energy, *kpsi*
DOT	drill-off test
DLL	dual later log tool
DPR	daily progress reports
DSS	decision support system
GTO	geo-technical order
GR	gamma-ray
HDI	hydraulic drilling impact, *ft/hr/kpsi*
HOOKLOAD	hookload acting at the deadline, tonne
HP	horse power
KCL	potassium chloride

MSFL	micro spherical focused leg tool
MD	measured depth, *m*
ML	machine learning
MPSI	area-specific mechanical energy power
MSE	mechanical specific energy, kpsi
MWD	measurement while drilling
NPT	non-productive time
ONGC	oil and natural gas corporation limited
PDC	polycrystalline diamond compact
PHPA	partially-hydrolyzed polyacrylamide
PPG	pounds per gallon
ROP	rate of penetration, *m/hr*
ROT-SPEED	rotational speed (RPM)
RUC	rig uncertainty compensation factor
SCADA	supervisory control and data acquisition system
SQL	structured query language
SOP	standard operating procedures
SP	self-potential
SWOB	surface weight on bit
TOT-DEP	total depth, *m*
TOT-SPM	mud pump flow in strokes per minute (SPM)
TVD	true vertical depth, *m*
UBHO	universal bottom hole orientation subs
WOB	weight on bit, tonne
WITSML	wellsite information transfer standard mark-up language

Contents

LIST OF FIGURES

LIST OF TABLES

Chapter

1

CHAPTER 1

Introduction

1.1. Foreword

Global energy demand has increased substantially in recent years due to economic and industrial growth. For a decade, this demand has been observed to be more in developing countries. Therefore, the oil companies are forced to drill high angled wells to explore more fossil fuels. Even though fossil fuels produce large amounts of greenhouse gases, fossil fuel is expected to be the key energy resource since there are no immediate alternate energy sources to meet the global need. Hence, noteworthy contributions are required in the drilling technologies to acquire fossil fuels beneath the earth's crust, and it requires energy-efficient technologies to produce low-cost fossil fuels. This thesis aimed to provide some energy-efficient solutions to the operator while operating the drilling rig.

1.2. Oil and gas as a primary source

The total energy consumption is an indirect measure of a country's primary energy sources. Energy is derived directly from natural resources such as coal, crude oil, solar, and wind. China is one of the largest energy consumers globally, and they consumed 141.7 exajoules in 2019 (Sonnichsen, 2020), as illustrated in Fig. 1-1. With the world's population expected to reach 9 billion in 2040 from 7.7 billion in 2019, the IEA expects the world's energy demand to grow by 19%. Over the last decade, energy consumption has increased, and it is projected to experience the largest growth in emerging economies like BRIC nations (Brazil, Russia, India, and China).

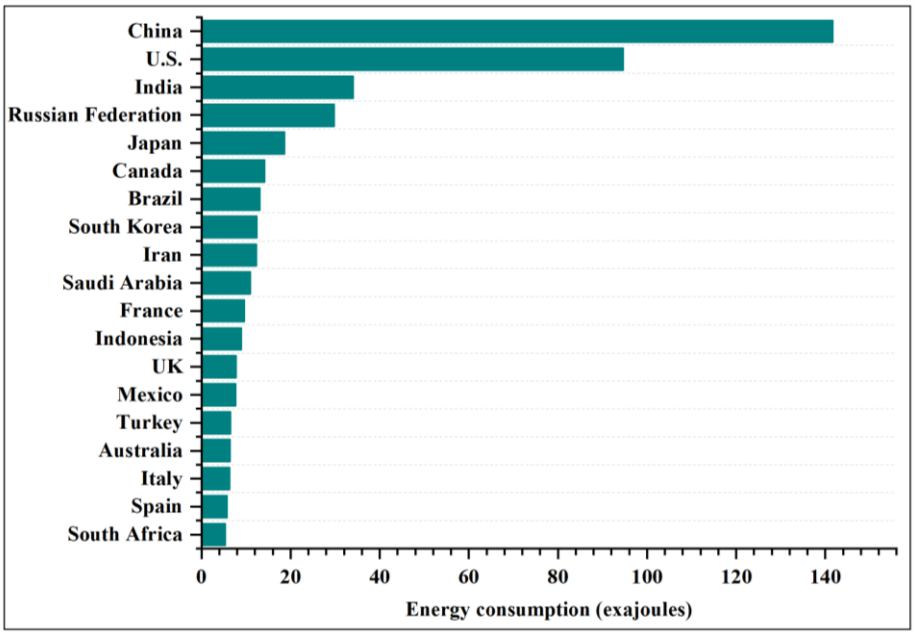

Fig. 1-1. Global energy consumption by individual countries

Among all the energy sources, global demand for crude oil in 2019 adds up to 100.1 million b/d and is decreased to 91.3 million b/d in 2020 due to the economic and mobility impacts of COVID-19 (Statista, 2021). The energy demand continues to multiply, and Energy Information Administration (EIA) forecasts that the global consumption of petroleum and liquid fuels is projected to be 97.7 million b/d for 2021, which is 5.4 million b/d higher than 2020 (refer to Fig. 1-2 (U.S. Energy Information Administration, 2021)).

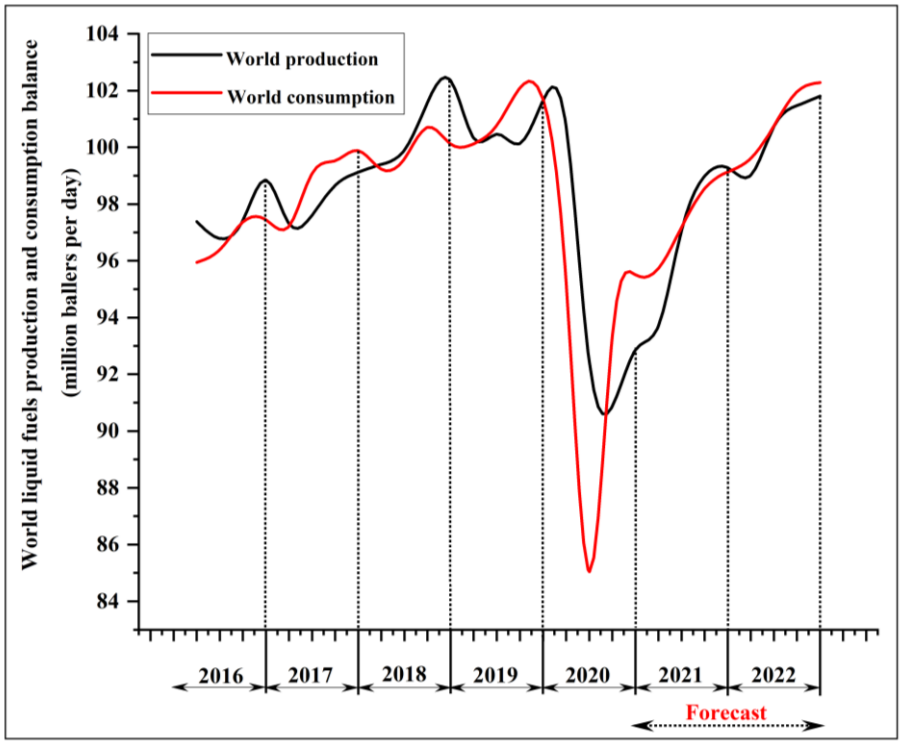

Fig. 1-2. World oil production and consumption

India is the world's third-largest energy consumer after China and the USA. India consumed 809.2 million tonnes of oil equivalent (MTOE) in 2018. With an equity share of 5.8% of the world's primary energy consumption, India's energy necessity is fulfilled in the order of coal, crude oil, natural gas, and renewable energy. India's primary energy demand is expected to rise at a compound annual growth rate (CAGR) of 4.2% during 2017-2040 and is comparatively much rapid growth than any other fastest growing economy across the globe (APR 2019-2020).

On the other hand, in India, Oil and Gas (O&G) sector play a predominant role as one-third of the required energy is met by hydrocarbons. The easy accessibility of advanced

technologies by developing countries has led to huge demand in O&G products. Energy-efficient drilling and exploration are very important to meet the supply and demand gap by using India's indigenous oil and gas resources. As means of progression, the O&G industry was forced to drill high-angled and extended reach wells. The major challenge in the drilling industry is to minimize the non-productive time (NPT) and make drilling more efficient while drilling deeper wells. Therefore, significant enhancement is required in the drilling industry, and this thesis presented here aims to address the fall-backs.

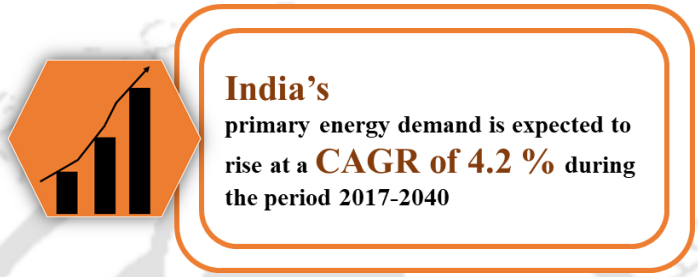

1.3. Oil and gas well drilling

The drilling process is performed to explore and extract the hydrocarbons available beneath the earth's surface. The hydrocarbon traces are identified in the early phase based on the well log data during an exploratory well drilling. The geo-technical order (GTO) for the production well is prepared considering the exploratory well drilling data. The following sequence of steps is universally followed for drilling oil wells.

(a) Well planning
(b) Performing a shallow gas survey
(c) Wellsite preparation
(d) Setting up the conductor casing
(e) Move-in and Rig-up (MIRU)
(f) Well spudding (spudding refers to the commencement of rotary drilling operations)
(g) Utilization of open-hole logs for well-logging
(h) Well-completion
(i) Rig down and move out

1.4. Complete rig and drill string configuration

The schematic structure of an onshore drilling rig with its associated components are illustrated in Fig. 1-3.

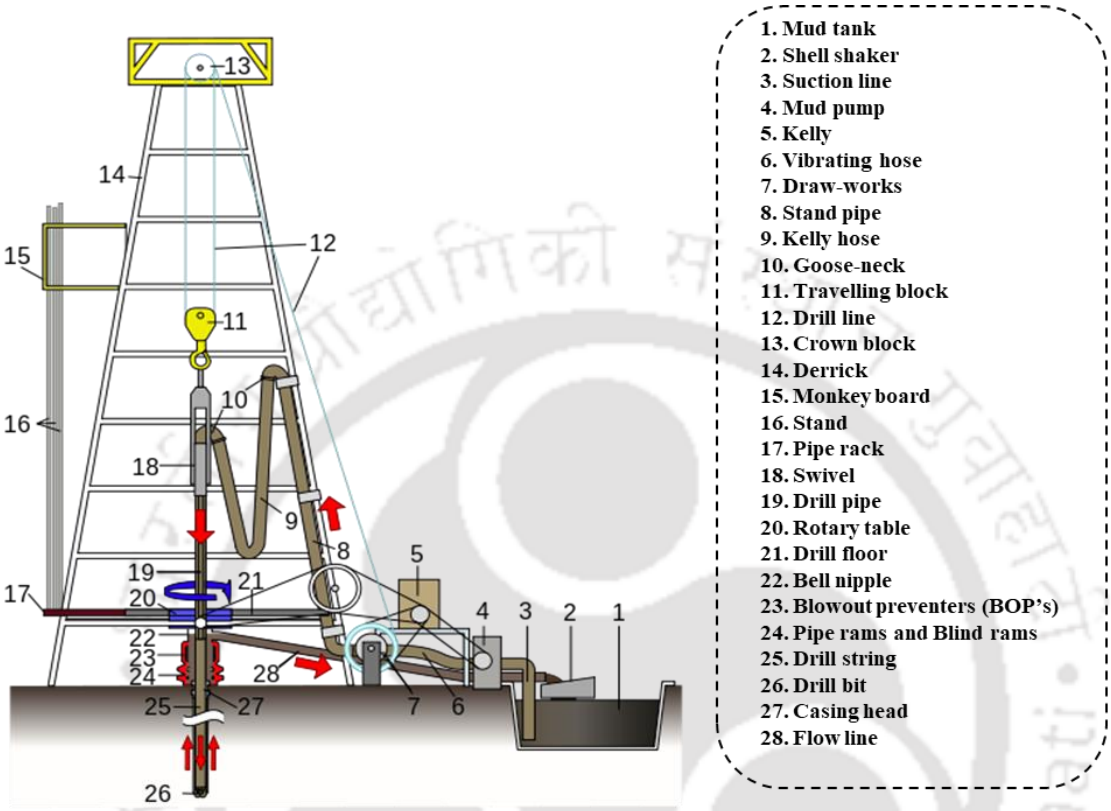

Fig. 1-3. Schematic structure of an onshore drilling rig

The important configuration to spud a well is listed down:

(a) Drilling rig
(b) Drill string
(c) Drill collars
(d) Rotary table drive
(e) Drilling mud
(f) Casing
(g) Downhole motors
(h) Measurement while drilling
(i) Logging while drilling

1.5. Drilling technology

Drilling technology has enhanced significantly since the advent of the Woodward-Clyde borehole design in 1983 (Brady et al., 2017). The technological advancements have been primarily associated with directional control and are a boom to the O&G drilling. Examples for advances in technology in O&G well drilling are described below:

1.5.1. Horizontal drilling technology

Horizontal drilling is the real engineering marvel and advancement in scientific innovation. It is a way of directing the drill bit along a horizontal track-oriented approximately 85˚ to 95˚ from a vertical axis (Azar, 2004). Horizontal well drilling consists of three phases (refer to Fig. 1-4): The first phase is a vertical section that starts from the surface and extends vertically downwards to a pre-determined depth (kick-off point). This phase is drilled using a rotary drilling technique employed in most vertical wells, wherein the complete drill string is rotated from the surface. The second phase is a deviated phase that beings at the kick-off point and ends at the entry point of the reservoir at approximately 90˚ from the vertical axis. And this section is drilled using a hydraulic motor mounted directly on the drill bit and powered by the drilling mud. Steering of the hole in this phase is accomplished by utilizing a steerable downhole motor (RSS – Rotary Steerable System). And the third phase is a drain hole section and is horizontally driven using the RSS.

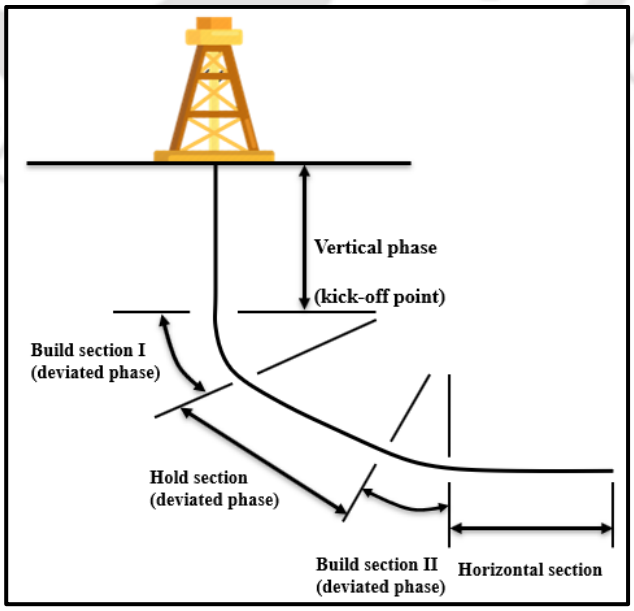

Fig. 1-4. Stages observed during horizontal drilling

In the mid-1970s, during the discovery of the Rospo Mare field by Elf Aquitaine (French oil major, now a subsidiary of TOTAL), it undertook a Research and Development (R&D) program called FORHOR (for Forage Horizontal Drilling) in partnership with French Petroleum Institute (currently known as Institut Francais du Petrole – Energies Nouvelles, IFPEN) (TOTAL, 2021). The program's main aim was to develop horizontal drilling technology that would streamline the oil and gas recovery and boost production. The R&D program involved five years of technical challenges and covered four broad topics: drilling, reservoir methodology, well equipment, production start-up, and electric logging. The efforts have quickly paid off, and in May 1980, the first horizontal well (LACQ 90) was drilled in Western Europe. At nearly 670 m depth, a horizontal section of 100 m was drilled successfully.

Many industrial trails, viz carried over this initial feat., the first offshore well drilled horizontally in Rospo Mare field in 1982 and then the Castera-Lou, CLU 100, which was drilled almost to a depth of 3000 m. The success of the FORHOR program is much beyond what is expected and gave rise to an array of downhole tools – such as LWD (Logging While Drilling), MWD (Measurement While Drilling), and SIMPHOR (System for Instrumentation and Measurement in Horizontal Wells). And these tools have enhanced the performance of horizontal drilling, which has completely revolutionized the O&G industry.

1.5.2. Multilateral drilling

The next step in the evolution of drilling technology was to drill several horizontal wellbores (well legs) in a formation from a single wellbore. The most common method was to drill a single horizontal wellbore and then branch off the initial wellbore in an open-hole to yield two or more (as many as five legs) horizontal legs (Themig, 1996). In general, the multi-lateral configurations include wellbores include: (a) multiple lateral branching from one main vertical wellbore, (b) multiple branched wellbores, (c) forked wells, (d) dual-opposing laterals, (e) wellbores with stacked laterals, and (f) multiple lateral branching from one main horizontal wellbore (Serintel, 2017) (refer to Fig. 1-5). With the advancement in state-of-the-art directional drilling technology, a successful multi-lateral well can substitute multiple vertical wellbores and aids in reducing overall drilling and completion costs.

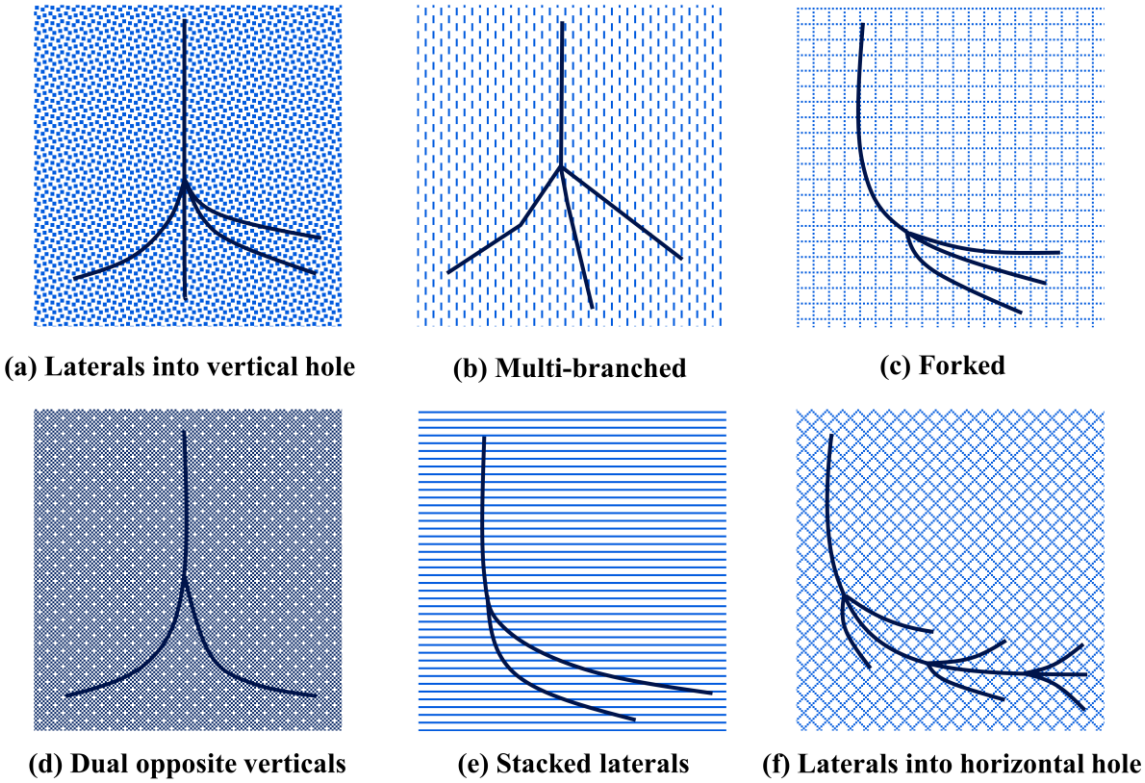

Fig. 1-5. Configuration of Multi-lateral wells

1.5.3. Extended Reach Drilling (ERD)

Extended Reach Drilling (ERD) refers to the practice of directional drilling and is an integrated practice of drilling high angled wellbores with long horizontal displacements (Agbaji, 2010). ERD wells are those in which the ratio of the measured depth (MD) and the true vertical depth (TVD) is at least 2:1, as shown in Fig. 1-6. ERD is employed in reservoirs where the hydrocarbons are either very deep into the formation or hindered with troublesome formations.

ERD technology has been implemented since the early 1980s, and the first ERD well was drilled with a horizontal reach of more than 5000 m from Statfjord Well C-10 in 1989-1990 (Agbaji, 2009). For the first time in 1999, the Statfjord Well C-3 holds the record for exceeding 6000 m drilling, and it had a horizontal departure of 6100 m. After the Statfjord development projects, numerous ERD wells were drilled, and in 2013, Exxon Neftegas Limited, Sakhalin Island, Russia, holds the record for longest well with a horizontal departure of 38514 ft. and a measured depth of 41667 ft. ERD allows producers to reach desired target zones from offshore platforms in offshore drilling, thereby minimizing the overall cost and number of platforms.

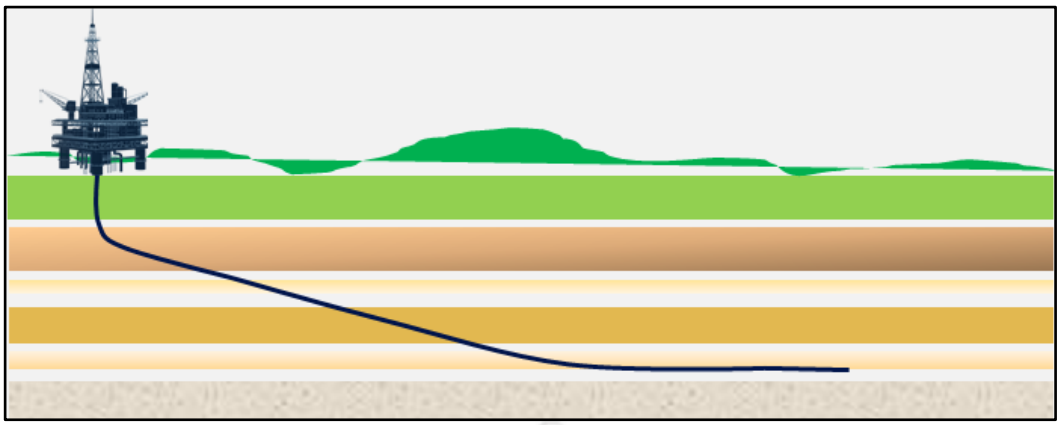

Fig. 1-6. Schematic of Extended Reach Wells (ERW)

Numerous challenges need to be addressed while drilling extended reach wells. For example, in directional drilling, the parameters such as torque and drag, hole cleaning, and casing flotation play a vibrant role in ERD wells. The top drive is utilized instead of a rotary table drive because the top drive enables a back-reaming capability and the capacity to push the casing down the wellbore when high drag is observed. Also, severe torsional variations are observed when the drill string traverses long distances. Therefore, the top-drive torque rating should be sufficiently high enough to house these peak values (Allen et al., 1997). The sliding mode results in several inadequacies that are compounded by extreme distances. The drill string needs to be turned 15 to 20 times at the surface to turn the downhole tool once, as the string absorbs the provided torque over long distances. Consequently, the downhole motor is oriented in a specific direction to follow a defined path, and the drill string torque needs to hold the motor in appropriate orientation against the reserve torque generated by the motor as the drill bit proceeds. Besides, the geo-steering tool is quintessential in ERD wells, as it can adjust the wellbore position (both inclination and azimuth angles) to reach desired targets.

1.6. Drilling complications

Drilling operations are constantly subjected to numerous factors that cause minor or significant drilling complications, exposing the rig personnel to hazards and danger. Some of the significant difficulties that result in non-productive time (NPT) are listed below:

a. Stuck pipe

Stuck pipe is one of the significant contributors to NPT, increasing the overall well-drilling cost. A stuck pipe is a position of the drill string where it cannot be moved or rotated freely from its actual state. The drill string might have partial movement and rotation, whereas circulation may or may not be possible depending on the severity of the stuck type. There are two types of stuck pipe mechanisms: mechanical and differential stuck pipe.

i. Mechanical stuck pipe

A mechanical stuck-up is usually observed when the cuttings accumulate around the BHA during drilling (Alhamed et al., 2020). The wellbore collapses due to loose formations and forcing the cuttings to surround the drill string region. And this happens when appropriate mud properties aren't designed properly to support cuttings suspension. These accumulated cuttings wield downward forces on the drill string and restrict its movement. Such scenarios are likely to be observed during making/breaking connections and no mud circulation. Fig. 1-7 depicts possible mechanical stuck pipe scenarios.

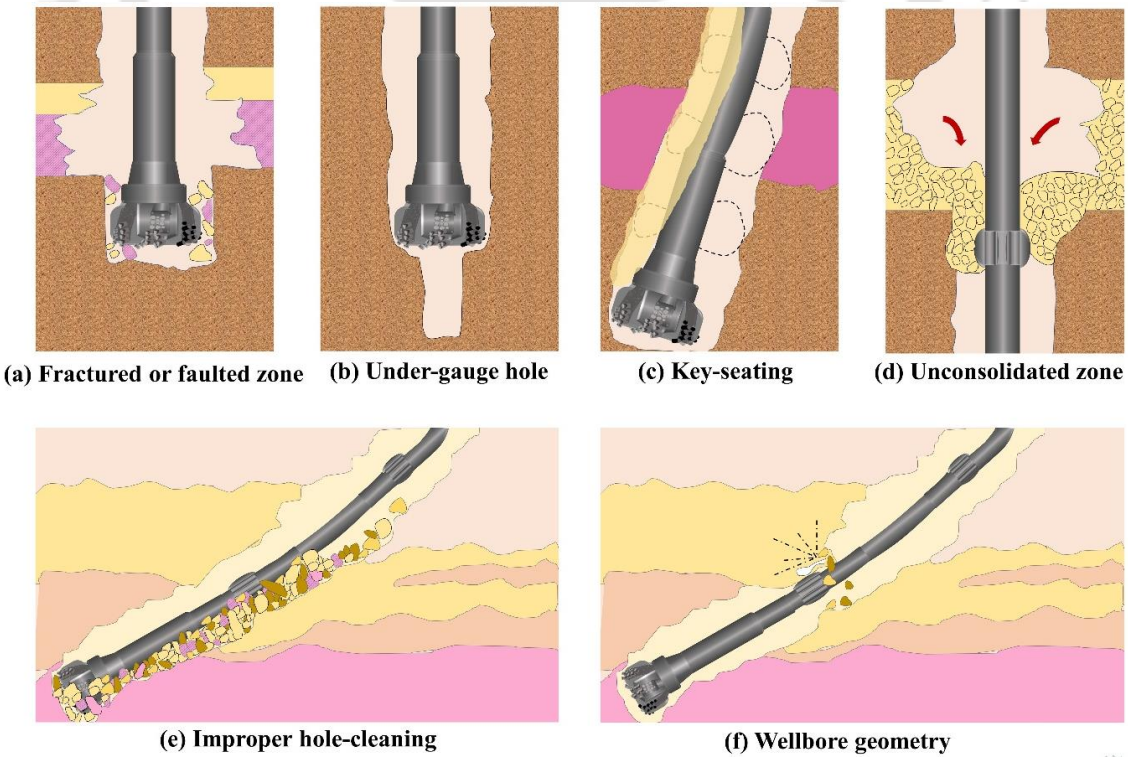

Fig. 1-7. Possible mechanical stuck pipe scenario cases

ii. Differential stuck pipe

Differential sticking is instigated by differential pressure force (where the mud pressure in the annulus exceeds the formation pressure) acting on the drill string against a mud cake deposited on the permeable formations. It can be determined when the drill string rotation and reciprocation are hindered with unrestricted mud circulation. Due to the restriction in the drill string movement, the sticking can be adverse as the larger drill string section can be embedded into the filter cake while drilling (Mahto, 2013). Few differential sticking scenarios are illustrated in Fig. 1-8: (a) reactive formation – the wellbore instability in reactive shales is due to physical and chemical reactions between the drilling mud and formation and eventually lead to osmotic swelling, water adsorption, and cuttings disintegration (Jain et al., 2015), (b) geo-pressure – refers to zones where the reservoir fluid pressure (mixture of liquid and gas) notably exceeds the hydrostatic pressure and even reach the overburden pressure, and (c) differential sticking. Symptoms prior to being stuck were listed in Table 1-1 (Inteq, 1995).

Table 1-1. Downhole complications related to stuck pipe and its indicators

Downhole Complications	**Indicators**		
	Torque	Standpipe pressure	Rate of penetration
Poor hole cleaning	Increase	Increase	Gradual increase
High overbalance	Gradual increase	No change	Gradual increase
Mobile formation	Gradual increase	Increase	Gradual increase
Fractured and faulted formation	Sudden erratic increase	Maybe unaffected	Sudden increase
Geo-pressured formation	Increase	Increase	Initial increase with the gradual decrease
Reactive formation	Gradual increase	Increase	Gradual decrease
Unconsolidated formation	Increase	Increase	Decrease
Junk	Sudden increase	No change	Sudden decrease
Cement blocks	Sudden increase	No change	Sudden decrease

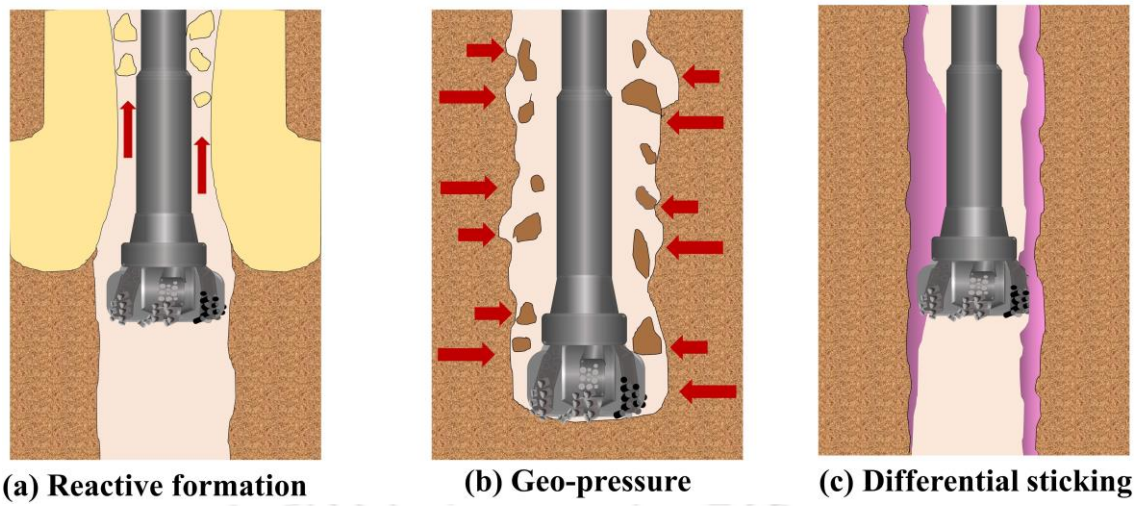

Fig. 1-8. Differential stuck pipe scenarios

b. Drill string washout

Drill string washout is a crack or a hole in the drill string caused by wear, severe fatigue, or corrosion effects, leading to erosion of drill string body and tool joints (Willersrud et al., 2015). This eventually results in a reduction in drill string strength during the continuous operation of drilling. The weakest point of the drill string leads to seepage of mud during drilling activities, and this seepage leads to damage of drill string. This phenomenon is termed as a washout (refer to Fig. 1-9 (Albdiry and Almensory, 2016)). The early identification of washout will help the operator pull out the complete string and replace the damaged portion. If it is not identified in the early stage, it leads to the parting of the drill string in the wellbore. Once parting has happened, the fishing operation is performed to remove the parted drill string. If it is not successful, then side-tracking is performed to reach the target depth of the reservoir.

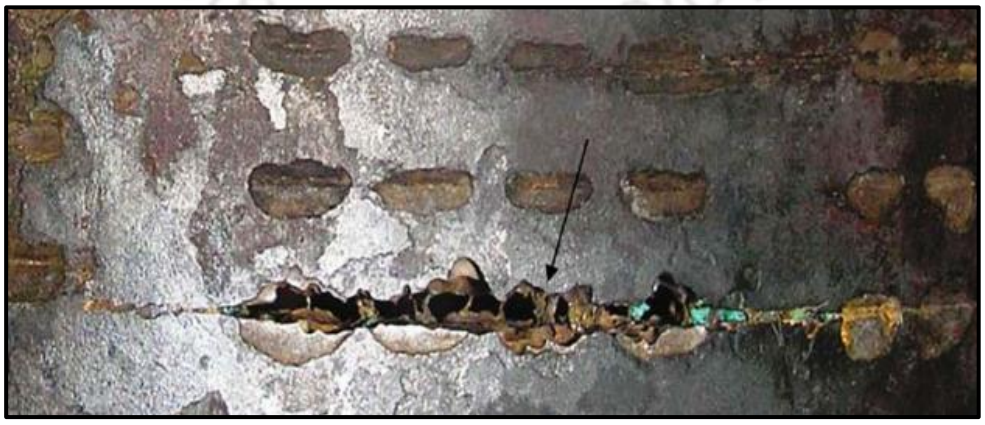

Fig. 1-9. Washout was observed on the drill pipe body

c. Twist-off

Twist-off is usually initiated with the fatigue crack extending around the drill pipe and causing the pipe to part off. The drill string twist-off occurs when the shear stresses due to high torque are more significant than the pipe material's ultimate shear stresses. Fig. 1-10 (Wikipedia, 2021) shows a typical drill string part off due to severe fatigue.

Fig. 1-10. Picture depicting the broken section of the drill string

d. Dogleg severity

Doglegs and inclination lead to increased torque and drag in the drill string. Drilling becomes a difficult task in inclined wells with doglegs because the stresses induced in the drill string may increase. So, the inclination should be within the permissible limits. Due to the dogleg, the portion of the drill string passing through the dogleg section will be subjected to compression and tension forces, as shown in Fig. 1-11. Both the forces' positions will be reversed when the drill string rotates 180º, i.e., the portion that experienced tension initially will undergo compression and vice-versa, resulting in severe fatigue of the drill string.

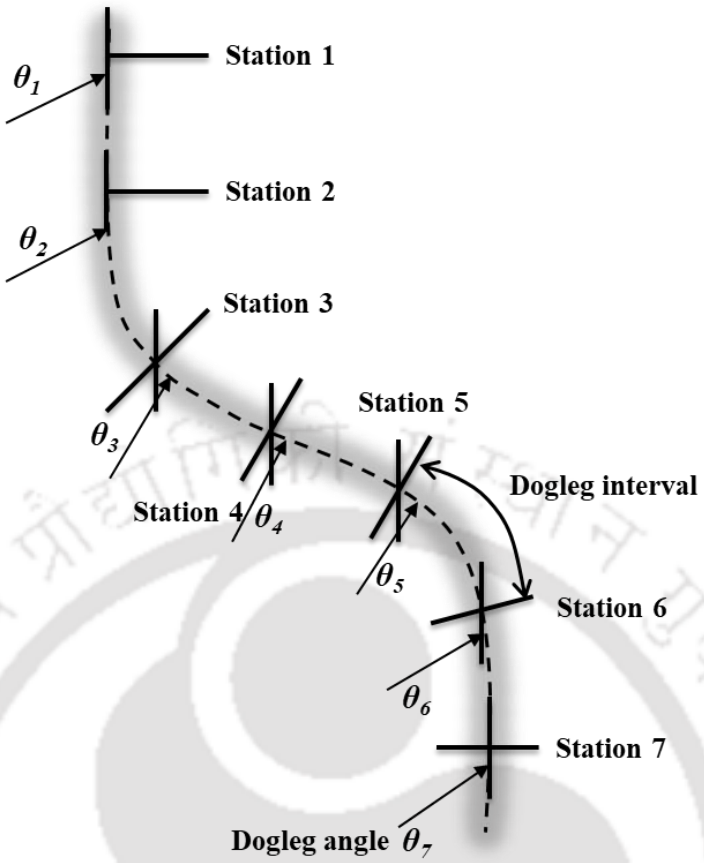

Fig. 1-11. Measurement of dogleg severity at specific intervals at each survey station

e. Kick and lost circulation

(i) Kick

Kick is generally a well control problem when the pressure inside the formation is greater than the hydrostatic mud pressure. When this situation occurs, the high-pressure compressed fluid from the formation will try to flow towards the surface in an uncontrolled manner, and this phenomenon is termed the kick. The kick is assumed to be killed if the fluid flow towards the surface is controlled. And if it is uncontrollable, it might upshoot in a blowout (Coelho Mariana, 2017). The kick is expected to occur while drilling the well with insufficient mud weight, shallow gas sands, excessive drilling rates in gas reservoirs, inappropriate swabbing, the improper fluid column in the wellbore, lost circulation.

(ii) Lost Circulation

Excessive loss of drilling mud to natural or artificially induced fracture zones leads to reduced or zero mud return to the surface, and that may result in mud level drop-down in the annulus section. The phenomenon of losing the wellbore fluids is termed lost circulation (Netwas Group Oil, 2021). Loss of circulation can occur in vulgar formations; sub-normally pressured zones or pressure depleted zones; naturally fractured regions; fractures induced due to surge and swab; annulus plugging due to sloughing shales; and excessive circulation breaking pressures due to the higher gel strength.

1.7. Drilling automation overview

The drilling automation enables monitoring, smooth drilling operation, and complete control of all rig operations from a single control source, as shown in Fig. 1-12 (Schlumberger, 2016). The level of automation can be improved by introducing more and more sensors and intelligence to monitor and control the drilling operation depending on the rig automation level. The rigs are categorized into the conventional rig, advanced rig, and full automated rig. The conventional drilling automation consists of the following key components: sensor, data collection input, and output devices, controller, control room with the appropriate graphical user interface. More accurate and more sophisticated sensors are integrated to operate the rig in a closed-loop with much intervention from the operator in an advanced rig. For example, maintaining constant ROP while manipulating the WOB and simultaneously ensuring the neutral point in BHA.

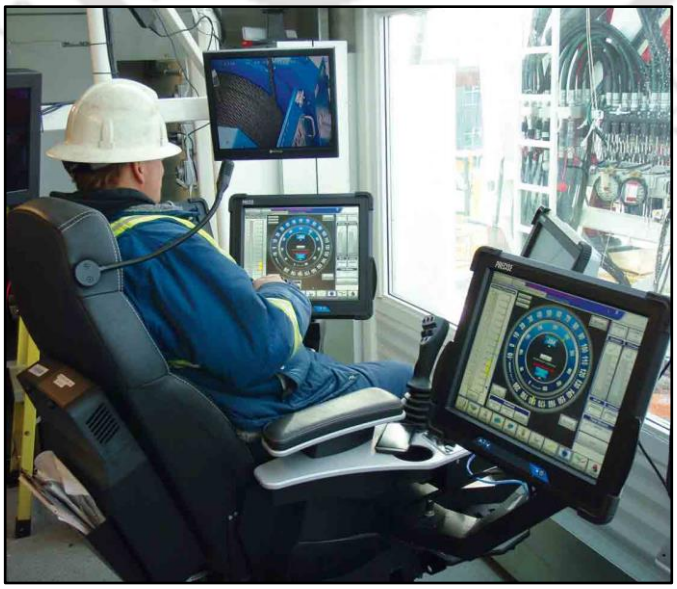

Fig. 1-12. Automated drilling system

The drilling automation can be in three hierarchy levels: (i) basic sensor-based well progress monitoring and manual open-loop operation by operator, (ii) integration of more sophisticated sensor and closed-loop control by the controller, (iii) online monitoring and optimization of drilling performance by combining AI and physics-based models. Depending on the level of automation, the cost of the rig is increased, and simultaneously, the well drilling cost is reduced (Tony Pink, Andrew Bruce, 2012). The rigs with the first two levels of automation are already being used in the drilling industry. For example, in 2011, Shell collaborated with China National Petroleum Corporation (CNPC), jointly developed a well manufacturing system called "SCADAdrill." The SCADAdrill can recurrently drill and complete standardized wellbores in an automated manner. With the help of sensors mounted on the drill bit, the SCADAdrill system has enabled smart monitoring wellbore trajectory and closed-loop control of the bit movement and its path precisely (Royal Dutch Shell, 2021).

In 2020, Statoil drilled the world's first automated exploration well on a floating rig using advanced drilling control (ADC) system with all three levels of automation hierarchy described above. Statoil had achieved a 15% – 20% improvement in the drilling rates with the help of an advanced automation system. This advanced rig has features like the prediction of drilling anomalies using advanced data analytics techniques. They claimed that early prediction of kick and loss circulation was viable (sekal, 2020). The reduction of drilling costs through real-time optimization is found to be a more attractive and accessible approach for O&G companies. ONGC has sponsored a research project to IIT Guwahati to develop a drilling decision support system (DSS) to reduce drilling costs. As a part of this project, IIT Guwahati developed a DSS framework for ONGC Ltd, and a part of the DSS feature is covered in this work.

1.8. Objectives of the thesis

The primary objective of the thesis is to develop a methodology and algorithm for detecting the upcoming complications and minimizing the non-productive time (NPT) and specific energy utilization during the rotary drilling process.

By considering the research gaps from the comprehensive literature review, the motivation of the thesis is to expand the research in the area of tubular mechanics,

detection of downhole complications and specifically contribute towards drilling optimization. To accomplish this, the specific goals for this work are as follows:

- To develop a 3-Dimensional frictional model for hookload estimation at the deadline by considering all the rig and wellbore uncertainties.
- To evaluate the structural integrity of drill string tubular with a workflow that estimates the overall stresses acting along the drill string during drilling activity.
- To integrate the developed model with a Decision Support System (DSS) developed for ONGC to minimize the potential downhole drilling hazards through dynamic predictions of hookload and neutral point.
- To develop a novel approach for optimum selection of drilling parameters with the help of historical drilling information, measured without MWD tools aid.
- To determine the inefficient drilling zones by using the concept of specific energy for different lithologies.

1.9. Organization of the thesis

The presented thesis is organized into six chapters. A thorough description of each chapter is explained in detail below:

In **Chapter-2**, the comprehensive literature survey is presented in detail as follows:

- Investigation on data pre-processing and rig state identification techniques.
- A detailed study on Torque and Drag (T&D) models and its applications.
- Studies on real-time monitoring techniques using surface and MWD measurements.
- A short literature describing the possibilities of differential sticking and its associated forces.
- Description of the methods developed for drill string fatigue management and tubular mechanics.
- Studies on various drilling optimization techniques to achieve better drilling rates.
- Exploring the utilization of specific energy concepts for drilling optimization.

Chapter-3 introduces a drag model that considers drilling rig and wellbore physical metrics. It also includes the subsequent enhancement of the 'Aadnoy's' 3D friction model to determine the deadline's load. The application of the drag model in both vertical and directional wellbore is illustrated in brief.

Chapter-4 discusses the evaluation of stresses along the tubular with an increase in depth. The enhanced effective tension and true tension model, which is utilized to estimate the neutral point and hookload at the deadline, is covered in this chapter. The application of the stress variation-based model was illustrated using an on-field case study.

Chapter-5 presents the optimum selection of drilling parameters using the improved playback methodology in directional wellbores. The optimum drilling parameters are further utilized to estimate the specific energies used to drill a particular section. In this work, the utilization of playback methodology and a field case study of both an exploratory and development well drilled in north-eastern India is presented.

Chapter-6 summarizes the present research and suggests the future scope of the present work.

Chapter

2

CHAPTER 2

State-of-the-Art of Drilling Technology

2.1. Foreword

Oil and gas (O&G) have made a massive contribution to humankind in economic growth and social advancement. Surplus energy enables the social division of labour and helps to grow cities and individuals. This expansion process has led to the unceasing finding and depletion of oil and fossil fuels as the whole world is looking forward towards peak oil period with substitutions. As per Canadian Association for Petroleum Producers (CAPP), the world is currently consuming nearly 100 million barrels of oil per day (CAPP, 2021). At the same time, the International Energy Agency (IEA) projects that oil continues to be in a demanding position for transportation and petrochemicals (which is used for daily manufacturing products extending from smartphones to footwear). The natural gas demand is increasing exponentially as an alternative for coal to reduce greenhouse emissions. It is proven to be cost-effective, plentiful, and reliable, with 40 to 65% lesser greenhouse emissions than coal. The IEA 2020 report stated that natural gas is projected to increase by 29% by 2040, meeting 25% of the total energy consumed worldwide (CAPP, 2021). To meet forecasted oil & gas demand, the industry is focused on developing energy-efficient technology for oil and gas exploration & production.

Consequently, researchers have focused on developing drilling technologies to explore oil and gas lying much beneath the earth's crust, and a considerable amount of research works have been reported. As described in the introduction section, in this chapter, the detailed literature review and state-of-the-art technology developed by both the academic and industry community is presented to intensify the technology gap that can be studied for the betterment of drilling process monitoring and optimization. The drilling monitoring and optimization solution require technology for online data collection, pre-processing, modelling of the drilling process, and a model-based approach for fault diagnostic and process optimization. The literature review of these topics is presented below.

2.2. Data pre-processing and rig state identification

To monitor well-drilling progress, the following sensors are installed in rig surface: rotary speed/ string RPM, mud flow, hookload, weight on bit, bit position, bit depth, total depth, block position, and many more. From these measured parameters, the following parameters are derived for drilling and monitoring purposes: rate of penetration (ROP),

weight on bit (WOB), hookload, rotations per minute (RPM), torque, bit depth, total depth, and mud flow rate – strokes per minute (SPM). The overall process of the drilling activity can be classified into the following sub-activity: drilling with rotation, drilling without rotation (sliding drilling), tripping-in with rotation and without rotation, tripping-out with rotation, and without rotation. The measured values from the above sensor are expected to vary based on the above-mentioned drilling sub-operation. This drilling sub-operation is also called a rig state. The state of the rig is important information to execute respective fault prediction algorithms. For example, the prediction of string washout has to be executed by monitoring the mud circulation rate during specific operations. Otherwise, the prediction can go wrong. Therefore, operations that require mud circulation needs to be identified.

Several sensor measurements are obtained from the drilling rig during the oil well drilling process. The high-frequency time-series data obtained from the sensor measurements are utilized in identifying the rig state and activities executed by the rig personnel. The rig state is mainly determined for mitigating undesirable drilling events using this surface/downhole information (Hoteit et al., 2005).

Ouahrani et al., (2018) focused on minimizing the invisible lost time (ILT) to improve the drilling performance. The ILT time includes wellbore problems, downhole tool failures, rig repair, and other complications. They implemented a tracking tool that utilizes real-time sensor data from surface and offline daily progress reports to measure the ILT. The tool analyses the cause of ILT on each drilling activity and suggests an action plan to be taken for future wells that may be drilled in nearby locations. The estimation of ILT and root cause analysis was able to reduce the ILT from 30% to 10% while drilling future wells during the next three years of duration. That resulted in increasing average footage/day and minimizing the well completion time.

Dunlop et al., (2004) have developed a method and system to automatically identify the rig state during the drilling process. The particle filtering algorithm, which is probabilistic, is utilized to identify the rig state. The algorithm requires at least two or more input information to determine the rig state (probably from 6 to 10 possible states). The rig states include rotary drilling, slide drilling, tripping-in with mud circulation (rotating), tripping-in with mud circulation (without rotation), tripping-out with mud circulation (rotating), tripping-out with mud circulation (without rotation), pump and slip

status. The algorithm requires measured hookload, torque, block position, and stand pipe pressure (SPP) to identify the rig state.

Recently, Ben et al., (2020) utilized both rule-based and machine-learning models for rig state identification for 10 wells in the Delaware basin and 12 wells in the DJ basin. Both approaches were used to classify seventeen rig states using real-time sensor data from the surface. The drilling state was sub-classified into 'rotary drilling' and 'slide drilling' using three machine learning models: convolutional neural network (CNN), random forests and a hybrid convolutional neural network, and recurrent neural network (CNN/RNN). The rule-based model resulted in 70% and 90% accuracy in both the basins, whereas machine learning models resulted in over 99% accuracy. The study concluded that machine learning models are superior to the rule-based models for the classification of rig states.

Chatar et al., (2021) developed machine learning models to classify the rig state from videos captured on the rig floor along with real-time sensors placed on the surface. The conventional neural network (CNN) is used to synchronize the video and real-time sensor data. The synchronized data is further processed using a graphics processing unit (GPU). The processed data is further used to train the ML models: visual geometry group (VGG) network, two stream models, and a convolutional 3-Dimensional model. These models were effective in detecting rig states using computer vision analytics and real-time sensor data.

The recent studies on rig state identification and its application to reduce the drilling cost are found to be more attractive for oil & gas industries. Further, the following technology gaps are observed while implementing AI & ML-based rig state identification algorithms for fault diagnosis.

(a) Validation of a single algorithm for multiple wells located in different regions (United States of America, India, and other nations)
(b) Integration of rig state identification algorithms to fault identification applications. Typical faults observed on the field include stuck pipe, drill string washout, twist off, kick and loss circulation, and downhole-related issues.

2.3. Modelling of drilling process and fault diagnostic

The data pre-processing and rig state identification algorithms will provide appropriate data to drilling engineers to analyse the data for improved drilling operation. The response time to avoid many critical faults can vary from 1 min to 30 mins. For example, to prevent washout in actual drilling conditions, by monitoring the SPP drop, the response time for the operator will be between 1 to 5 mins. Otherwise, the drill string may washout and may result in a twist-off. Therefore, appropriate input to the operator within the response time can save from drill string washout considering the importance of real-time data analysis and fault prediction. Many researchers focused on developing fault prediction algorithms, and these can be developed by adopting first principle models, data-driven models, and a combination of both. The literature on fault diagnosis for drilling operation is presented in this section.

Numerous studies have been done to detect stuck pipes based on machine learning techniques. Hempkins et al., (1987) demonstrated the utilization of multivariate analysis for stuck pipe detection, and the same had been used for differentiating the type of stuck. Later, Biegler & Kuhn, (1994) developed a second-generation engineering statistical model incorporating physical stuck pipe parameters and vast amounts of drilling information to determine the stuck pipe possibility. The statistical inferences are less precise when compared to machine learning approaches (Bzdok et al., 2018). Siruvuri et al., (2006) established an Artificial Neural Networks (ANN's) model to estimate the risk of stuck pipe occurrence during well planning and drilling. The study further extended using Support Vector Machines (SVMs), and SVMs provide an edge over ANNs due to fewer parameters for model development (Al-Baiyat & Heinze, 2012). Some of the drilling process variables are discontinuous and non-linear; incorporate the same in the predictive model. Murillo et al. introduced the adaptive fuzzy logic and ANNs to predict the pipe sticking symptoms (Murillo et al., 2009). Apart from the machine learning techniques, stuck pipes can also be detected by analyzing torque and drag (T&D) acting on the drill string with the help of the first principal model approach. The section below lists the enhancement and application of T&D models to detect stuck pipe and their associated symptoms. The work progress in the T&D model development for drilling analysis and its application in detecting stuck pipe and associated complications is summarized below.

2.3.1. Torque and Drag (T&D) models

While drilling high-angle wells, the operators are expected to have downhole complications at a higher rate. Specifically, keyseating would occur in directional drilling when the diameter of the wellbore is insufficient for free movement of a drill string due to low radius of curvature, resulting in pipe stuck (Edy Soeiinah, 1985). Further, to predict the downhole complications, the drilling industry requires improved technologies to minimize the non-productive time (NPT). The prediction and monitoring of measured hookload in real-time drilling can mitigate downhole problems and aid in optimized drilling by reducing the NPT and making drilling more efficient. For example, the following downhole complications can be predicted using measured and calculated hookload: stuck pipe, improper hole cleaning, lost pipe situations, and excessive tortuosity. The hookload is the total weight force needed to move the drill string up or down (Frafjord, 2013). It is measured at the deadline and indicates the severity of the friction between the drill string and the borehole surface. Numerous contributions are reported in the literature about the fundamental understanding of friction in the directional wellbores.

Falconer et al., (1989) developed a technique for determining side forces, torque, tensional forces, rotating and sliding friction factors using real-time MWD and surface measurements. The estimated friction factors can be utilized to quantify the drilling anomalies, such as the onset of buckling, improper wellbore conditions, and stabilizers hanging up. They have also formulated an algorithm to identify the need for wiper trips and circulation to improve poor drill bit performance. Jardine et al., (1992) developed a real-time wellbore friction monitoring algorithm to identify borehole conditions. Their algorithm uses the following real-time measurements: hook load and torque to generate a wellbore friction profile with respect to depth. The calculated friction profile can be compared with the design phase value to identify drilling anomalies.

In general practice, the WOB is maintained by manipulating the hook load manually. Such manual operation may lead to variations in WOB. Further, by maintaining constant WOB, the operator can achieve optimal drilling performance. Recently, Zha et al., (2018) developed closed-loop control to maintain consistent WOB. Wherein the WOB is calculated from surface hook load measurements. The inferential control algorithm is implemented to maintain consistent WOB. The inferential model was aimed to predict

the downhole WOB with the following model inputs: friction factor, surface hook load, and wellbore geometry. The inferential model was validated using measured downhole WOB on multiple horizontal wells and found to accurately predict friction factors throughout the lateral section of the wellbore.

The wellbore conditions in terms of improvement and deterioration can be identified by monitoring the calculated friction factor (Bible et al., 1991). An increasing friction factor indicates the obstructions in the wellbore and vice-versa. Hookload has a uniquely complex character, exhibiting different trends during drilling/tripping operations (Salem Al Gharbi, Moataz Ahmed, 2018). By monitoring the friction factor, measured and calculated hookload, the following analysis can be performed, and that will improve the drilling operation.

(a) The identification of abnormal fluctuations in measured hookload would help identify improper hole cleaning and reaming operations (Freithofnig, H.J., Spoerker, H.F., Thonhauser, 2003).
(b) The analysis of hookload variation with respect to depth will provide input to the design of a new mud system and hydraulic conditions for optimized drilling (Elgibaly et al., 2017).
(c) The accurate prediction of hookload deviation from theoretical value will help the operator identify drilling complications such as drill pipe failures, buckling, box swelling, and the inability to send the liners and casing to the target depth (McCormick et al., 2011).
(d) The accurate prediction of the hookload during stuck pipe can provide maximum load that can be applied during jarring (Kenneth R.Newman, Ray Procter, 2009).

The first two analysis doesn't require the mathematical model to predict the hookload and last two analysis requires the mathematical model for anomaly identification and decision support to operators.

For these analysis, the hookload is measured by a tensiometer fixed at either wire rope or at the deadline, which is attached to the draw-works and tackle system (Wylie et al., 2013). When it is fixed in the wire rope, the actual hookload acting on the drill string can be measured directly. But in other cases, the hookload is measured at the deadline, and it includes travelling block weight, sheave friction, number of drilling lines running over

the sheave. Therefore, hookload measured at the deadline will be subjected to load generating forces such as the imperfect tension transmission across sheaves, inertia forces associated with weight and rotation of drilling lines, the weight of the mud hose attached to the top drive (Eric et al., 2015).

To predict the hookload acting on top of the drill string, the torque and drag model for deviated wellbores was first developed with a basic set of frictional equations (Johancsik et al., 1984), and the same was modified to incorporate the effect of hydraulic and hydrostatic pressure inside the wellbore. The revised model resulted in a one-dimensional momentum balance along the drill string length (Sheppard et al., 1987). Subsequently, a method to evaluate the overall friction coefficient between the drill string and the wellbore is developed, and this method uses an iterative procedure to estimate the friction coefficient by minimizing the error between the measured and calculated hookload (Maidla & Wojtanowicz, 1988). While developing a hookload model, the friction factor is assumed to be a function of dogleg severity. Further, to include such effects, the model for friction factor is developed as a function of hydrodynamic viscous drag, and tortuosity (Mason & Chen, 2007). And, this friction factor is expected to vary with respect to the well profile for a given formation type. The same can be incorporated by dividing the well profile (straight, drop-off, build-up), and different analytical equations were derived and analyzed for deviated wellbores (Bernt S. Aadnoy, 2010). To further improve the accuracy of hookload calculation, the variation of hookload as a function of block position for one complete stand (approx. 28.5 m) is considered. The pull force exerted by the mud hose and other electrical umbilical's on the top-drive system starts decreasing as the travelling block gets closer to the derrick floor (Eric et al., 2015).

Further, to predict the hookload at the deadline, the model developed by Eric et al., (2015) can be improved by integrating the factors affecting the tensiometer's position at the deadline (J.W. Dangerfield, 1987). The studies on block and tackle system by Luke and Juvkam Wold concluded that the hookload is a function of deadline tension, sheave efficiency, number of drilling lines, and direction of pipe movement (Luke & Juvkam-Wold, 1993).

The application of a mathematical model for predicting downhole complications is one of the essential aspects of the drilling industry. For example, the hookload prediction model indicates the wellbore condition and expected complications in advance. The

success of this approach is entirely dependent upon the quality of the model used for hookload prediction. The literature reported three approaches: data-driven/ statistical model, first principle model, and combination of both (hybrid). The data-driven model requires historical drilling data from the exploratory wells, and the availability of such data is minimal. Wesley, (2016) developed a technique to identify the tight spots based on the moving average of hook load and depth in two different time intervals. For example, the average value of hook load and depth is calculated for a time interval of 30 sec and 240 sec (4 mins). By analysing the moving average hookload and depth profile, they were able to identify the tight spots (refer to Fig. 2-1).

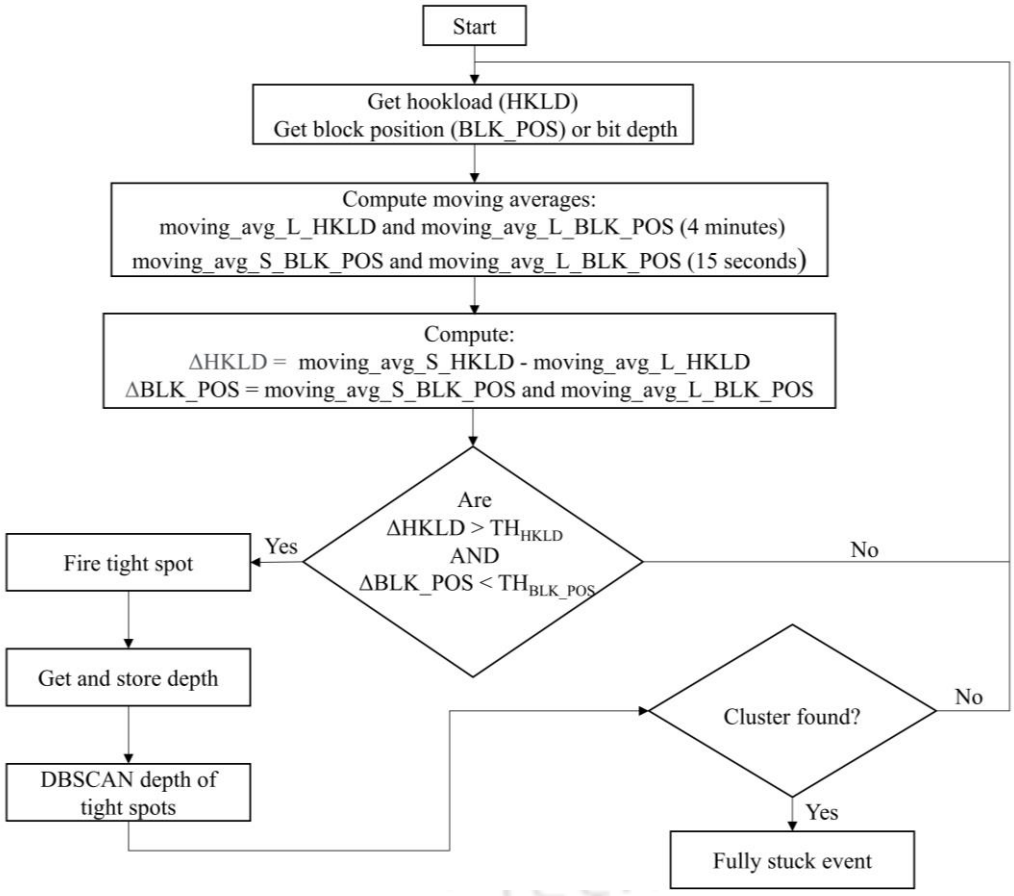

Fig. 2-1. Flowchart depicting the identification of stuck pipe

On the other hand, developing the first principle model for drilling applications may not be possible considering many complex phenomena during drilling. Therefore, the hybrid model will provide flexibility to tune the model constants to match the measured hookload with the predicted hookload.

The drilling industry started developing real-time monitoring and anomaly detection systems by two approaches to evaluate the wellbore's health and mitigate the downhole complications. Firstly, the measured hookload and other drilling parameters are used to identify anomalies based on expert knowledge and artificial intelligence (AI) (Fruhwirth et al., 2012). In the second approach, in addition to the first approach techniques, the new variable, i.e., a deviation between the measured and calculated hookload, is used along with other drilling parameters. Wherein hookload can be calculated using the above-mentioned literature reported models. Salminen et al., (2016) has evaluated the above said two approaches to predict the stuck pipe event. Also, they have come up with a hybrid approach by combining both model prediction and measured data analysis. The results conclude that anomaly detection techniques by using an expert rule approach may not predict all the anomalies. In another aspect, the efficiency of the hybrid approach is found to be superior to the stand-alone expert rule approach.

After identifying the anomaly by monitoring hookload and its allied parameters, the alarm's triggering in real-time is important before the situation gets aggravated (Cayeux & Daireaux, 2009).

2.3.2. Modelling of axial and radial forces acting on the drill string

The optimal well design requires a detailed analysis of the forces acting along the drill string's length, which helps the operators to achieve trouble-free drilling in directional wells. The wells designed without such an analysis are more prone to lead downhole complications, increasing the non-productive time (NPT). The detailed analysis of forces acting along the drill string can provide drill string stability in directional wellbores. Also, it can help the operator to have an optimistic plan for drilling activities during the well design phase. Further, the real-time analysis of the force acting on the drill string can help the operator to predict the downhole complications and make a mitigation plan. For example, accurate prediction and real-time monitoring of hookload and forces along the drill string may indicate upcoming downhole complications like excessive tortuosity, unsuitable hole conditions, improper cutting transportation, stuck-pipe.

To understand the various loads acting on the drill string in the presence of external fluid pressure, in the early 1900s, Bridgman demonstrated an experiment where a glass bar of cylindrical shape was mounted in a chamber and pressurized until the bar got parted

(Arnfinn, 2015). The mounted specimen was unmasked to radial pressure alone, and therefore, this amazing effect was termed as Bridgman's paradox. Furthermore, Bridgman's study was conducted at the University of Stavanger in 2013-2014 on a rigid bar and came up with a conclusion that "The tensional surface is comparable to the fracture surfaces in either of the conducted experiments." The Bridgman test concludes that tension on the bar is majorly affected by the forces due to external pressure than the forces due to other sources. In the late 80s, Sheppard et al. modified their model equations into differential form by incorporating the effect of mud pressure on forces acting on the drill string as concluded by Bridgman experiments (Sheppard et al., 1987).

The effective tension is a function of both the true tension acting on the drill string and the drilling fluid's pressure forces. The presence of drilling fluids in the wellbore entails hydrostatic forces as an essential part of operations and well design. Lubinski et al., (1962) concluded that if the outside pressure is less than the inside pressure, the tubing may helically buckle even if it was in tension. Further, Sparks et al. provided an analysis of effective tension and true tension of cylindrical pipe when it was exposed to external pressure (C.P.Sparks, 1984). Later, Samuel & Kumar, (2012) have extended a similar analysis for drill string at different operating conditions. Along with T&D, calculated axial and radial forces can even be utilized to estimate the hookload and neutral point acting along the drill string in some circumstances.

Statistics showcase that 50% of drill string failures arise due to severe fatigue (W.-C. Chen, 1990), and they cause major rig downtime. In directional and extended-reach wells, the drill string is subjected to severe loads such as tension, compression, torsion, and bending pressures and temperatures. Under these circumstances, the drill string is more likely to undergo failure when the drill string is exposed beyond the allowable number of cycles, i.e., duration to drill string fatigue (Vaisberg et al., 2002).

Lubinski, (1961) and Hansford & Lubinski, (1964) investigated drill pipe fatigue during rotary drilling operations of the well with high dogleg severity. They concluded that stress analysis is a critical aspect to avoid drill string failure due to severe fatigue. Silva et al., (2009) conducted fatigue experiments and numerical stress analysis on drill pipe made of Al-Cu-Mg and Al-Zn-Mg alloys systems as per ASTM E466-96 standards. The aluminium drill pipes are connected using the shrink fit concept, and it uses the concept of heating before threading and cooling after threading. They observed that drill pipe

material fatigue in the transition region between tool joint and pipe. Remarkably, the contact between box and pin threads plays a crucial role in fatigue analysis.

Collins & Vaghi, (2002) have attempted this problem through numerical stress analysis on rotary shouldered connections to understand the stress variation and fatigue resistance. The stress analysis of different types of joints and thread forms are performed to predict drill pipe connection strength. They recommended that the bending strength ratio (BSR) greater than 3 corresponds to an excessive weak pin, and BSR less than 2 relates to the weak box. Wu, (1996) presented a detailed analysis of drill pipe bending and fatigue during rotary drill activity in horizontal wellbores. The analysis aimed to predict the drill pipe fatigue damage by determining drill pipe contact status with wellbore and maximum bending stress. These derived equations are incorporated into the computer program DPLIFE, which will aid the field engineers to perform quick prediction and monitoring of cumulative fatigue damage, permissible build rate, and the total number of rotating hours before failure.

Skoczylas, (2014) presented a method for fatigue life estimation of drive strings in progressive cavity pumps (PCP) applications. The method includes determining the drive string's effective curvature, and then the alternating bending stress and mean stress are estimated. Further, the S-N curves are obtained for the drive rod, and various correction factors (size, corrosive environment, and surface finish) are incorporated. The effective stress obtained from the alternating mean stresses is utilized in the S-N curve to determine the number of cycles to failure. The S-N curves correspond to relating alternating stress to the total number of cycles before failure. The mean stress is zero for any specimen during the development phase of S-N curves, and since there is no torque or axial load action on the specimen. These curves can’t be used directly for drilling-related applications, as the drill string is constantly subjected to extreme torque and higher axial loads. Therefore, the S-N curves are corrected and altered to M-N (moment – no of cycles to failure at the moment level) curves with the modified Goodman diagram application, which considers the influence of axial stress (Inoue et al., 2008).

Zoanni et al., (2009) demonstrated a cumulative fatigue damage analysis technique for real-time monitoring applications. Their technique aids in approximating the fatigue levels within the drill string and intelligently handling pipe positioning and inspection frequency. The monitoring starts at spud and is executed on each joint of the drill pipe as

it traverses along the wellbore path to total depth. This technique acts as a quantitative measure of relative fatigue damage accumulated across the joints of complete drill string and assistance in managing logistics, forecasting drill string inspections, and position string sections to reduce the cumulative fatigue damage.

2.3.3. Preventive measures for stuck pipe and remediation

The main objective of identifying the drilling anomalies using the techniques described in the above section is to prevent major downhole complications. In this section, the preventive and mitigation measures taken to avoid stuck pipe after noticing symptoms are briefly discussed. A drill string is considered to be stuck in the wellbore if it cannot be moved or pulled out of the hole. Based on the mechanism, the stuck pipe is classified into two types: mechanical stuck pipe and differential stuck pipe (refer to section 1.6). Mechanical stuck pipe is caused due to crooked wellbore geometry, improper hole cleaning, junk accumulation, severe doglegs. Several studies were conducted to identify the root cause of the mechanical stuck pipe. Oketch, (2014) conducted a study on a geothermal well in Menengai, Kenya, which was abandoned due to a stuck pipe. The study mentioned that sticking due to fracture and faulted formation can be mitigated by decreasing the drill string vibrations, reducing the surge pressures, and proper hole cleaning to reduce pack-off. Due to poor hole cleaning, mechanical sticking can be reduced by maintaining good mud rheology, gel strength, controlling the drilling rate and annular velocities, and checking the output flow rate.

Differential sticking is one of the significant contributors to NPT (Al-Ansari et al., 2009), and it contributes to 40% of the well cost (Alshaikh & Amanullah, 2018). It may occur when the drill string is stationary or moving slowly across the permeable or depleted rock formations, such as sandstones, where there is always a possibility for mud cake deposition (Reid et al., 2000). A rapid recovery solution to free the differential stuck pipe would eventually cut down the well cost and NPT. To understand the interaction between the drill string and mud, Courteille & Zurdo, (1985) conducted theoretical and experimental studies resembling actual field conditions. A pressurized mud circuit was developed in the laboratory to record the pressures at critical interfaces. Their impact on interfaces among the mud cake, formation, and drill string were studied. The study concluded that the drill string, mud cake, and formation interface are mainly affected by the pore pressure at the stuck pipe region. Later, Hale & Tutuncu, (2005) introduced an

ultra-sonic horn-type device that would be lowered into the drill string before applying freeing force. The ultra-sonic energy would aid in reducing the contact force between the drill string and the mud cake, thereby minimizing the effort to pull out in the case of differential stuck up.

Further, Heitmann & Burgos, (2015) engineered a U-tubing model which would aid in the rapid injection of nitrogen into the annulus by making way through the closed annulus preventer. The nitrogen would displace the mud in the annulus and push the mud through the drill string, and eventually lower hydro static pressure in the annulus section. The developed solution is demonstrated in the Heavy oil Faja Orinoco Belt, Venezuela. Al-Qasim et al., (2019) patented a system to release differential stuck pipe by coupling fluid releasing tank to the centralizer or stabilizer present in the BHA. Heat-sensitive nozzles are shoved on the fluid-releasing tanks, and the fluid (HCL) is released when there is an attempt to move the drill string. During the pipe movement, the portion of the drill string which is adhered to the external material would get heated up and releases the fluid when the temperature of the nozzle exceeds the threshold temperature. Javeri et al., (2011) came with an innovative solution to prevent loss circulation, kick, and differential sticking by including silicon nanoparticles into the drilling mud. The silicon particles allow the mud cake to be continuous and uniform, thereby preventing all the stuck pipe associated complications.

In the case of a stuck pipe scenario, the preliminary step is to determine the depth of the stuck up. Currently, two conventional approaches are followed in the industry: (i) measurement using sensor log tools and (ii) theoretical calculation based on the surface sensor. For precise measurement of stuck, the sensors such as radial cement bond tools, acoustic log tools, and free point indicators are run into the wellbore. However, these techniques are expensive, time-consuming, and require experts to handle specialized instrumentation. The theoretical calculations are performed on-field by conducting a stretch test. As per Hooke's law, the strain or distortion in a material is directly proportional to the pull force applied if the material's elastic limit is not exceeded (Degeare et al., 2003). The stretch of the drill string due to the force's application is recorded, and the free pipe's length is estimated using Hooke's law, as given in Eq.2.1.

$$\Delta L = \frac{F \times L \times 12}{E \times A} \tag{2.1}$$

where F indicates the pull force in lbs, L & ΔL represents the length of free pipe and stretch, respectively, E denotes modulus of elasticity of steel, and A indicates the cross-sectional area.

2.3.4. Modelling of ROP

To drill a well successfully and to achieve a better rate of penetration (ROP), the following three drilling process parameters have to be maintained at their optimal value: as weight on bit (WOB), rotations per minute (RPM), mudflow in terms of strokes per minute (SPM). The WOB is manipulated by controlling the draw-works brake such that the neutral point will move towards the drill bit. The RPM is controlled by top-drive systems/ kelly drive systems/ mud motors, and mudflow is controlled by varying the pump speed to remove all the cuttings generated at the bottom. Among these three parameters for the top-drive system, WOB and RPM will be critical parameters that must be monitored and optimized in real-time.

Similarly, the other drilling parameters such as torque, standpipe pressure (SPP), mud weight, and mud rheological properties also play a critical role in achieving optimal ROP. However, these parameters cannot be manipulated in real-time since they are a function of formation type, lithology, and temperature (Alali et al., 2021). The drilling without having real-time monitoring and optimization solution may lead to sub-optimal drilling, i.e., high drilling costs with reduced ROP. Also, applying excessive WOB to achieve maximum ROP can eventually result in higher torques and further lead to drill string snapping off, buckling, severe stick-slip, and other downhole complications. The selection of optimal drilling parameters further reduces energy consumption and NPT.

A mathematical model that relates ROP and other drilling process parameters is essential for determining the optimal parameters. Therefore, numerous researchers have established the mathematical model for the drilling process by using traditional physics-based models ((Hareland & Rampersad, 1994), (Motahhari et al., 2010), (Hegde et al., 2017)) and data-driven approaches. One of the early attempts for establishing a technique for determining optimal drilling parameters was made in the late 1950's by Graham & Muench, (1959). The work is mainly minimizing the drilling cost by an optimum selection of WOB and RPM. Galle & Woods, (1963) presented a graphical method to find optimal WOB and RPM to achieve maximum ROP. Also, they

came up with a simplified empirical relationship to find optimal drilling parameters. Bourgoyne & Young, (1999) have developed a mathematical model for drilling using multi-non-linear regression analysis. In their analysis, the following drilling parameters were considered as a model input: formation depth, formation strength, formation compaction, bit diameter, weight on bit, rotary speed, bit wear, hydraulics, and pressure differential across the hole bottom. Maidla & Ohara, (1991) have proposed a new model by including additional parameter namely formation compressive strength component in the model developed by Bourgoyne and Young (B&Y). Later, the performance of both models was compared and the latter was found to have better ROP. Their analysis concluded that the inclusion of more drilling process data may improve the model prediction ability.

Similar to the B&Y model, Eren & Ozbayoglu, (2010) developed a model for drilling optimization using the multi-linear regression technique. The developed model utilizes actual field data collected through data recording and well-monitoring systems as an input to predict ROP. The input parameters are namely: mud weight, WOB, RPM, and formation characteristics. Etesami et al., (2021) developed an improved version of the B&Y model for predicting ROP. To achieve such an improvement, the parameters such as differential pressure function from the downhole motor, equivalent circulating density (ECD), and wellbore inclination are included as input. As a result, their model was more precise than the B&Y model in deviated wellbores drilled by polycrystalline diamond compact (PDC) bits. Daireaux et al., (2021) have proposed a framework for optimizing the drilling process that determines optimal ROP without violating the operational risk of rig components and borehole stability in real-time. The proposed framework was demonstrated using the Detournay model, and the model parameter was estimated by validating the model using dynamic surface measurement while drilling. The major limitation of the Detournay model is that it requires various unknown parameters for model calibration, and the determination of these parameters in actual field conditions is a difficult task. Keshavarz Moraveji & Naderi, (2016) studied the effect of six variables on ROP by utilizing the actual field data. Response surface methodology (RSM) was utilized to develop a mathematical relationship between ROP and six variables. The variables include total depth, weight on bit, bit rotary speed, bit jet impact force, 10 min to 10-sec gel strength ratios (10 MGS/10 SGS), yield point to plastic

viscosity ratio (Yp/PV). Further, bat algorithm (BA) was utilized for optimization of ROP, and its objective function is as follows:

$$obj.func = \min \sum_{i=1}^{n} \frac{\left(ROP^{i}_{actual} - ROP^{i}_{estimated} \right)^{2}}{n} \tag{2.2}$$

where 'n' represents the total data points and $ROP_{estimated}$ is the estimated ROP. The study concluded that the ROP is estimated at 95% accuracy. However, the utilization of uncontrollable parameters for ROP prediction is unproductive, as the operator cannot alter these in actual drilling conditions.

2.4. Optimization of drilling specific energy

Teale, (1965) developed a Mechanical Specific Energy (MSE) model to evaluate the total energy spent to drill a unit volume of rock. The MSE estimation depends on mechanical rock properties such as friction angle, unconfined compressive strength (UCS), and the cutting environment. The work reveals that MSE can be utilized as an index to determine mechanical efficiency and concluded that the ROP is maximum when a minimum MSE is spent. Recently, F. E. Dupriest et al., (2005) presented the pilot project undertaken by ExxonMobil Fast Drill Process (FDP), where MSE is monitored in real-time drilling conditions. Even though MSE can be utilized to find optimal WOB and RPM, further detailed analysis of MSE in real-time may also provide better insights into drilling complications. In their work, the MSE is used to detect the changes in drilling system efficiency.

But later, many attempts have been made to determine the optimal drilling parameters by maximizing the ROP and minimizing the MSE ((X. Chen et al., 2014), (W. Chen et al., 2019), (Alsubaih et al., 2018)). For example, Pessier & Fear, (1992) utilized the ROP and MSE cross plot to study the overall drilling performance and efficiency. Amadi & Iyalla, (2012) used MSE to determine the drilling efficiency. The determined MSE is compared with the unconfined compressive strength (UCS) to evaluate the downhole drilling conditions, and it is estimated from both surface and downhole measurements. Pinto & Lima, (2016) have used MSE for geo-mechanical analysis, and that provides a method for optimization of ROP and non-productive time (NPT), simultaneously minimizing the excessive energy utilization and preventing the BHA failures. Nascimento et al., (2017)

has introduced a new concept to analyze ROP and MSE together to identify downhole complications. Wherein they have observed downhole complications when MSE increases with reduction in ROP while increasing WOB and RPM. The literature has verified that quadratic regression is a way to model the relationship between WOB and ROP (Xuyue et al., 2018). The model for determining the foundering WOB was adopted from play-back methodology, and R^2 value of the model was found to be very low. And these low values might have been due to data inconsistency and other problems associated with data pre-processing. Hegde et al., (2018) had developed a data-driven approach (random forests algorithm) to build three different objective functions, namely ROP, MSE, and torque on bit (TOB). The inputs to the model include WOB, RPM, flow rate, and rock strength. Later, the particle swarm optimization technique was utilized to optimize all the objective functions in a single objective mode. For example, while maximizing ROP, they observed ROP increments by 28%, MSE, and TOB by 4% and 10%, respectively. While minimizing TOB, they observed a 12% reduction in TOB, ROP, and MSE increment by 9% and 13%, respectively. Further, MSE optimization resulted in a 15% decrement in MSE, a 7% decrement in torque, and a 20% increment in ROP. Overall, the MSE optimization alone provided maximum benefit, simultaneously aiding in increase in ROP, and reduction in TOB and MSE. One has to note that the model used in their work requires considerably large number of input parameters from downhole tools, which is not available in majority of the drilling operation.

Armenta, (2008) enhanced the concept of using MSE more appropriately by combining it with bit hydraulics parameter called DSE determines the amount of energy required to excavate the unit volume of rock and lift the cuttings to the surface. The DSE will also act as a quantifier for hydraulic energy necessary to drill faster and efficiently when the MSE increases. From drilling data, they have observed a non-linear power function relationship while plotting DSE Vs. ROP. From the non-linear plot, they were able to identify different regions of drilling, namely: (1) Inefficient drilling (high DSE and low ROP), (2) Efficient drilling (low DSE and high ROP), (3) Transition zone (placed in between region 1 & 2). Al-Rubaii et al., (2020) has improved DSE use for drilling optimization by introducing the constraint on cutting concentrations in the annulus (CCA). For example, introducing this constraint (CCA < 0.05) improved the ROP by 44% and reduced the DSE by 48%. The specific energy concept was always utilized distinctively for monitoring purposes.

2.5. Literature gap

Modelling of Torque and Drag in the drill string

- For accurate hookload prediction at the deadline, the forces acting on a block and tackle system can aggregate up to several pounds of load. Apart from the influencing forces, all the measurements have some degree of uncertainty, for example, wear out of drilling lines, stick-slip in rotating sheaves, tilting of travelling block, and other uncertainties from unaccounted sources. The detailed impact analysis of these uncertainties in calculated surface measurements is not well studied. In one of the studies, the rig and wellbore uncertainties are incorporated to calculate the load at the deadline (Eric et al., 2015).
- The above-reported literature primarily focused on data-driven approaches for the detection of downhole complications ((Fruhwirth et al., 2012), (Ben et al., 2020), (Tsuchihashi et al., 2020)). Even though much literature is reported with first-principle models and their validation, very few of them are used for anomaly detection compared to the data-driven approach (McCormick et al., 2011).

Modelling of Axial and Radial Forces Acting on the Drill String

- There is still a technical gap in evaluating hydro-mechanical loading on different components of the drill string. The existing literature does not conclude the importance of using true tension and effective tension to achieve stable drilling operation for optimal drill string design. Specifically, the relationship between the drill string failure conditions concerning both of these forces has to be established for the case of directional drilling.
- The drill string operational data history is mandatory to conduct fatigue analysis. Without such a database, the fatigue analysis is not the right choice for determining tubular and downhole complications.
- The actual forces acting on the drill string in directional drilling are relatively complex than the vertical wellbore due to the action of numerous forces. Limited research has been reported on studies of drilling fluid effects on drill string during drilling operations (Samuel & Kumar, 2012), and there is scope for improvement in model development and utilizing these forces for detecting tubular and downhole complications.

- The neutral point needs to be considered before designing the BHA, depending on the target depth. The neutral point variation along the BHA is dynamic and needs to be monitored in real-time. There is a lack of profound investigation on neutral point determination when the drill string is on-bottom (e.g., rotary drilling).

ROP modelling optimization

- Several ROP models were proposed in the recent past, and the simplest models contain very few variables (Nascimento et al., 2017), while a majority of them requires as many as more variables such as rig/bit related variables, formation variables, associated mud variables ((Yi et al., 2015), (Shi et al., 2016), (Hankins et al., 2015)). All these variables are categorized as controllable and uncontrollable parameters. The controllable parameters can be altered instantaneously to improve the ROP without compromising the well-economics. In contrast, uncontrollable parameters such as formation type, formation pressures define the selection of mud type and well trajectory for that specific wellbore (Al-Abdul Jabbar et al., 2018).
- Most of the literature includes both surface and downhole sensor information, and access to all this information is a daunting task. And in the wells driven by the potential of cost reduction, the MWD tools aren't utilized in the BHA.
- The concept of MSE had been used in the improvisation of ROP ((F. Dupriest & Koederitz, 2005), (Alsubaih et al., 2018)), and the trend change in MSE with depth can be quantitively utilized to identify drilling dysfunction. To include the impact of hydraulic energy consumption with the MSE concept, the term Drilling Specific Energy (DSE) was introduced (Armenta, 2008). Different approaches were made for ROP optimization by utilization of MSE and DSE (a function of MSE and bit hydraulic contribution) profiles distinctly ((Hegde & Gray, 2018), (Armenta, 2008)). However, there are not enough attempts to combine them with the bit hydraulic contribution to achieve maximum ROP with better hole cleaning and a smooth wellbore.

2.6. Scope of the thesis

The extensive literature study shows that the real-time prediction of drilling downhole complications will enable the operator to perform energy-efficient drilling operations. To enable real-time prediction, accurate online drilling measurements are essential. The online measurements include hook-load, torque, rate of penetration (ROP), rotation per minute (RPM), standpipe pressure (SPP), strokes per minute (SPM), weight on bit (WOB), bit depth, measured depth, block position, and ton-of-mile. Analysing these measurements using an appropriate mathematical model of the drilling phenomena may provide a detailed real-time analysis of drilling activity. For example, the stuck pipe event may be predicted by analysing the torque and drag measurements with an appropriate mathematical model in real-time (Vos et al., 2000). Similarly, one can expect all significant events using real-time measurements of drilling activity. Currently, the Oil and Natural Gas Corporation of India Ltd (ONGC) uses a sophisticated SCADA system to acquire online drilling measurements from the drilling rig. Therefore, the main objective of this work is to make use of real-time streaming drilling parameters for predicting downhole drilling complications. Given the capital and operating expenses of the drilling rig, the oil & gas industry is focused on reducing the drilling rig's non-productive time (NPT). The drilling rig NPT is coined from many unpredicted and unwanted events such as stuck pipe, drill string washout, improper hole cleaning, kick and loss circulation, and other downhole complications.

Consequently, there's a necessity for detecting these anomalous conditions during drilling activities to progressively reduce the NPT. Besides, to minimize the NPT, establishing a design procedure for maximizing the drilling rates is crucial. Therefore, the current thesis work focuses on reducing the NPT by detecting downhole complications with the aid of first-principle models and maximizing the drilling rates by the optimal selection of drilling parameters. The scope of work is wholly pertained to drilling operations, i.e., starting from well spudding until the target depth is reached.

Chapter

3

CHAPTER 3
Anomaly Detection Methodology Using Predicted Hookload and Neutral Point

Content in this chapter is published as the following research article:

- Viswanth Ramba, Senthil Selvaraju, Senthilmurugan Subbiah, Muthukumar Palanisamy, "A Robust Anomaly Detection Methodology Using Predicted Hookload and Neutral point for Oil Well Drilling," *Journal of Petroleum Science and Engineering*, 195, 107787-[2020], https://doi.org/10.1016/j.petrol.2020.107787

3.1. Problem background

The rig operators are expected to have downhole complications during high angled drilling. To predict these downhole complications, the drilling industry requires better technology for trouble-free drilling and minimizes the non-productive time (NPT). For example, monitoring the hookload parameter during drilling operations can be utilized to provide information about the downhole complications like stuck pipe, improper hole cleaning, lost pipe situations, and excessive tortuosity.

Therefore, in this chapter, the improved methodology for predicting the hookload at the deadline is presented and validated with real-time use cases established from Assam Asset, ONGC, India. To predict the hookload at the deadline, the load acting at the top of the drill string has to be integrated with some of the unknown factors that are affecting the tensiometer's position at the deadline (J.W. Dangerfield, 1987). The methodology to include those unknown factors while calculating the hookload at the deadline is established in this chapter. The improved method uses the 3-Dimensional friction model to estimate real-time hookload, where the real-time weight-on-bit is utilized to estimate the neutral point, load acting at the surface and deadline. Due to the unknown forces acting on the block and tackle system, in literature, the hookload is derived as a function of deadline tension, sheave efficiency, number of drilling lines, and direction of pipe movement (Luke & Juvkam-Wold, 1993). The unknown forces acting on a block and tackle system can aggregate up to several pounds of hookload. Apart from these unknown forces, all the real-time sensor measurements have some degree of uncertainty, which may arise from several sources (i.e., drilling lines weight, stick-slip in rotating sheaves, tilting of traveling block, etc.). To incorporate all the above said unknown forces and uncertainties in the measurement, a new parameter “Rig Uncertainty Compensation” (RUC) factor is introduced in this work. It has to be estimated at regular intervals to reflect the change of real-time rig conditions.

To deploy this improved hookload prediction model, the decision support system (DSS) is established. The architecture of the DSS enables the real-time data collection, the estimation of RUC factor, prediction of hookload at the deadline, and finally identifying the anomaly to avoid downhole complications. The conventional method of anomaly detection involves combining both hookload and torque derived out of WOB, ROP, torque, SPM, and other drill string, wellbore and rig configurations. The method proposed

in this chapter is improved by utilizing a single key parameter, i.e., hookload to detect the anomaly and later, the anomaly is confirmed by analysing the other rig sensor parameters in real-time.

The developed DSS that combines the mathematical model of the drill string assembly with surface connection and alarm generation module was validated by using drilling data collected from multiple sources of drilling operation in real-time, such as drilling SCADA, well directional log information, well design data, and mud chemistry data. The whole framework was implemented in MATLAB and SQL server is used as the data base, and the DSS's human user interface (HUI) and alarm generation module were developed by using HTML and python respectively.

3.2. Model development

In literature, multiple mathematical models were proposed for calculating drill string hookload at the surface, torque, stresses (bending, buckling, and normal) along the drill string. They can be classified either as a data-driven model or the first principle model. Most of the reported models in the literature have ignored some of the essential contributing factors such as, the tension in the deadline and sheave efficiency of the block and tackle system, frictional forces acting along the drill string, and tensional forces exerted by the mud hose, hydraulic lines, and electrical umbilicals. Considering all these uncertainties, for accurate estimation of hookload at the surface, all these contributing (non-measurable) parameters are grouped into a metric termed as Rig Uncertainty Compensation (RUC) factor (refer to section 3.2.2). As described, the proposed mathematical model in this work has two components: (1) the model equations for drill string (2) the block and tackle system. For drill string, literature reported Aadnoy's 3-Dimensional friction model is used, and the model for block and tackle system is derived based on Luke's work (Luke & Juvkam-Wold, 1993).

3.2.1. Model to estimate the force at the top of the drill string

The Torque & Drag model in the drilling industry is mainly developed considering the string as either a soft or stiff string. The soft string is vastly available and signifies the industry standard. The basic assumptions of the soft string model to predict the drag are listed below

i. The drill string is assumed to be acting like a chain or cable.
ii. The radial clearance effect between the drill string and the borehole is negligible.
iii. The drill string trajectory is assumed to be similar to the wellbore trajectory.
iv. The bending moment of the drill string is neglected, which will project the contact forces lower than the actual.
v. The drill string stiffness is negligible when dogleg severity is less than 3°/30 m (DrillScan, 2013).

According to Aadnoy's 3D model for soft string (Bernt S. Aadnoy, 2010), the different forces acting on the drill string during the drilling process are presented in Fig. 3-1. The model equations used to calculate the load forces acting on drill string in both vertical and curved sections are given below.

Eq. (3.1) gives the load force required to pull the entire drill string on an inclined plane. In addition to the load component, the frictional force acts in the direction of the motion.

$$F = mg\cos\alpha + \mu mg\sin\alpha \tag{3.1}$$

Similarly, if the drill string is lowered, the frictional force acts opposite to the direction of the motion, resulting in the top load force

$$F = mg\cos\alpha - \mu mg\sin\alpha \tag{3.2}$$

In straight sections, the frictional force is contributed by the normal weight component (cosα term), and the sinα term gives the additional force required to move the drill string. Therefore, the drag force acting on the drill string body on a straight inclined section without rotation:

$$F_2 = F_1 + \beta w\Delta L \times \left(\cos\alpha \pm \mu\sin\alpha\right) \tag{3.3}$$

where '+' and '–' indicates hoisting and lowering of the drill string, respectively.

Eq.3.3 determines the static weight acting in the straight section during the drilling operation when the friction coefficient μ is zero. The Eq's 3.1-3.3 are applicable for estimating drag in straight sections.

Further, the directional survey data has to be integrated with drag equations to estimate the drag for curved sections. Aadnoy et al., have developed torque and drag equations for

curved sections. In curved sections, the normal contact force between the drill string and the bore hole depends on the tensional force and weight of the string. In the top section of the string, the side force generated by tension plays a vital role compared to weight. Therefore, to accommodate this effect in model equations, the drill string is assumed to be weightless initially, and the curved segment estimates an infinitesimal normal force. Later, the weight of the string is summed up to the normal force as given in Eq.3.5.

The dogleg angle is calculated for curved sections using the inclination and azimuth angles between two survey stations. Using this dogleg angle given in Eq.3.4,

The dogleg angle (θ) is given by

$$\cos\theta = \sin\alpha_2.\sin\alpha_1.\cos\left(\phi_2 - \phi_1\right) + \cos\phi_2.\cos\phi_1 \tag{3.4}$$

Drag for a curved section without rotation (buildup, drop-off, side bends, or combination of these) is reported in (Aadnoy et al., 2010).

$$F_2 = F_1 e^{\pm\mu|\theta_2-\theta_1|} + \beta w \Delta L \left\{ \frac{\sin\alpha_2 - \sin\alpha_1}{\alpha_2 - \alpha_1} \right\} \tag{3.5}$$

where '+' and '–' indicates hoisting and lowering of the drill string, respectively. In the case where the friction component $\mu = 0$, then the above Eq.3.5 determines the static weight component in the curved section.

In a buildup section, for the circle segment $\Delta L = R\alpha$, the above equation can be rewritten as

$$F_2 = F_1 e^{\pm\mu|\theta_2-\theta_1|} + \beta w R \sin\alpha_1 \tag{3.6}$$

The friction can be computed for any wellbore path by dividing the entire path into both straight and curved sections.

The above Eq's.3.1-3.6 are used to calculate the drag acting on drill string without rotation. Further, the resultant angle has to be included in the drag equations to include the effect of drill string rotation. Rotary drilling is carried out by simultaneous axial and rotational motion of the drill bit. There is a large amount of drag associated with only axial motion. So, the axial drag can be reduced by providing axial and radial movement to the drill string (Aadnoy & Andersen, 2001). While combining axial and radial

movement of the drill string, the resultant velocity ψ is given by the axial velocity V_h and tangential speed V_r. The angle between axial and tangential velocity is given by

$$\psi = tan^{-1}\left(\frac{V_h}{V_r}\right) = tan^{-1}\left(\frac{60V_h\left(m/s\right)}{2\pi N_r\left(rpm\right)r\left(m\right)}\right) \tag{3.7}$$

The drag force for straight pipe sections with axial and radial movement

$$F_2 = F_1 + \beta w\Delta L\cos\alpha \pm \mu\beta w\Delta L\sin\alpha\sin\psi \tag{3.8}$$

The drag force for curved pipe sections with both axial and radial movement

$$F_2 = F_1 + F\left(e^{\pm\mu|\theta_2-\theta_1|}-1\right)\sin\psi + \beta w\Delta L\left\{\frac{\sin\alpha_2-\sin\alpha_1}{\alpha_2-\alpha_1}\right\} \tag{3.9}$$

$\psi = 90°$, there is no rotation during axial movement and

$\psi = 0°$, there is no axial movement during rotation.

Eq's.3.8-3.9 are used to estimate the drag force in both straight and curved pipe sections with both axial and radial movement. In Eq's.3.1-3.9, the only model parameter that has to be tuned to predict the load force at the surface is the friction factor.

3.2.2. Model to estimate the force at the deadline

It is vital to distinguish between the force acting on the top of the drill string and hookload measurement at the deadline. Typically, the hookload measurement was performed relatively far away from the top of the drill string, as shown in Fig. 3-1.

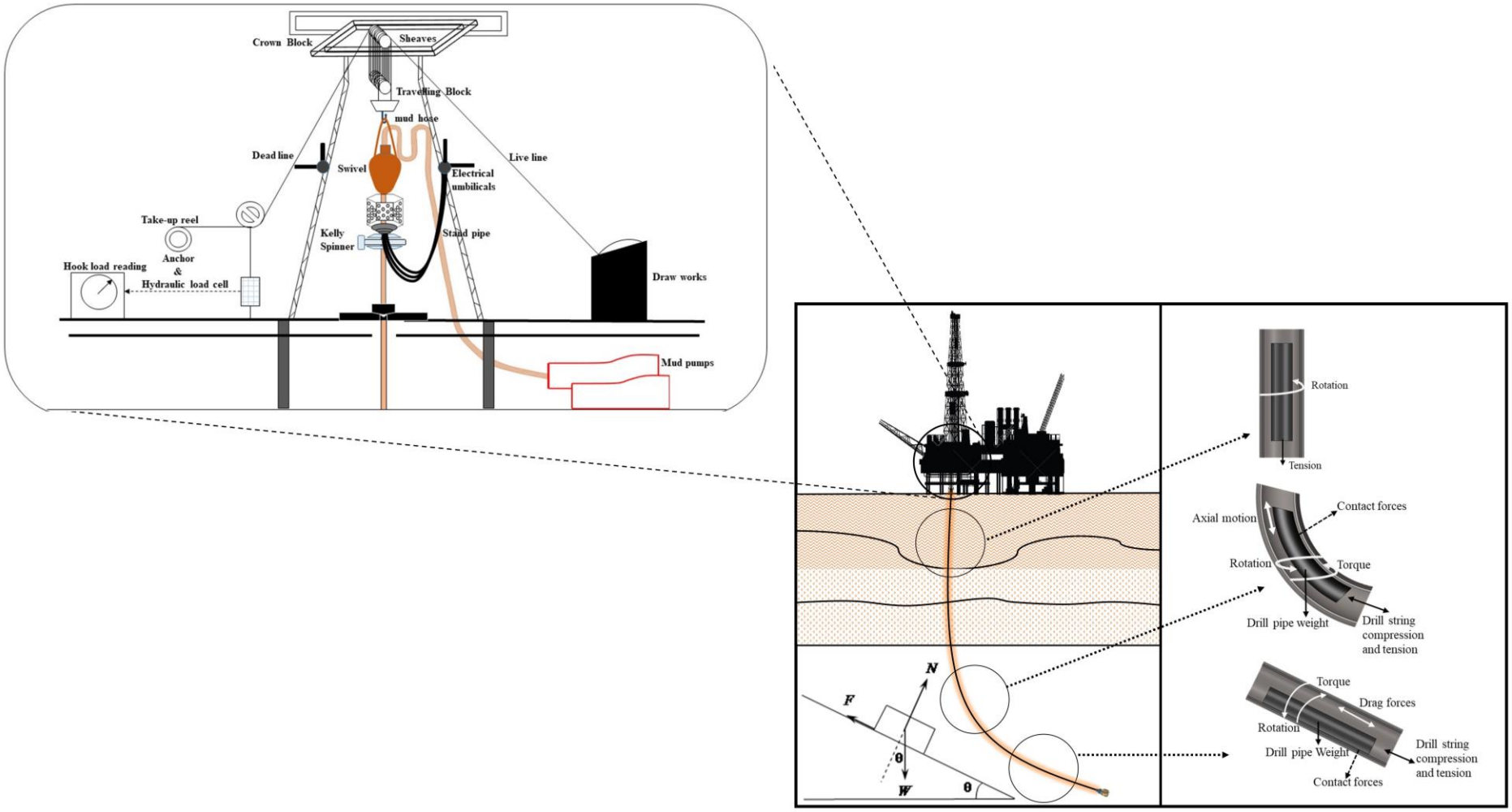

Fig. 3-1. Schematic of block and tackle system

Depending on the location of the hookload measurement, there will be additional physical singularities that interfere with the system, such as frictional forces between the drilling lines and sheaves and the number of drilling lines. Therefore, the sheave friction corrections are incorporated into Aadnoy's 3D friction model (Luke & Juvkam-Wold, 1993) and are based on Eq.3.10 and Eq.3.11.

The hook load acting at the deadline when raising the drill string

$$W_r = \frac{n(E_s - 1)(W_{hr} + W_{block})}{\left(1 - \frac{1}{E_s{}^n}\right)} \tag{3.10}$$

The hook load acting at the deadline while lowering the drill string

$$W_r = \frac{n(1 - E_s)(W_{hl} + W_{block})}{E_s\left(1 - E_s{}^n\right)} \tag{3.11}$$

In addition to sheave friction correction, there are numerous physical phenomena and uncertainties that affect the accuracy of the hookload measurement. Further, to explain these uncertainties in brief, actual drilling data from one of the ONGC wells is chosen and depicted in Fig. 3-2, where the wellbore is drilled from a total depth of 3334.01 m to 3371 m. The total depth signifies one complete stand of drill pipe, and the remaining depth belongs to the next consecutive stand. This section of drilling was spud on auto-drilling mode, and that will maintain optimum drilling conditions, i.e., constant ROP was maintained. As the drilling progress, the hookload started to decrease while moving the block from top to bottom (approximately 30 m), and similar variations can be clearly observed in the surface weight on bit (SWOB), and it was changed from 13.8 tonnes (block at the bottom) to 11.5 tonnes (block at the top) (refer track 6, Fig. 3-2). Such variation in hookload may be due to either (1) gradual change in formation strength along with the depth, (2) variation of self-weight of surface equipment, and (3) variation in the efficiency of a block and tackle system and its associated components.

The gradual change in formation strength can be included in equations using formation data. Similarly, the self-weight of the block & tackle system and its associated components can be captured using appropriate model equations. Further, the sheave efficiency term will provide additional hook load generated by the sheave system;

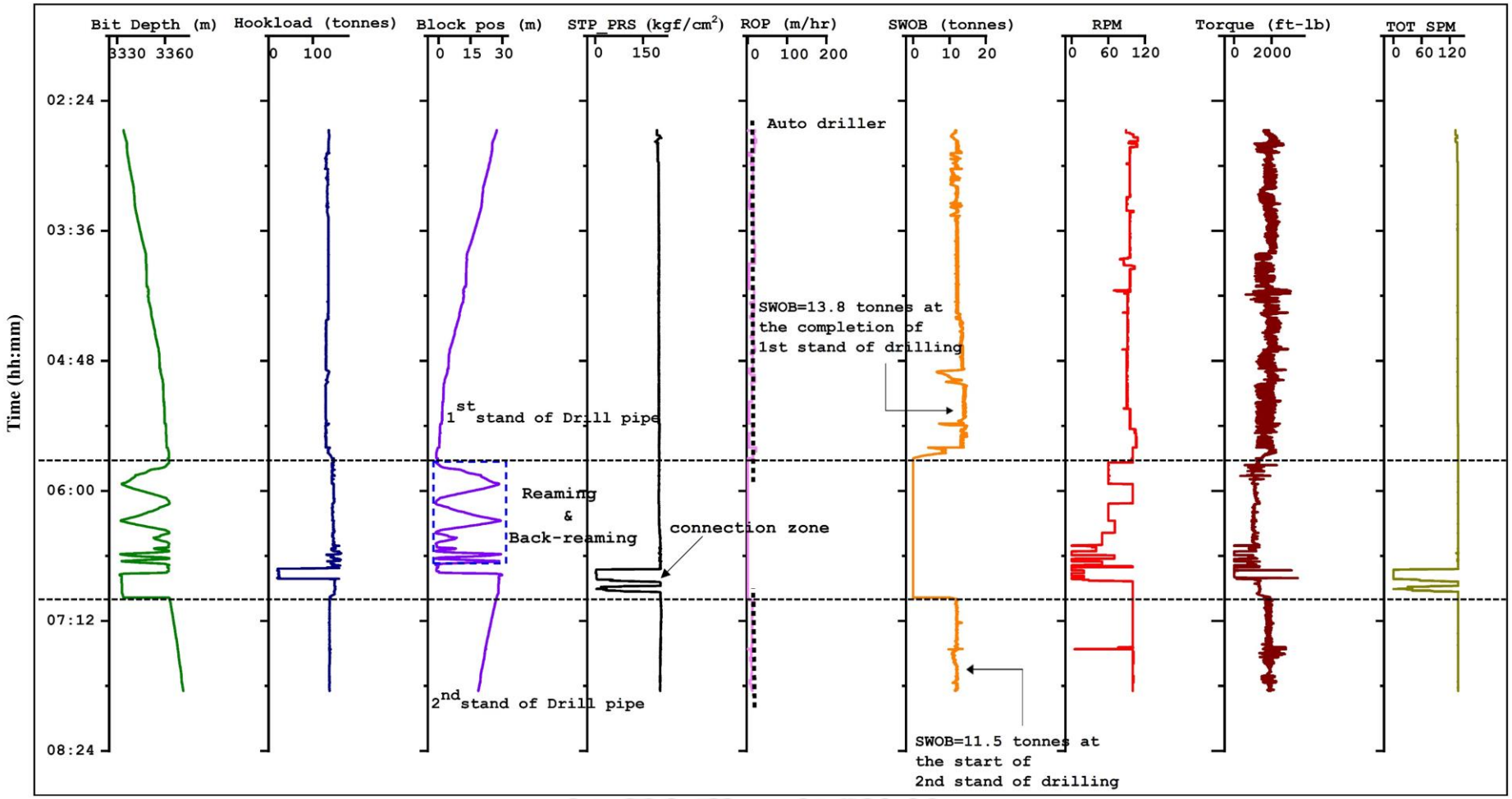

Fig. 3-2. Illustration of hookload variation during auto operator function mode

similarly, the weight parameter is introduced to include extra hook load contributed by other mechanical and electrical components present in between drill string and deadline.

While drilling, many other uncertainties may introduce different hook load components. For example, (i) the weight of the drilling lines has a considerable effect on the measurements made at the deadline, and it is expected to vary based on drilling requirements (Eric et al., 2015), (ii) traveling block may tilt from its normal position during dolly retracing, and there might be an alignment issue (refer Fig. 3-3 (a)), (iii) The tilting of the traveling block due to the difference in the tensional forces between the sheaves (refer Fig. 3-3 (b)) and (iv) pulley efficiency might deteriorate due to stick-slip condition. In this study, to include this uncertainty factor in load acting at the deadline, the Rig Uncertainty Compensation factor (RUC) is introduced. This factor is expected to vary for each rig, and it has to be estimated using actual drilling data. Therefore, to estimate the theoretical hookload at the deadline, the proposed model in this work requires the relationship between the force at the drill string pivotal position and the hookload reading at the deadline. And such a relationship requires the following three parameters: weight parameter, sheave efficiency, and RUC factor.

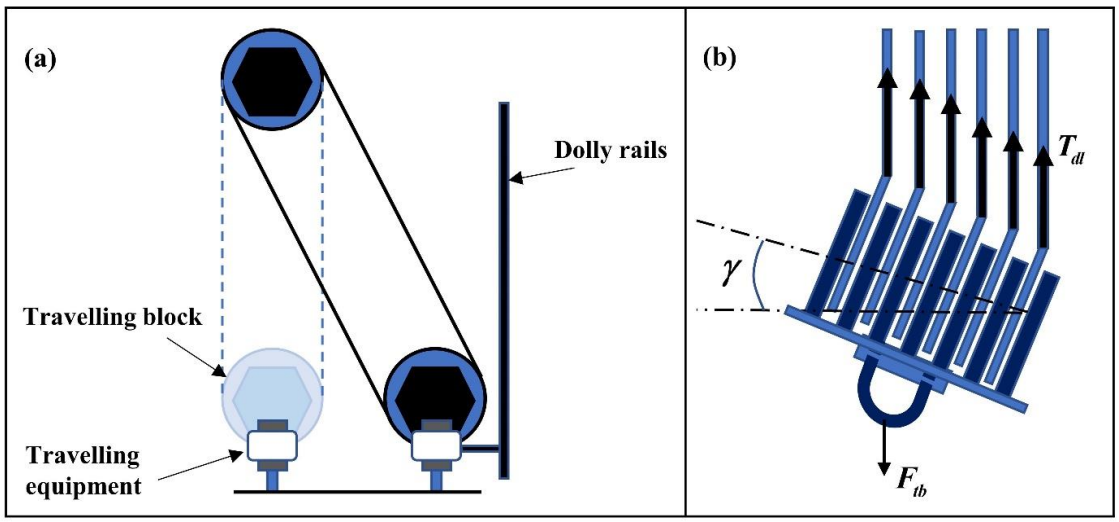

Fig. 3-3. (a) Depiction of travelling block misalignment, (b) Tilting of travelling block

The final hookload acting at the deadline during drilling operation is computed considering the Eq.3.12.

$$W_r = \left(\left(\frac{n\left(1-E_s\right)}{E_s\left(1-E_s^{\,n}\right)} \right) \left(W_{hl} + W_{block} + \lambda_{bp}.x + RUC \right) \right) \tag{3.12}$$

The above-described model equation has following model parameters: sheave efficiency (E_s), global friction factor (μ), weight parameter (λ_{bp}), and RUC factor (for one complete stand of drilling). These parameters need to be back-calculated from the existing real-time drilling data to determine the physical wellbore and rig conditions. The residuals between predicted hookload and actual hookload are minimized by tuning model parameters. The tuned parameters are initially utilized to determine a neutral point of a drill string. During the actual drilling activity, the neutral point may vary due to changes in frictional drag, pressure losses, weight on the bit, and other relevant factors. As the model has to process the parameters in real-time, assuming that the sheave efficiency, global friction factor, weight parameter, and RUC factor does not change, incremental tensile load from the neutral point is cumulatively summed up to determine the hookload at the deadline. However, the historical information of at least one stand of drilling data is needed for the model to obtain actual wellbore and rig parameters. And the developed model only considers all the uncertainties pertained to rigs that are equipped with top-drive systems.

3.3. Data input, pre-processing and system overview

The model type is distinguished to be 2-D or 3-D based on the well trajectory. The 2-D model is selected in the case where the well survey was made in a single plane (i.e., negligible azimuth angle). In this study, the 3D model is considered as the directional survey includes both inclination angle and geographical azimuth. Both 2D and 3D models are expected to provide a similar prediction for hookload (Elgibaly et al., 2017). For estimating the hookload, using the above-used model equations requires listed parameters in Table 3-1.

Table 3-1. Input data requirement to the hookload model

Time series and static data	Input data
Real-time rig sensor data	• Hookload (Tonnes) • WOB (Tonnes) • ROP (m/hr) • ROT-SPEED (rpm) • TOT-SPM (Strokes per min) • TOT-DEP (m) • BIT-DEP (m) • Block position (m)
Mud properties	• Mud weight (ppg)
Directional Survey	• Inclination (deg) • Azimuth (deg) • TVD (m) • BIT-DEP (m)
BHA details	• Unit weight (lb./ft) • Length (m) • Count (Nos) • ID (inch) • OD (inch)
Rig specifications	• No of rope lines • Drive system (Kelly or top-drive system) • Block weight (Tonnes)

3.3.1. Decision support system architecture

The following steps describe the architecture of DSS (refer Fig. 3-4):

1. Both the static data and time series data are stored in the MS-SQL database.
2. Time series data (rig-sensor) is retrieved from the database, and drilling data is segregated in the data pre-processing module and again sends back the pro-processed data to the database.
3. Both the static data and pre-processed data are fetched from the MS-SQL database to calculate neutral point and hookload at the deadline.
4. The calculated hookload and neutral point are stored back in the database.
5. The logics for alarm generation was executed in real-time. Threshold values for alarm were updated in the database using a user interface developed in python.

6. The alarm flags are generated using a Python application, and model outputs are displayed by means of a web application (i.e., CSS, HTML).

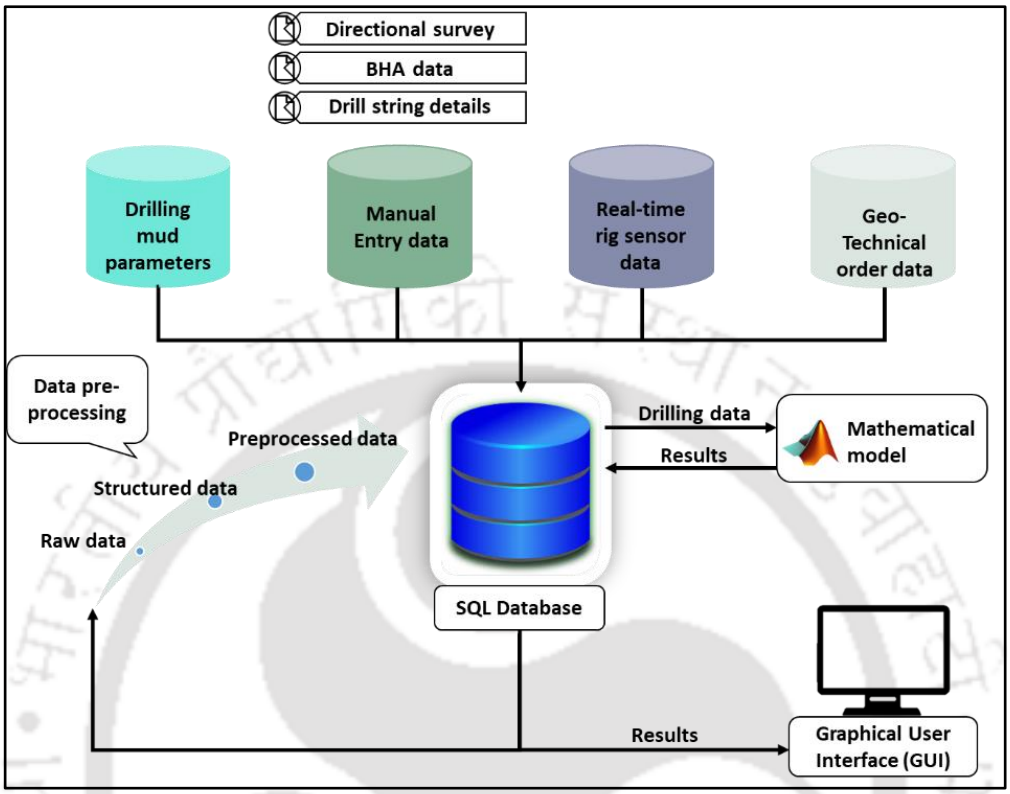

Fig. 3-4. Decision support system (DSS) architecture

3.3.2. Data types and frequency

The availability of more rig sensors and its connectivity with real-time SCADA at the rig site will allow the operator to better interpret the downhole conditions. The common problems identified with data collection were that the data's type, frequency, and quality were not consistent from time to time and well to well. The number of online measurements coming into the WITSML server might even range up to 50. However, for hookload analysis, the below-listed measurements are chosen. They can be categorized into static and time-series data (refer to Table 3-2). For example, static data relates to laboratory data, daily progress reports (DPR), including inside and outside diameters of the drill string, geotechnical order, and other geometrical information. Time series data is collected in frequent intervals, and static data will vary with different drilling sections and expert knowledge. For example, as shown in Fig. 3-2, the streaming time series sensor measured data is observed at the rate of one data point per 7.2 s (0.138 Hz) frequency.

The method and corresponding system of equations to be solved will be varying with respect to the type of drilling operation. The following below listed rules are utilized to identify the rotary drilling operation:

- HOOKLOAD (Tonnes) > 0
- TOT-SPM > 0
- WOB (Tonnes) > 0
- ROT-SPEED (RPM) > 0
- ROP (m/hr) > 0
- BIT-DEP (m) > 0
- BIT-DEP (m) > 0
- 0.25 > (TOT-DEP (m) – BIT-DEP (m)) >= 0

Table 3-2: Depiction of Static data and Time-series data

Static data	Time series data
Daily drilling mud reports	Rig sensor data (SCADA)
Geotechnical order	Directional survey data
Daily progress reports (DPR)	MWD data

Fig. 3-2 shows the output of the high-frequency rotary drilling data after filtering utilizing the above-mentioned rules. Fig. 3-2, Tracks 1-9 (from left to right) are recorded rig sensor measurements such as bit depth, hookload, block position, standpipe pressure, ROP, WOB. In track-1, the bit depth tends to increase, track-5,6 shows a positive rate of penetration and weight to the bit, track 7-9 represents the drill string RPM, generated torque, and total mud flow rate (TOT-SPM), respectively depicting a drilling operation.

3.4. Implementation procedure

The methodology and computational algorithm utilized for estimating the hookload at the deadline and neutral point can be summarized as follows (refer Fig. 3-5):

1. The real-time sensor data obtained is checked for validity, which includes (but not limited to) rules such as:
    - Hookload within prescribed bounds
    - WOB above threshold

- ROP/ROT-SPEED being non-zero
- Total depth and bit depth are closer/nearer
- Mud flow rate (TOT-SPM) being non-zero

2. After data validity check, the real-time data and history data (latest rig sensor data) is utilized to identify the drilling activity (refer to section 3.3.2)
3. Once the activity is confirmed as drilling and data validity is asserted, hookload estimation is initiated. The hookload estimation doesn't work if the activity is not recognized as drilling or if the data validity cannot be asserted.
4. In the hookload estimation process, the following data is retrieved from the database:
    - BHA details
    - Directional survey data
    - Rig specification information
    - Mud properties
5. Using the above retrieved data and real-time rig sensor data, the neutral point of the drill string is calculated.
6. Then, using the Aadnoy model (refer to section 3.2.1), the calculated load force will indicate the load acting at the top of the drill string. Further, the load force computed at the top of the drill string is modified to accommodate the variation from the measurement made at the deadline to estimate the hookload (refer to section 3.2.2).
7. The above computed neutral point and hookload at the deadline are then employed for further analysis, like identifying risky drilling when the neutral point crosses BHA and enters the drill pipe region, or abnormal hookload deviation, which might indicate a probability of stuck up, drill string parting and other related issues.

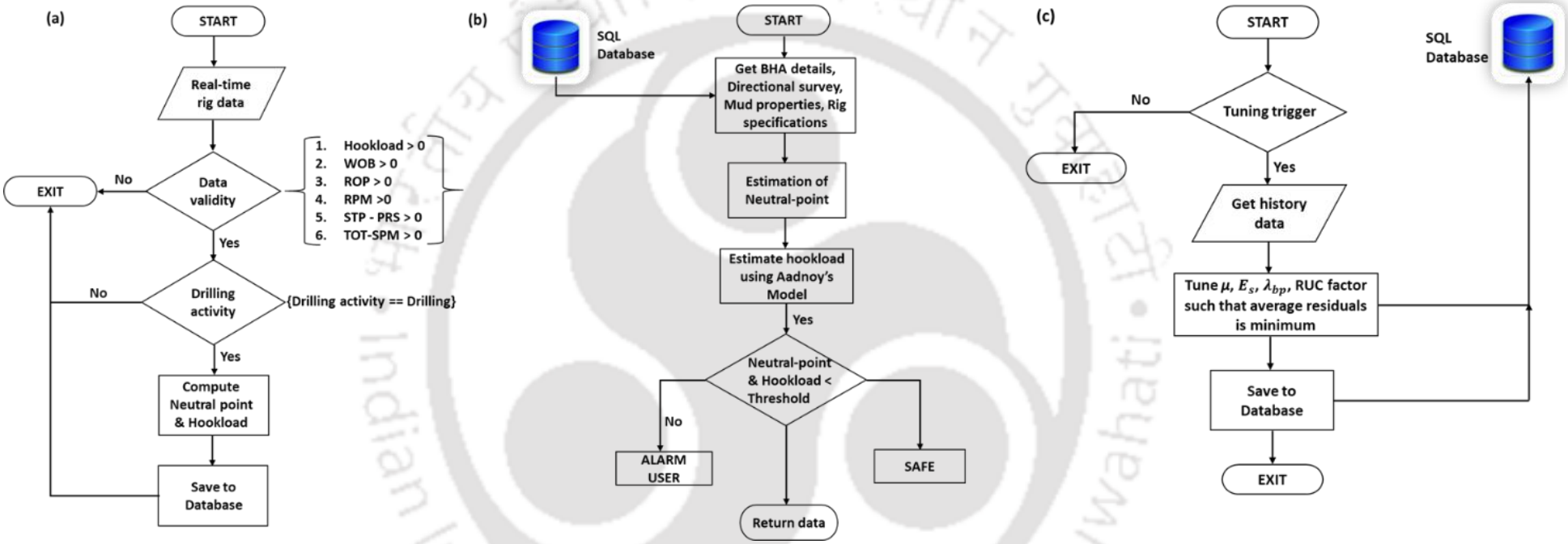

Fig. 3-5. (a) Module overview, (b) Neutral-point and hookload estimation workflow, (c) Real-time tuning module

3.5. Results and discussions

3.5.1. Case study 1: Vertical well monitoring

The presented case study of well-A was drilled in the north-eastern parts of India. The well-A is an exploratory well of vertical profile. The drilling is terminated at 4960 m as the objective was covered against the planned target depth of 5000 m. The drilling rig has a hoisting capacity of 250 tonnes and a top drive torque of 50000 lb-ft. The water-based mud system was used for the complete section of drilling. In general, hydrocarbon exploration in exploratory wells is associated with a number of uncertainties. The wellbore and casing information was given in Table 3-3, and as shown in Fig. 3-6 (a), The first phase of drilling with 26" drill bit is done up to 405 m followed by 20” casing and cementing. The next phase of drilling started with a lowering of 17 ½" TCR bit. The hole was cleared down to 405 m by drilling cement shoe of the previous casing. The drilling of 17 ½" open-hole section consumed a lot of time due to wellbore and auxiliary equipment complications, which led to high non-productive time. Drilling of fresh formation started from 405 m and drilled down to 1371 m as per the GTO plan.

The bit was changed after pulling out of the hole and, while lowering the PDC bit, observed held up at 750 m. Held up was cleared and drilled down to 1772 m. At this depth, a 568.93 psi pressure drop was observed. After pulling out of the string, fish of 19.23 m was found left in the hole (fish details: crossover + 2 singles of 8" DC + bit sub + drill bit), and the fish top is at 1752.77 m. Lowered 13 3/8" casing with centering device + 6 5/8" bit sub, engaged and recovered the complete fish. Then drilling was resumed, and the well was drilled down to 2550 m. Logging tools were run in, and GR-CAL-SP-DLL-MSFL-BCS-IS logs were recorded from 297 m to 2555 m. Then 13 3/8" casing was lowered down to 1176.5 m. Held up was observed while lowering the 100th joint. Subsequently, the casing got stuck in the hole. Moreover, the stuck casing could not be released even after working on the string and spotting high-speed diesel (HSD). After backing off, 32 singles of 13 3/8" casing were pulled out of the hole. In this situation, 67 casing pipes had still remained in the hole as fish and fish top was at 377 m. Several efforts were made to recover the fish, but all efforts went in vain. While attempting to recover the fish, the drill string got disengaged from the kelly joint and fell in the hole (fish details: (kelly saver sub + 14 stands of left-handed drill pipes + cross over + spear).

Table 3-3. Wellbore and casing information of Well-A

Section			**1**			**2**			**3**	**4**
Casing Length	(m)		297			2547.8			4001.5	4969
Casing Diameter	OD (in)		20			13.375			9.625	5.5
	ID (in)		19.124			12.715			8.755	5.044
Drill Collars (DC)	Section of DC	DC 2	DC 2	DC 1	DC 2		DC 1	DC 2	DC 1	DC 1
size	OD (in)	6.5	8	9.5	6.5		8	6.5	8	6.5
	ID (in)	2.813	2.813	3	2.813		2.813	2.813	2.813	2.813
	Length (m)	56	28	28	108		56	108	56	154
Drill Pipe	OD		5			5			5	5
	ID		4.777			4.276			4.276	4.276
	Unit Wt. (lb/ft.)		19.5			19.5			19.5	19.5
Drill bit Diameter	(in)		26			17.5			12.25	8.5

This fish was recovered completely. As the remaining fish of casing could not be recovered, the diverter tool was lowered and placed bottom cement plug from 415 m to 470 m followed by top cement plug from 290 m to 370 m. After waiting on cement, bit and BHA were made up and lowered. The cement top was tagged at 242 m. As depicted in Fig. 3-6 (b), the string was pulled out after drilling cement down to 303 m, and directional assembly was lowered for side-tracking the well. The well was side-tracked from 303 m to 436 m. The string was pulled out along directional assembly. The drill string was lowered without directional assembly; drilling was resumed, and the 17 ½" section was side-tracked/drilled down. Thus, to discern the performance of the developed model in offline mode, the same section of wellbore was selected for post-analysis.

The complete bottom hole assembly (BHA) configuration is tabulated in Table 3-4. As the well profile is near vertical, the BHA was not complex. To increase the BHA rigidity and minimize the wellbore deviation, a new BHA 16 ¾" stabilizer was used for the 17 ½" section. The following assumptions were considered to validate the accuracy of the model:

i. The wellbore was ideally vertical with a minimal constant inclination
ii. The side forces were quite negligible as it is a near-vertical wellbore
iii. There is a complete transfer of weight to the drill bit

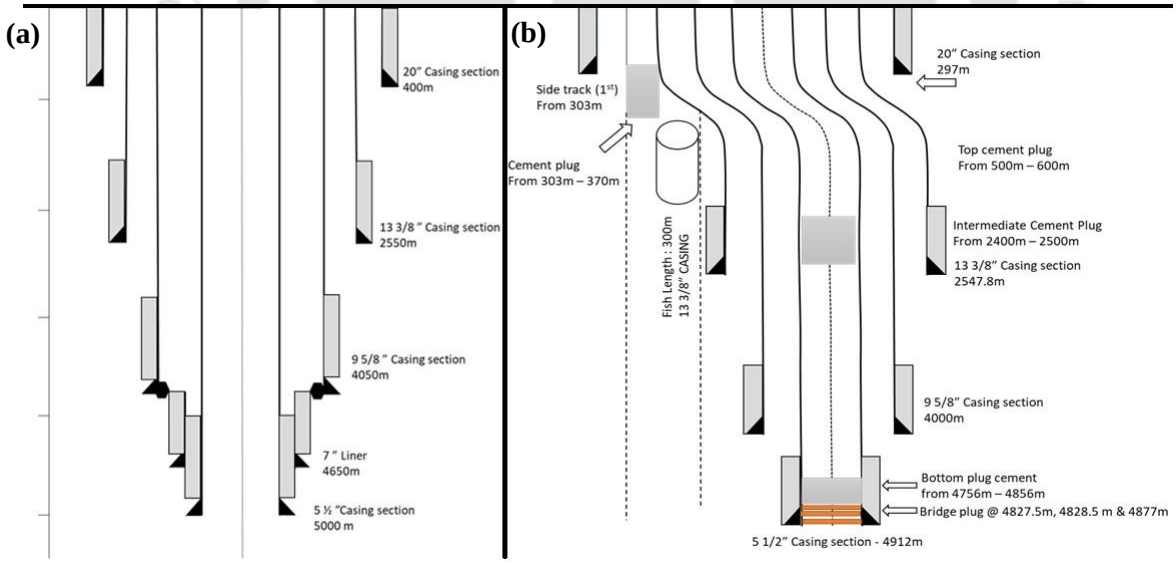

Fig. 3-6. (a) Planned depth and casing profile as per Geo-Technical Order (GTO) (b) Actual on-field well casing profile after side-tracking

Table 3-4. BHA specifications utilized in 17 ½" hole section of Well-A (Vertical)

Description	Count	Fish Neck		OD	ID	Unit Weight	Length	Accumulated
		OD	Length			(lb./ft)	(m)	Length
PDC BIT	1			17 ½	N.A.		0.45	0.45
BITSUB	1						0.48	0.93
SGL 8" Drill Collar	2			8	2.813	148.01	17.75	18.68
8" STABILIZER	1	8	0.48	8	3	138	2.2	20.88
SGL 8" Drill Collar	4			8	2.813	148.01	36.06	56.94
X-Over							0.5	57.44
SGL 6 ½" Drill Collar	9	6 ½	N/A	6 ½	2.813	91.6	82.65	140.09
X-Over	1						0.5	140.59
SGL 5" HWDP	6		N/A	5	3	42.7	56.16	196.75

3.5.1.1. Parameter sensitivity analysis

Sensitivity analysis is performed to determine the considerable influence of the input parameters on the model behavior and signify upper and lower bounds of the selected model parameters (Wang et al., 2012). In this section, the sensitivity analysis was performed to investigate the uncertainty in output hook load reading with change in the input parameters (refer to Fig. 3-7). The hookload is highly sensitive with respect to the sheave efficiency (E_s) of the block and tackle system. Lower sheave efficiencies of the block and tackle system project higher hookload reading than the actual hookload acting at the deadline. Similarly, in directional wellbores, the hookload increases with an increase in friction factor (μ). However, due to the low rate of penetration (ROP) and revolutions per minute (RPM), the resultant angle between the axial and tangential velocity is low (refer to Eq.3.7). Therefore, for a specific rig configuration, the friction factor effect seems to be nullified and doesn't have much influence on the hookload. Further, the study was conducted with the novel rig uncertainty compensation (RUC) factor. The RUC factor is the most sensitive parameter for hookload determination. It implies that the rig uncertainties are essential to be considered to have a precise estimation. Likewise, the hookload is sensitive to the weight parameter (λ_{bp}), as the load keeps varying for each stand of drilling. It might be due to tilting of traveling block, the effect of drilling lines weight, and other possible uncertainties that may arise from hookload components (refer to section 3.2.2).

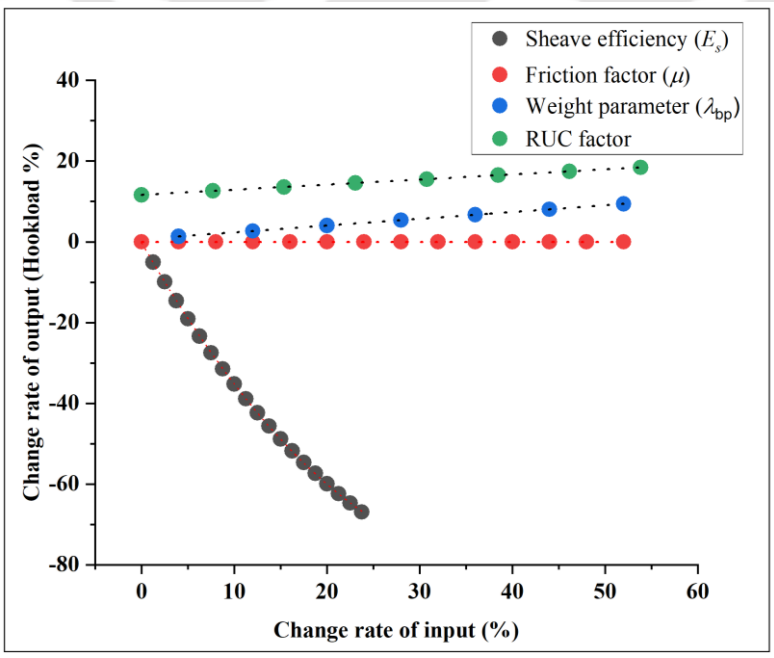

Fig. 3-7. Sensitivity analysis of key input parameters

3.5.1.2. Model validation

The friction factor is assumed to be constant over the entire wellbore length during drilling (Kucs et al., 2008). Likewise, the sheave efficiency, weight parameter, RUC factor, and global friction factor are assumed to be constant over a certain length of the wellbore for simulation of the hookload curves. And it is decided on a case-by-case basis, and it may vary with respect to the type of the well plan, casing design, type of well, and other wellbore and formation parameters. The model performance was evaluated by utilizing on-bottom drilling data. After several trials, the hookload pattern was observed to be similar for each drilling stand (refer to Fig. 3-8). Therefore, at least one stand of drilling data is required to train the model, another stand of drilling for model validation and optimized model parameters are utilized for further prediction. Moreover, the prediction can be performed until the operator observes a significant deviation in hookload or whenever the operator wants to train the model again.

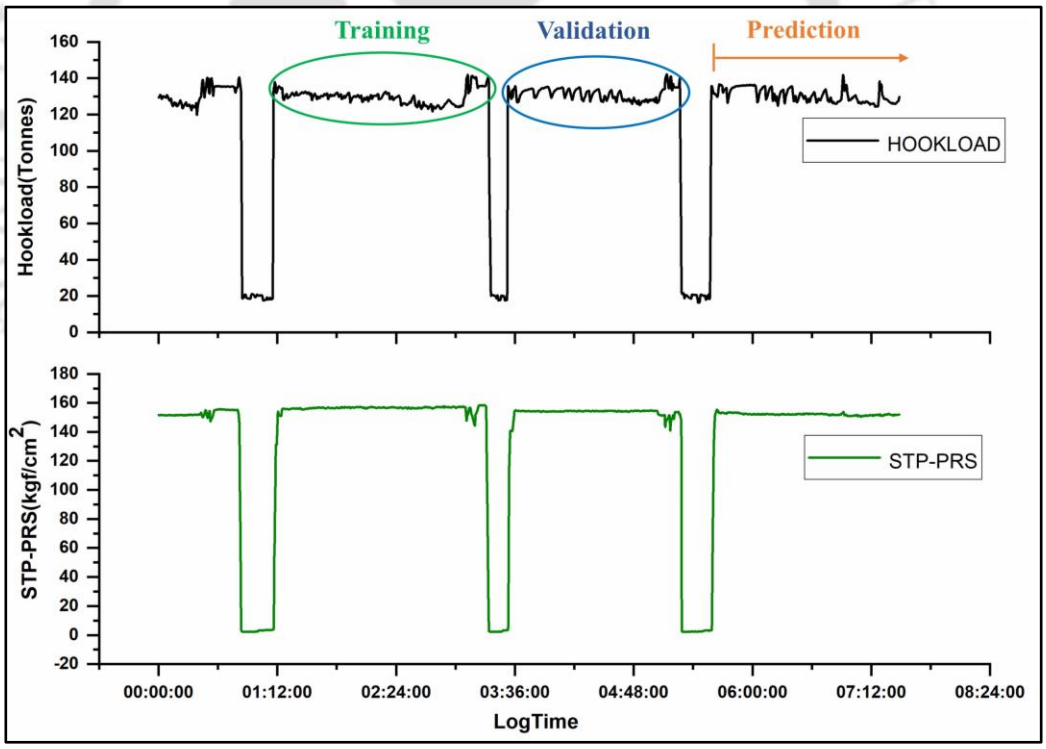

Fig. 3-8. Illustration of training, validation, and prediction during drilling activity

The developed mathematical model utilizes the model parameters (refer to Table 3-5) to predict the hookload at the deadline during the normal rotary drilling operation. Both the estimated and actual hookload follow a similar variation in trend, but the estimated hookload falls much below the actual hookload. The average residuals (E) between the

actual hookload and predicted hookload is expressed in terms of percentage (refer to Eq.3.13) and was found to be 25.37 % using nominal values of the key model parameters. Therefore, for calibration of hookload, an approximate one complete stand of drilling data was taken for tuning the model parameters to fit the chosen rig and wellbore conditions.

Table 3-5. Input model parameters

Model Parameters	Nominal value	Lower bound	Upper bound
RUC factor (tonnes)	12.5	0	30
Friction Factor (for water-based mud)	0.30	0.25	0.40
Weight parameter (tonnes/meter) $(\boldsymbol{\lambda_{bp}})$	0.015	0	3
Sheave Efficiency $(\boldsymbol{E_s})$	0.94	0.80	0.99

$$E(\%) = \left(\frac{1}{n} \sum_{i=1}^{n} \left| \frac{HL_{act} - HL_{est}}{HL_{act}} \right| \right) \times 100 \tag{3.13}$$

The calibration is performed by minimizing the average residuals between the actual hookload and predicted hookload, and it is considerably reduced to 0.9% for the same depicted depth. Then, the test data set for 2 hrs of drilling data is chosen to evaluate the model performance. The average residuals between the actual and estimated hookload were found to be 0.78%. Under normal drilling conditions, the model predictions are in good agreement with the actual hookload. Therefore, to further evaluate the performance of the model, abnormal drilling data is chosen where the well experienced downhole complications. The tuned model parameters are further chosen to predict the hookload at the deadline during drilling.

As shown in Fig. 3-9, Zone A, the drill string marginally confronted a sudden deviation of 5.64 tonnes hookload starting from 1633.7 m. The standpipe pressure starts shooting up without a change in flow rate, which may be due to kick, pack off, inadequate hole cleaning, obstruction to mudflow, or simply a mud pump problem. The mud pumps were shut down as continuous pumping might have severe complications as per the standard operating procedures. The operator tried to reciprocate the string with a low mud flow rate for dislodging the packed cuttings. The drill string was run in the back, followed by proper conditioning and circulation (C&C). As depicted in zone B, the reciprocation of

the string and mud circulation couldn't reduce the deviation of hookload and further steering towards problem intensification. Proper mud-circulation and conditioning with wiper trip up to the casing shoe followed by reaming down might have reduced the aggravation of the situation. However, after reaching 1642.57 m, the hookload starts to slowly deviate much further in zone C even when the WOB is dropped down. The well condition was drastically reduced at this depth, leading to a complete pull-out of the string that increased non-productive time (NPT) and BHA change.

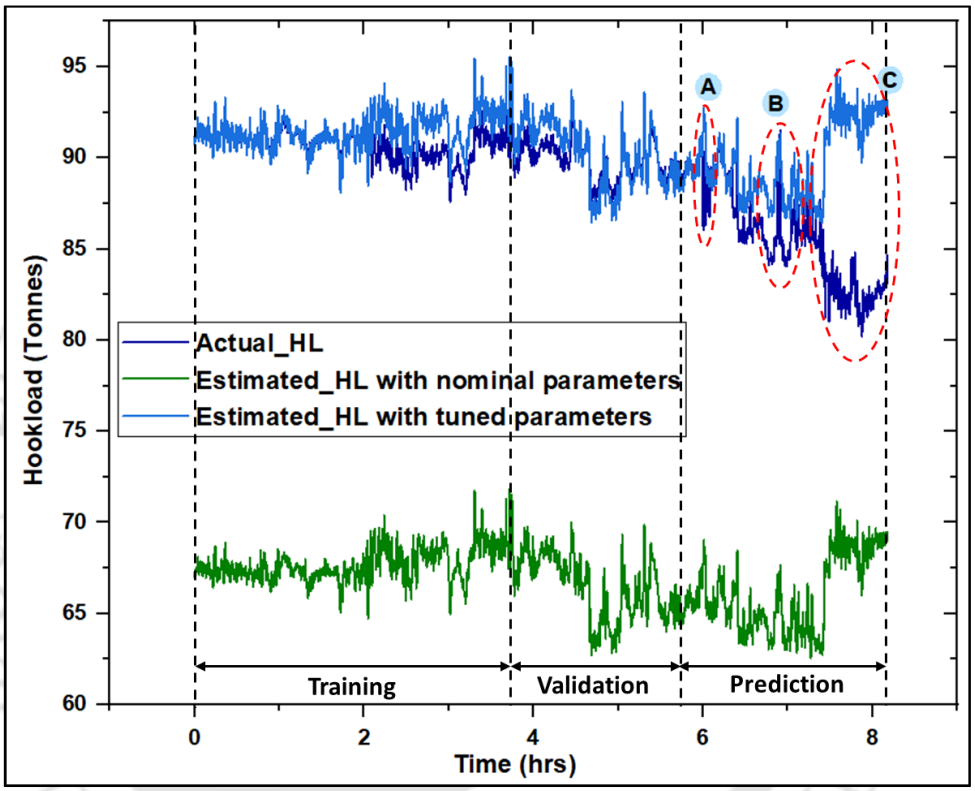

Fig. 3-9. Training, validation, and prediction of hookload

The actual and modeled hookload did not converge to desired or acceptable levels (± 2.5 tonnes). The crucial rig sensor measurements were monitored to confirm the anomaly, as shown in Fig. 3-10, which displayed abnormal behavior in the crucial rig sensor measurements. Fig. 3-10, Tracks 1-7 (from left to right) are real-time drilling parameters such as weight on bit, rate of penetration, standpipe pressure, total flow rate, hookload, rotational speed, and total depth. The RPM gradually drops down to 78 RPM, and ROP tends to be nearly zero even after the operator maintains a positive WOB. The standpipe pressure starts to shoot up to 177.91 kgf/cm^2 (2530.46 psi) even when the pumps are maintained at a constant flow rate.

The BHA got packed down in the cuttings, due to which the force acting at the top starts to drop down. The filter cake deposited on the loose unconsolidated formation might be insufficient, resulting in formation collapse, and the drill string would have packed off. Due to wellbore packing, the standpipe pressure (SPP) shoot up was observed. Even if the weight on bit was available, the ROP decreased gradually to minimal which indicates BHA was packed and bridged with conglomerates and due to which the force acting at the top of the drill string dropped down as described in Track 5, Fig. 3-10. In addition to hole packing, the wellbore was under-gauge, due to which the stabilizer got stalled down in the abrasive formation, and cuttings slowly accumulated, which worsened the situation. In the stated scenario, the model can be used to evaluate the situation and pre-warn in certain situations about upcoming problems.

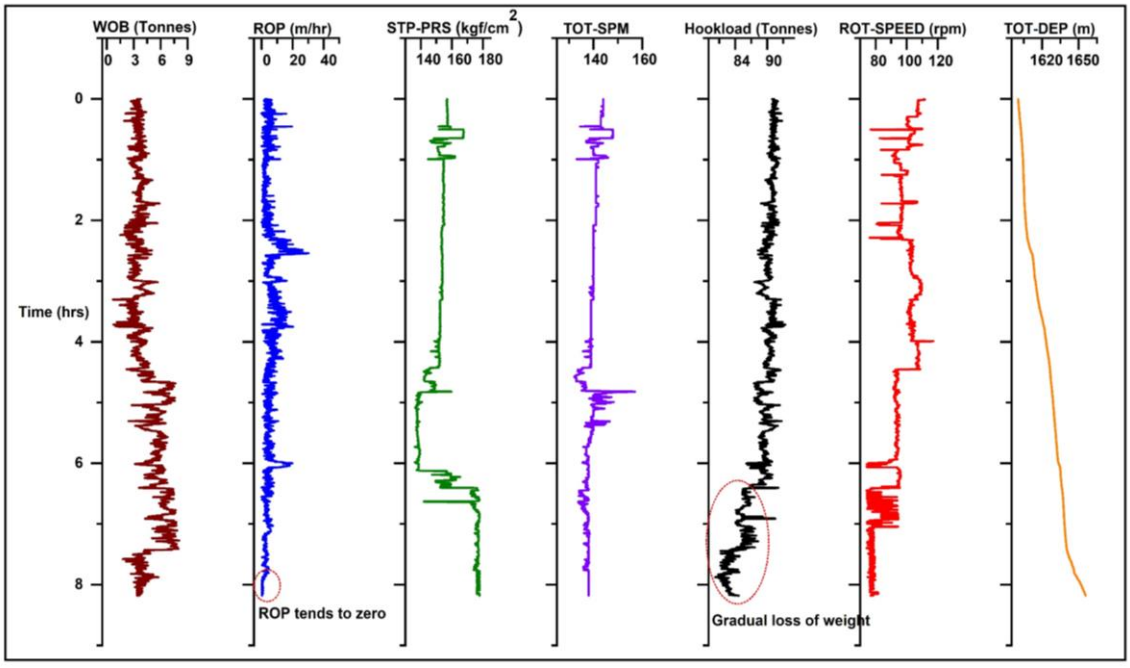

Fig. 3-10. Monitoring of secondary parameters for anomaly identification depicting hole pack-off and stabilizer stalling

The wellbore stability is caused by a combination of controllable and uncontrollable (natural) factors (Pašić et al., 2007). The operator has to consider all the above-mentioned circumstances, which might not be taken care of while planning the well. Proper mud weight, optimized BHA design, and controlled drilling parameters would make the drilling process much smoother.

Furthermore, during drilling, the drill string can be subjected to both tensional and compressive loads. The application of excessive WOB can cause the drill string to buckle and may probably fracture. Therefore, for safer drilling operation, the neutral point is calculated using data collected in real-time, as shown in Fig. 3-11. The DSS tool developed in this study can generate the alarm to the operator when the neutral point shifts near the drill pipe. As shown in Fig. 3-6 (a), the wellbore is near vertical, so the neutral point variation is directly proportional to the weight on bit and buoyancy factor and independent of inclination. The position of the neutral point with respect to depth is monitored and compared to the total BHA length. The weight on the bit applied by the operator is ideally low, and consequently, the neutral point lies in the drill collars. The DSS tool will generate the alarm to the operator if the neutral point crosses 85% of the BHA length (i.e., drill pipe length + 15% BHA length) as depicted in Fig. 3-11. In the case of harder formations, the operator tries to increase the ROP by increasing the WOB. Therefore, in these conditions, the DSS will suggest the operator take necessary actions to prevent buckling of the weakest component of the drill string (i.e., drill pipes).

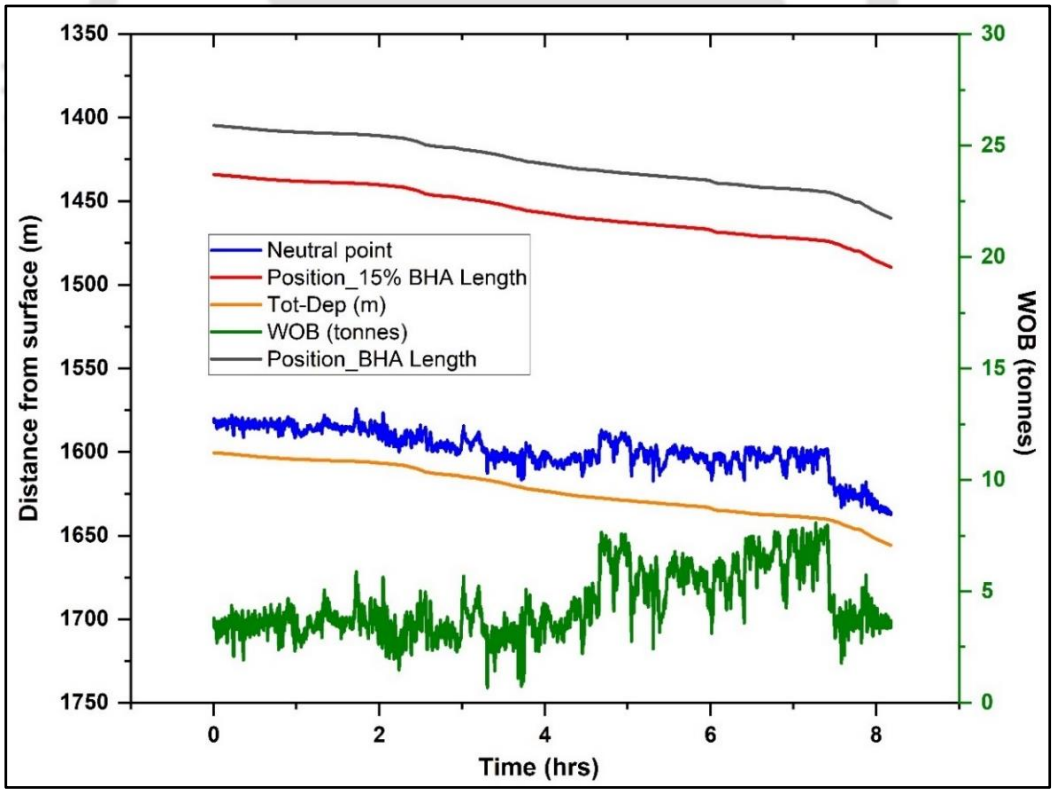

Fig. 3-11. Real-time monitoring of variation of the neutral point along the drill string

3.5.2. Case study 2: Real-time validation in directional Well-B

Unlike the vertical wellbores, the frictional forces represent an important interaction between the drill string and the wellbore in directional wells. Well-B is the directional well (refer to Fig. 3-12 (a)) with a proposed total target depth of 3752 m. The hookload variation is studied at deeper sections using Aadnoy's model for the said well-B. Water-based drilling fluid with a mud weight of 10.495 ppg was used for the considered depth range. The 12 ¼" section experienced a severe dogleg at 2410.79 m, and thereafter, the 8 ½" section (2800 m – 3256 m) was planned to drill with nominal doglegs.

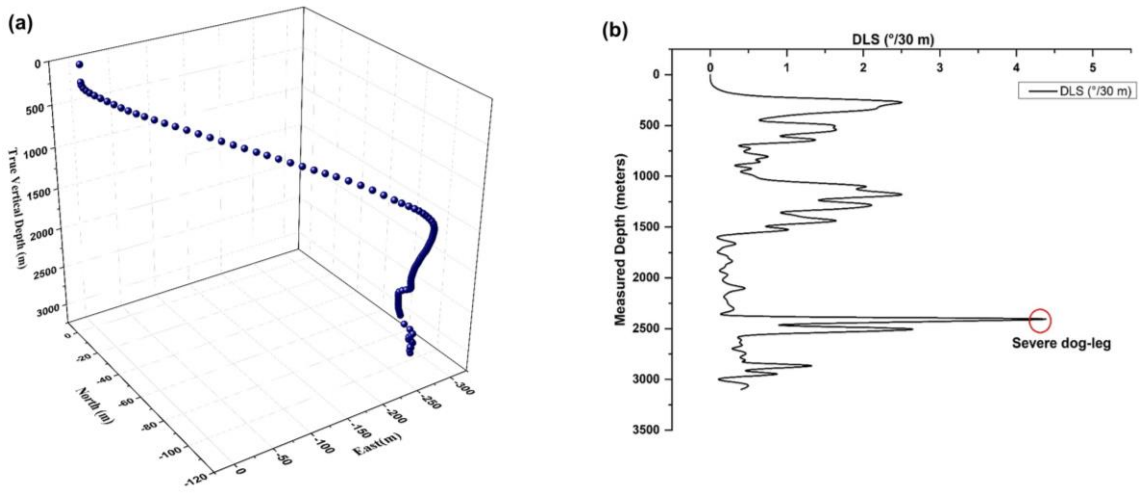

Fig. 3-12. (a) The 3D directional profile of Well – B (b) Dogleg severity profile with an increase in total depth

The BHA in the hole was run with a universal bottom-hole orientation sub (UBHO) to provide fluid flow control at the bottom of the drill string and prevent the cuttings from blocking the drill bit jets. A non-magnetic drill collar (NMDC) with an inbuilt MWD tool that comprises a gamma-ray sensor to indicate the possibility of shale formation was a part of the BHA. The complete BHA configuration is listed in Table 3-6. The BHA is equipped with an 8 ½" PDC bit, and it is designed to avoid deviation from the planned directional survey and achieve optimized ROP and proper bit performance. As there is a possibility of stuck up in deep sections, a 6 ½" drilling jar is placed to release the stuck in the case of a stuck-up.

Table 3-6. BHA specifications of 8 ½" hole section of Well-B

Description	Count	Fish Neck		OD	ID	Unit Weight (lb./ft)	Length (m)	Accumulated Length (m)
		OD	Length					
PDC BIT	1	N/A	N/A	8 ½	N/A	147.19	0.27	0.27
BITSUB	1	6 ½	0.3	6 ¾	N/A	88.7	0.48	0.75
SGL 8" Drill Collar	2			8	2.813	148.01	17.75	18.50
8 " STABILIZER	1	8	0.48	8	3	138	2.2	20.70
SGL 8" Drill Collar	3			8	2.813	148.01	27.04	47.74
6 ½" UBHO	1	6 ½	0.79	6 ½	2 ¾	88.7	0.79	48.53
X-Over		6 ½	9.23	6 ½	3 ¼	88.7	9.23	57.76
SGL 6½" Drill Collar	9	6 ½	N/A	6 ½	2.813	91.6	82.65	140.99
X-Over	1	6 ½	0.43	6 ½	2.813	88.7	0.80	141.79
6 ½" jar	1	6 ½	0.43	6 ½	2.312	88.7	7.04	148.83
SGL 5 " HWDP	5		N/A	5	3	42.7	46.80	195.63

To accommodate the physical wellbore and rig conditions, the model is calibrated by tuning the model parameters for one complete stand of drilling (3053 m - 3082 m). The average residuals were found to be 0.09 % after calibration of hookload. Further, the tuned model parameters are utilized to validate the model performance for approximately two hours of drilling data, and the average residuals in percentage were found to be 1.01%. The global friction factor tends to be 0.39 as the well is tortuous with doglegs, as shown in Fig. 3-12 (b). The tuned model parameters are utilized to predict hookload for the rest of the drilling in the 8 ½" section of the wellbore. As depicted in Fig. 3-13, Zone A, the actual hookload starts deviating from 3092.84 m and gradually incurred a gain of nearly 4.001 tonnes, which provided the operator with an indication of a possible downhole anomaly. Since the wellbore is completely tortuous and had experienced severe doglegs in the previous section, the actual hookload is expected to vary drastically. The operator focused on key rig sensor parameters to keep them well in control by checking for possible anomalies (refer to Fig. 3-14). The ROP suddenly dropped to zero during positive weight on bit, and the remaining parameters didn't show any indications.

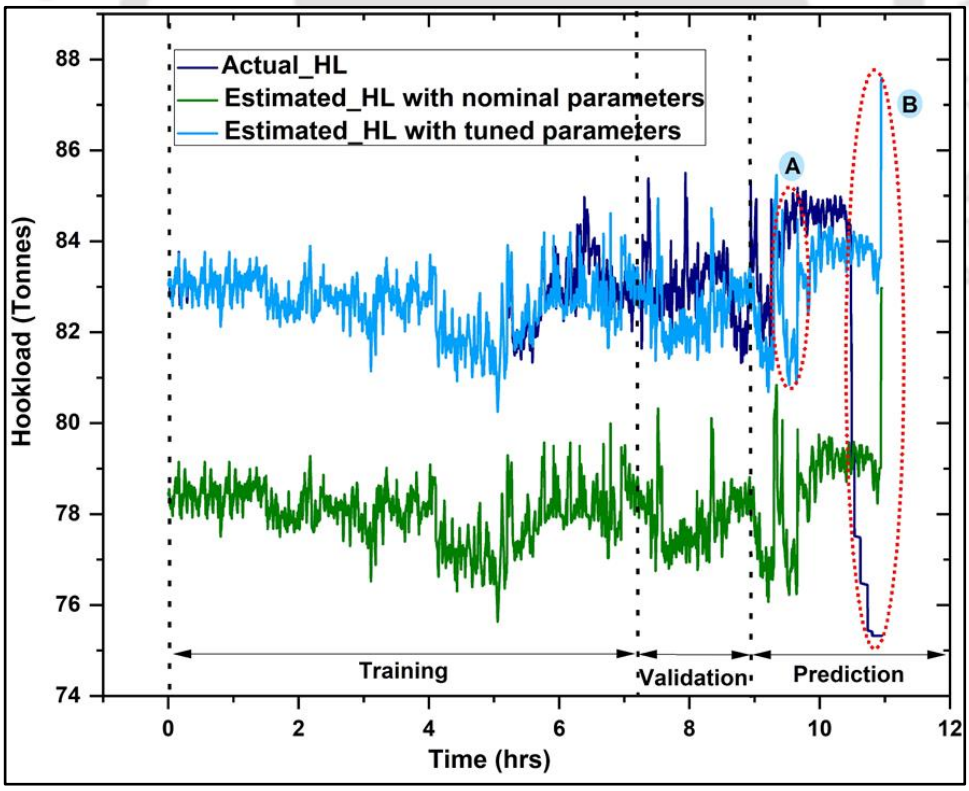

Fig. 3-13. Sudden deviation of hookload during field-testing in Well-B

Thereafter, the operator decided to pull out the drill string (as per SOP), to check the complete BHA and drill bit condition. However, either of them did not show up with any

breakdown or wear out. After proper gauging of the BHA, the drill string was run back to the total depth and drilling resumed. Further, the ROP started to increase and the variation in hook load was within the permissible limits. However, after reaching the depth of 3095.07 m, the ROP suddenly dropped down to zero, and the operator tried to increase the WOB to increase the ROP. As soon as the WOB started to increase, the drill string observed a sudden loss in standpipe pressure (729.65 psi) at a constant flow rate and it also incurred a weight loss of 9.09 tonnes, along with the drop in ROP (refer Fig. 3-14).

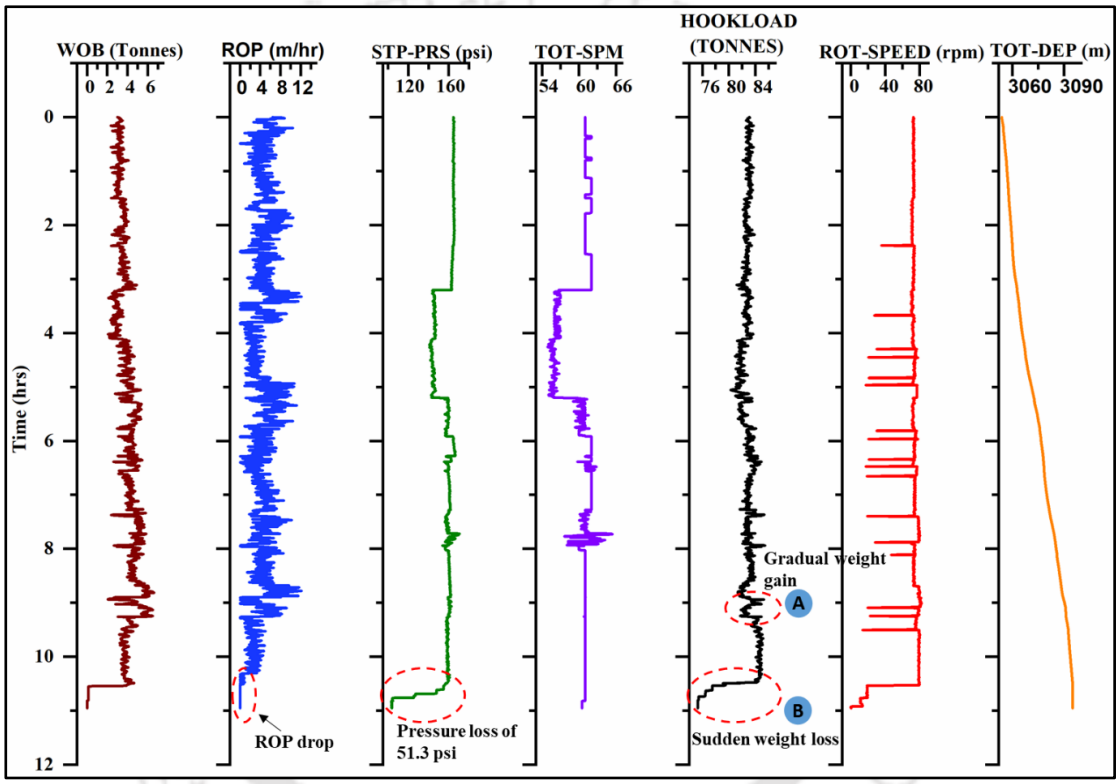

Fig. 3-14. Variation of secondary SCADA parameters indicating the occurrence of an anomaly during field testing

An abundant number of factors can lead to weight loss, including wellbore tortuosity, severe dogleg, unadorned stress zones, fatigue, and lack of life cycle estimation. And due to which the drill string might have bowed and eventually broken due to permanent damage. Additionally, pin joints take up more stress when compared to the complete section of the body, due to which the string might have sheared at the pin section. The hookload deviations were observed well in advance, indicating an upcoming downhole anomaly. Based on the variations in hookload, the operator would have chosen optimal

drilling parameters and followed many more precautions to avoid failure. Therefore, the test was considered to be successfully implemented in the real-time drilling activity.

Fig. 3-15 illustrates the variation of neutral point with a change in weight on bit and increase in total depth. Monitoring the variation of neutral point in the operator's console will alert the operator to take proper actions when there is a miscalculation in the required weight on bit due to tight time schedules and human errors. In directional wellbores, due to severe doglegs and tortuosities, the operator might increase the weight on the bit to achieve the optimal rate of penetration, and with an increase in weight on bit, the neutral point shifts upward near to the drill pipes. Moreover, in case the neutral point reaches 85% of the BHA, the DSS tool will alarm the situation to the operator, indicating the possibility of a neutral point shift into the drill pipes. Preventing the buckling event before it gets aggravated would save the wellbore a lot of time and cost.

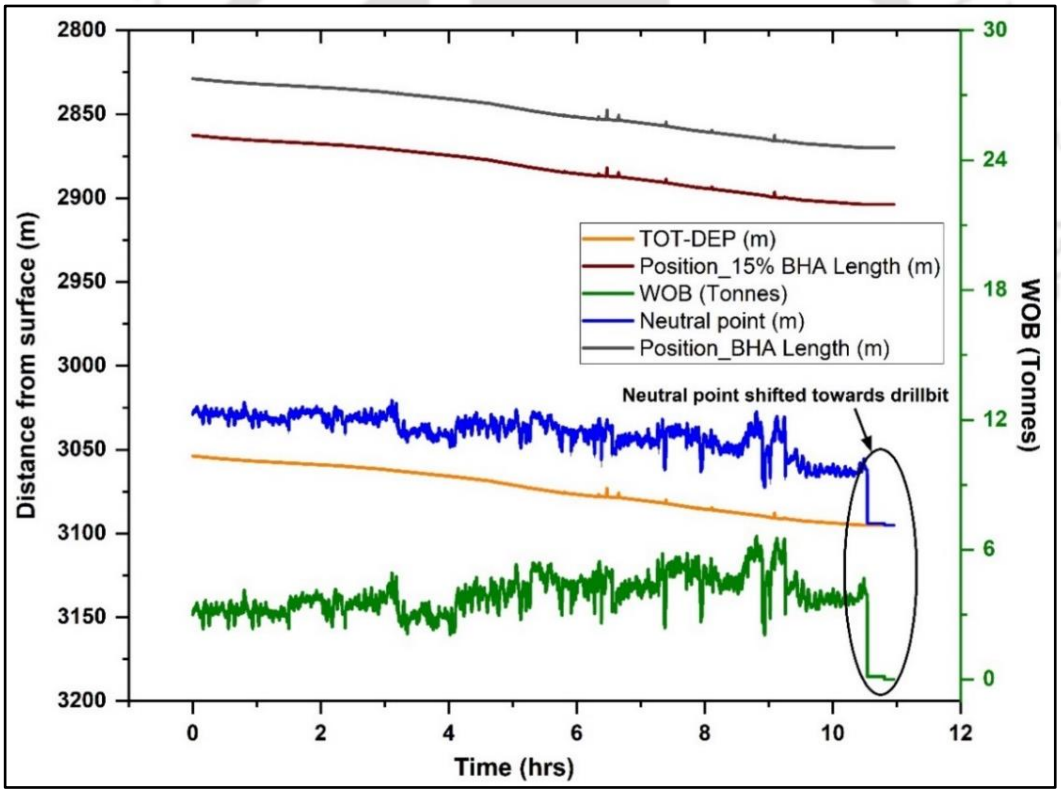

Fig. 3-15. Neutral point variation along the drill string in directional well (Well-B)

3.6. Challenges in real-time implementation

The challenges faced during real-time implementation are similar to the challenges faced by other automation industries. These includes:

1. Data pre-processing: Data pre-processing has been a daunting task in this current study. The streaming drilling information contains a lot of missing data, erroneous data, and quite many outliers. Most of the time has been consumed in improving the quality of data
2. Directional survey tool: Due to the non-utilization of gyroscopic and magnetic survey tools, the directional survey input is manually fed to the model every 30 m or 100 ft. To have accurate dynamic predictions from the model, the directional survey data from the MWD tool needs to be hinged to the SCADA system.
3. Decision expertise: The drilling engineers are responsible for the overall safety of the rig and the personnel, rig floor management, rig equipment maintenance, and environmental integrity. The work overload may preclude the operators from monitoring the overall rig sensor parameters. Human expertise also plays a key role in making vital decisions in the field.
4. Service agreement: For successful on-field implementation, the operator and service company teams should have a mutual understanding in terms of utilization of available data, training, and technical support.

3.7. Summary

This chapter introduces the development and deployment of a real-time hookload prediction model using actual wellbore parameters and tubular information. The presented hookload estimation technique at the deadline in real-time is superior to the conventional methods. The model performance is improved by including several uncertainties related to the complete rig structure affecting the hookload measurement. The DSS utilizes real-time rig sensor parameters in combination with a large body of drilling experience in quantifying the risk of upcoming downhole complications. To evaluate the model robustness, it was tested on both vertical and directional wellbores. The developed hookload model can be applied to the exploratory wells and can be utilized in developing countries where the potential of cost reduction drives the wells.

Chapter

4

CHAPTER 4
Evaluation of Structural Integrity of Tubulars in Directional Wellbores

Content in this chapter has been published in the following research articles:

- Viswanth Ramba, Senthil Selvaraju, Balakumara Vignesh Muppidathi, Senthilmurugan Subbiah, Muthukumar Palanisamy, “Evaluation of Structural Integrity of Tubulars in Directional Wellbores: A Case Study in North-Eastern Parts of India,” *Journal of Petroleum Science and Engineering*, P.P 109067-[2021], https://doi.org/10.1016/j.petrol.2021.109067
- Viswanth Ramba, Senthil Selvaraju, Senthilmurugan Subbiah, Muthukumar Palanisamy, Sanjay Kumar Gauba, Suresh Jandial, S. "Real-Time Evaluation of Structural Integrity of Tubulars in Directional Wellbores." *Proceedings of the ASME 2020 39th International Conference on Ocean, Offshore, and Arctic Engineering*. Volume 11: Petroleum Technology. Virtual, online. August 3–7, 2020

4.1. Problem background

In chapter 3, the load acting on the deadline is calculated from Aadnoy's model, where in the effect of drilling mud on the drill string is neglected. Therefore, in this chapter, the effect of mud pressure forces on drill string is incorporated. In presence of mud pressure, the drill string is subjected to both internal and external pressures, and it can be well explained in terms of true tension and effective tension. Estimating these tensional forces and other load forces acting on the drill string is essential for efficient drilling operation and selecting optimum operational parameters. Excessive tensional and load forces on drill strings for longer period during rotary drilling may lead to unexpected drill string failure. Therefore, these load forces have to be monitored in real-time to avoid drill string failures.

To estimate both the tensional and load forces in presence of mud pressure, in this chapter, the forces acting along the length of the drill string are calculated by combining Robello Samuel's and Johancsik's model. Wherein, the model equations for tensional force are adopted from Robello Samuel's model and the model equations for load forces are adopted from Johancsik's model. As described in chapter 3, along with the RUC factor, these forces are further utilized to estimate the neutral point and load acting at the deadline. The improved model is incorporated in the DSS to predict the drilling anomalies in real-time. Later, the improved model performance is validated by installing the DSS in Galeky field, ONGC, Assam Asset, India.

4.2. Model development

The following assumptions are considered for the model development

- The drill string material is premier grade and un-utilized.
- The whole length of the wellbore is a cylinder structure.
- The drilling mud (drilling fluid) is incompressible.

This section briefly describes the methods to estimate the axial force on the drill string, the neutral point, and the hookload acting at the deadline. The two commonly used methods to estimate the axial force are the true tension (pressure-area method) and effective tension (buoyancy method). The simplest way is to initially begin with the true

force illustration and modify under the working internal and external pressures using Eq.4.1 (Newman & Bhalla, 1999).

$$F_{eff} = F_{true} + \left(P_e A_e - P_i A_i\right) \tag{4.1}$$

The influential forces and stresses are the important parameters for the dimensioning of drill string exposed to internal and external pressures. In the below Fig. 4-1, the total force/pressure system acting on the drill pipe of length (δL) is disintegrated into three force components, namely Archimedean upthrust forces ($\rho_e . g . A_e . \delta L$), weight forces ($\rho_i . g . A_i . \delta L$) and the true weight forces ($W . \delta L$). And sum of all these forces is equivalent to the apparent weight of the pipe section (C.P.Sparks, 1984).

The internal pressure and external pressure acting on the drill string is specified by Eq's below:

$$P_i = P_{sp} + \sum \rho_{gp} \times TVD \tag{4.2}$$

$$P_e = P_{sa} + \sum \rho_{ga} \times TVD \tag{4.3}$$

Even though the axial force is estimated using two effective tension and true tension methods, both approaches converge to the same tensional value at the surface when there is no mud circulation in the wellbore. On the other hand, the pressure forces are not zero on the drill string side for the case of mud circulation. Therefore, the effective tensional force is greater than the true tensional force at the surface.

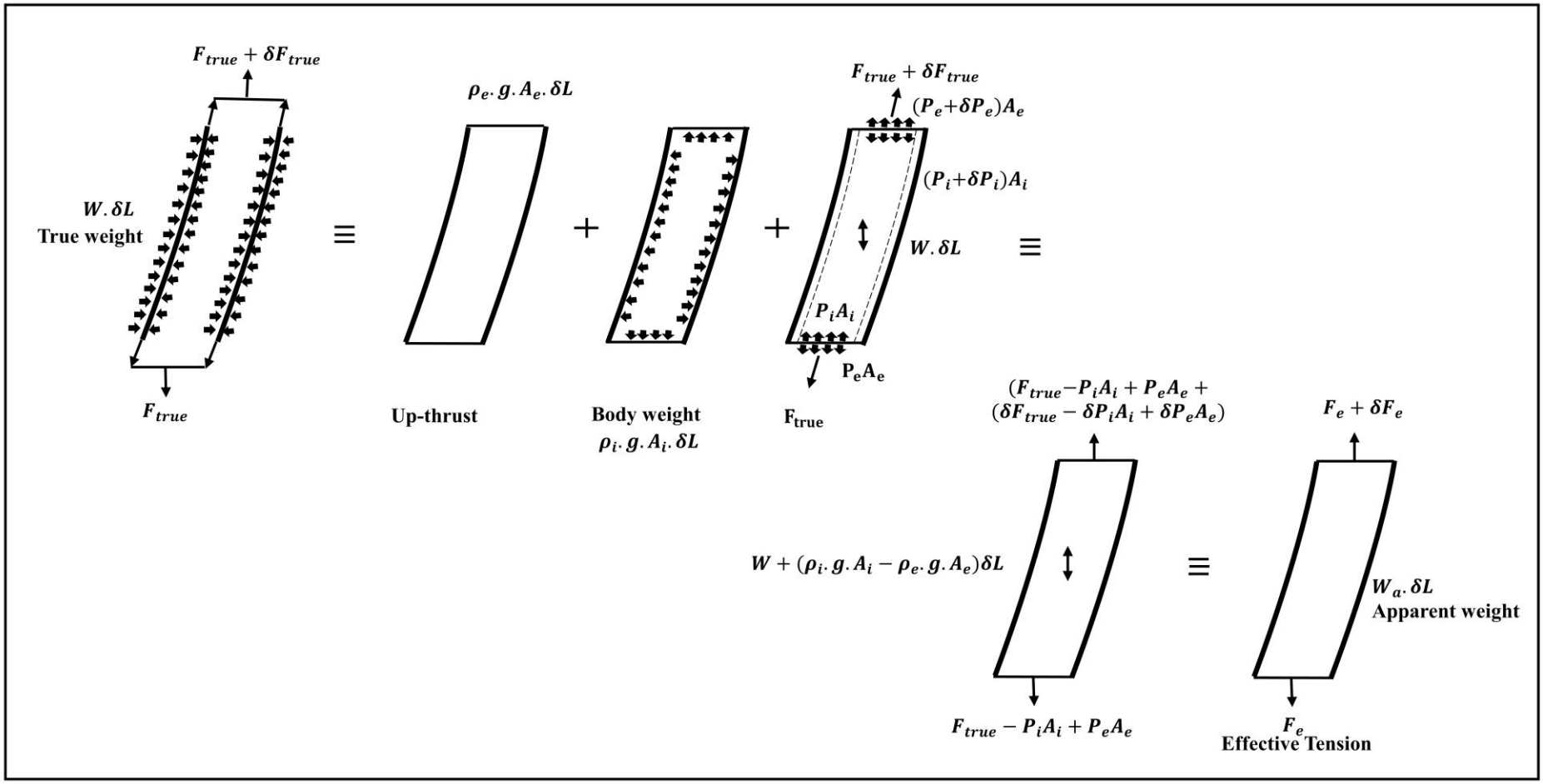

Fig. 4-1. The influence of pressure, weight, and tension for a drill pipe segment of length (δl)

True Tension (Pressure Area Method)

The pressure area method is used to compute the true tension force, and Eq.4.4 is utilized to calculate stresses in the tubular.

$$F_{true} = \sum \left[LW_{air} \cos\alpha + F_{drag} + \Delta F_{area} \right] - \left[F_{bottom} + WOB \right] \tag{4.4}$$

Pressure force due to change in cross-sectional area

The change in force due to change in the cross-sectional area during the transition phase from drill pipe to drill collars and drill collars to drill bit is given as

$$\Delta F_{area} = P_{hyd\_sta} \left(A_2 - A_1 \right) \tag{4.5}$$

Bottom Force and Buckling Stability Force

The compressive force exerted over the drill bit cross-sectional area is attributed to the fluid pressure. In large diameter wellbores, this bottom force has limited impact on the wellbore, but in the case of small diameter, it may create downhole complications such as total circulating loss, bit bouncing. When the drill string gets submerged in the mud, a hydrostatic force acts on the drill bit, providing a lift upward. This force is equivalent to the bottom hole pressure times the cross-sectional area of the bit as given by Eq.4.6.

$$F_{bottom} = P_e \left(A_e - A_i \right) \tag{4.6}$$

At the drill string bottom position, the bottom pressure force is equivalent to the buckling stability force. The bottom force is estimated at the drill bit, and the buckling stability force is determined at different depths.

$$F_{buc.stab} = \left(P_e + \rho_e u_e^{\,2} \right) A_e - \left(P_i + \rho_i u_i^{\,2} \right) A_i \tag{4.7}$$

Effective Tension (Buoyancy Method)

Effective tension is sometimes referred to as fictitious tension. The buoyancy method is used for examining the onset of buckling. This is because the critical buckling force calculations are based on the assumptions regarding hydrostatic pressure.

If the fluid flows uniformly internally and externally, the rate in change of momentum of fluid entering and leaving should be included in the determination of effective tension

(C.P.Sparks, 1984). The momentum of the fluid inside the tubular is given as $\rho_i A_i u_i^2$, and the fluid outside the tubulars is given as $\rho_e A_e u_e^2$.

$$F_{eff} = F_{true} + P_e A_e - P_i A_i - \rho_i u_i^2 A_i + \rho_e u_e^2 A_e \tag{4.8}$$

By rearranging the above equation,

$$F_{eff} = F_{true} + \underbrace{\left(P_e + \rho_e u_e^2\right)}_{F_o} A_e - \underbrace{\left(P_i - \rho_i u_i^2\right)}_{F_i} A_i \tag{4.9}$$

The additional terms F_o and F_i are termed impulse functions, which are the thrust forces produced by the fluid flow. These functions don't impact effective tension but are affected even due to small changes in these functions (Samuel & Kumar, 2012).

$$F_{eff} = \sum \left[LW_{air} \cos\alpha + F_{drag} + \Delta F_{area} \right] - \left[F_{bottom} + WOB \right] + F_{buc.stab} \tag{4.10}$$

When the tensile force on the drill string exceeds its limit, then the drill string may part-off. During the drilling operation, the drill string will experience both tensile and compressive forces, which won't create any complications until the forces are within the designed limits. If the string is operated within the elastic range, it tends to return to its original state. Fig. 4-2 describes the list of force components acting along the drill string. To further demonstrate the concept of effective tension and true tension, in brief, the following possible wellbore conditions were illustrated in Fig. A-1 and Table A- 1 (Appendix -A). Appropriate examples are presented to demonstrate the influence of true and effective tensional forces on simple hydro-mechanical systems. The drill string will experience severe fluidic and mechanical stresses in actual working scenarios, and establishing an accurate, effective tensional force illustration will be much more challenging.

Determination of buckling criteria

Buckling initiates when the compressive axial forces along the drill string exceed the critical buckling forces. The axial force estimated using the effective tension (Buoyancy method) is utilized to define the buckling criteria as given below

- The drill string is stable but tending to buckle if $F_{eff} < -F_c$
- The drill string is stable but not tending to buckle if $F_{eff} > -F_c$

- The drill string undergoes neutral stability and is an intermediary between the above two conditions if $F_{eff} = -F_c$

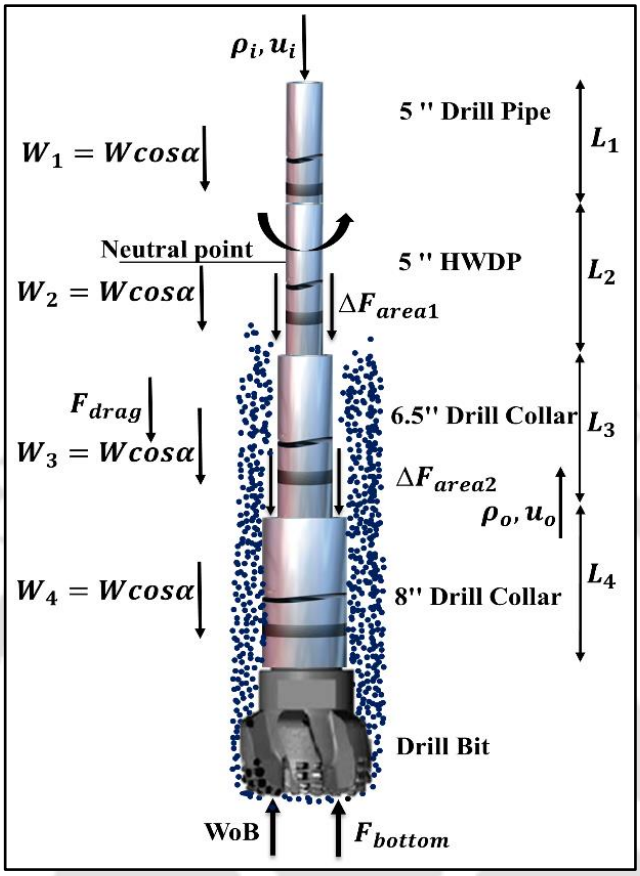

Fig. 4-2. Depiction of force distribution along the length of the drill string

Axial stress

Axial stress is caused by the combination of both mechanical and hydrostatic loading. The pressure-area method is utilized for estimating the axial stress as given in Eq.4.11. Axial stress is expressed as a combination of true axial stress, bending stress, and buckling stress. The buckling term is considered only if the critical buckling force exceeds the axial force (G.Robello Sameul, 2010).

$$\sigma_a = \frac{F_{apa}}{A_c} + \sigma_{bend} + \sigma_{buck} \tag{4.11}$$

Bending stress

The bending stress is the most critical alternating stress that should be considered during the well design and drilling phase. The bending stress acting on the drill pipe when subjected to a bending moment is given by

$$\sigma_{bend} = \frac{M_{ds} \times D_2}{2I} \tag{4.12}$$

where the bending moment acting on the drill pipe is given by M_{ds}

$$M_{ds} = (EI) \times \delta \tag{4.13}$$

where EI signifies the drill string flexural rigidity. The bending stress can also be expressed as,

$$\sigma_{bend} = \frac{E \times D}{2R} \tag{4.14}$$

where R denotes the borehole radius of curvature
and the bending stress is defined as presented in Eq.4.15.

where $R = 1/\delta$

$$\sigma_{bend} = f(F_{true}, DLS, BSMF) \tag{4.15}$$

Bending Stress Magnification Factor (BSMF)

In the absence of axial tension in the drill pipe, the drill pipe curvature is constant and is equal to the borehole curvature. For example, severe dogleg can induce high tensional force in the drill pipe. Further, the laterally unsupported drill pipe tends to flatten such that the drill pipe curvature is more at the tool joint position than at the centre of the body. Therefore, the local maximum curvatures are determined to accurately estimate the bending stress in the drill pipe sections. BSMF is defined as the ratio of maximum curvature in the drill pipe body to the hole axis curvature. This magnification factor can be used as a multiplier in accurately determining the bending stress. Paslay re-derived the Bending Stress Magnification (BSM) factor for all possible axial tensile and compressive loads in drill pipe from Lubinski's results (Paslay & Cernocky, 1991). The final bending stress is determined as given in Eq.4.16.

$$\sigma_{bend} = \frac{rE\delta(BSMF)}{68754.9} \text{ psi} \tag{4.16}$$

From the derivations obtained from Paslay, the BSMF can be expressed as follows

If $L_{tj}^{\,2} / R\Delta D \cong 1.0 - 4.0$,

$$\text{then, } BSMF = 1.1213\left(PL^2/4EI\right)^{0.4789} \tag{4.17}$$

and if $L_{tj}^{\ 2}/R\Delta D \cong 5.0$

$$\text{then } BSMF = 1.1975\left(PL_{tj}^{\ 2}/4EI\right)^{0.4594} \tag{4.18}$$

Buckling stress

Due to compressive force, the drill string may undergo buckling phenomena. The corresponding buckling stress can be estimated using the equation below.

$$\sigma_{buck} = \frac{\left|F_{apa}\right|(r)(r_{cl})}{2I} \tag{4.19}$$

Normal force and Drag forces (Johancsik's Model)

In general, 50% of the stuck-up problems are reported in deep hole drilling (Edition, 2015). One of the significant phenomena that leads to the stuck pipe is key-seating. Also, severe dogleg issues were experienced in deviated wellbores due to large diameter tool joints in the BHA. The side force (normal force or lateral force) is the load impacted by the drill string on the borehole wall. During lowering or drilling activity, the weight component acts downwards, and drag force acts in the opposite direction to the motion of the drill string. In contrast, the side force normally acts to the surface in contact. The side forces between the drill string and borehole wall are imperative to determine the torque, drag, and buckling forces are given by Eq.4.20.

$$F_{side} = \sqrt{\left(F_{eff}.\Delta\phi.\sin\alpha_{avg}\right)^2 + \left(F_{eff}.\Delta\alpha + W_b.\sin\alpha_{avg}\right)^2} \tag{4.20}$$

The limiting force at which the buckling force starts to increase dramatically is yet unclear (Menand, 2012). As per the API recommendations, the drill string's side forces shouldn't exceed 2000 lbf (0.9 ton) during severe dogleg.

The mud drag force acting on the drill string due to pipe movement is given below.

$$F_{drag} = \mu \times F_{side} \times \left(\frac{V_t}{V_r} \right) \tag{4.21}$$

Determination of Neutral point

During the drilling operation, the upper section of the drill string is in axial tension, and the lower section of the string is in axial compression. The drill string section, which is under compression, is responsible for imparting weight on bit. The point at which the state of stress changes from compression to tension is termed as the neutral point (Edwards & Hills, 2012). The monitoring of neutral point during a drilling operation in real-time is vital for stress management and reduction to avoid sudden disruption of the drilling jar in high inclined wellbores.

The pressure-area method determines the axial forces on the drill string, which can be used to estimate the neutral point by doing the force balance, i.e., the axial force and axial stress are exactly zero at a depth of neutral point. The axial force and stress are equal to the hydrostatic pressure at the neutral point position in the buoyancy method. This method is employed whenever the string buckles, as hydrostatic pressure alone isn't responsible for drill string buckling (Halliburton, 2014).

When the operator experiences hard formation, the weight on bit is eventually increased for a higher rate of penetration. In these conditions, the operator will be unaware of the neutral point position and might cross the critical limits, and may cause string buckling. Therefore, the neutral point is monitored in a real-time environment for safe drilling operations in this work. The neutral point position is compared to the total length of BHA, and the operator can choose operating parameters such that it doesn't fall near to drilling jar (which may lead to misfire) and drill pipe.

Estimation of Hookload at the Deadline

The effective tension derived at the surface signifies the overall tension acting at the drill string's pivotal position. The final effective tension obtained at the surface doesn't represent the hookload measured at the deadline. At zero block weight and sheave friction, the hookload graph will show the value of effective tension. Therefore, sheave friction correction is applied to account for the changes in the position of hookload measurement (refer to Eq.4.22 & Eq.4.23) (Luke & Juvkam-Wold, 1993). The schematic

diagram of the complete block and tackle system with mud-hose, electrical umbilicals, and other hydraulic lines is shown in Fig. 3-1.

The hook load acting at the deadline during hoisting activity is given by

$$W_r = \frac{n(E_s - 1)(W_{hr} + W_{block})}{\left(1 - \frac{1}{E_s^{\,n}}\right)} \tag{4.22}$$

The hook load acting at the deadline while slacking off activity (drilling activity)

$$W_l = \frac{n(1 - E_s)(W_{hl} + W_{block})}{E_s\left(1 - E_s^{\,n}\right)} \tag{4.23}$$

The above set of equations doesn't account for the uncertainties in the rig structure and the variations in the hookload due to the effects of mud-hose, umbilical systems, and other hydraulic lines (described in section.3.2.2). Therefore, to enhance the precision in determining the hookload at the deadline, Eq.4.23 is modified to Eq.4.24 by considering the variation of the above-mentioned effects.

The final hookload acting at the deadline during rotary drilling operation is estimated by using Eq.4.24.

$$W_l = \left(\left(\frac{n(1 - E_s)}{E_s(1 - E_s^{\,n})}\right)\left(W_{hl} + W_{block} + \left(\lambda_{bp}.x + RUC\right)\right)\right) \tag{4.24}$$

The complete flow diagram of the stress calculations, hookload estimation, and neutral monitoring is illustrated in Fig. 4-3.

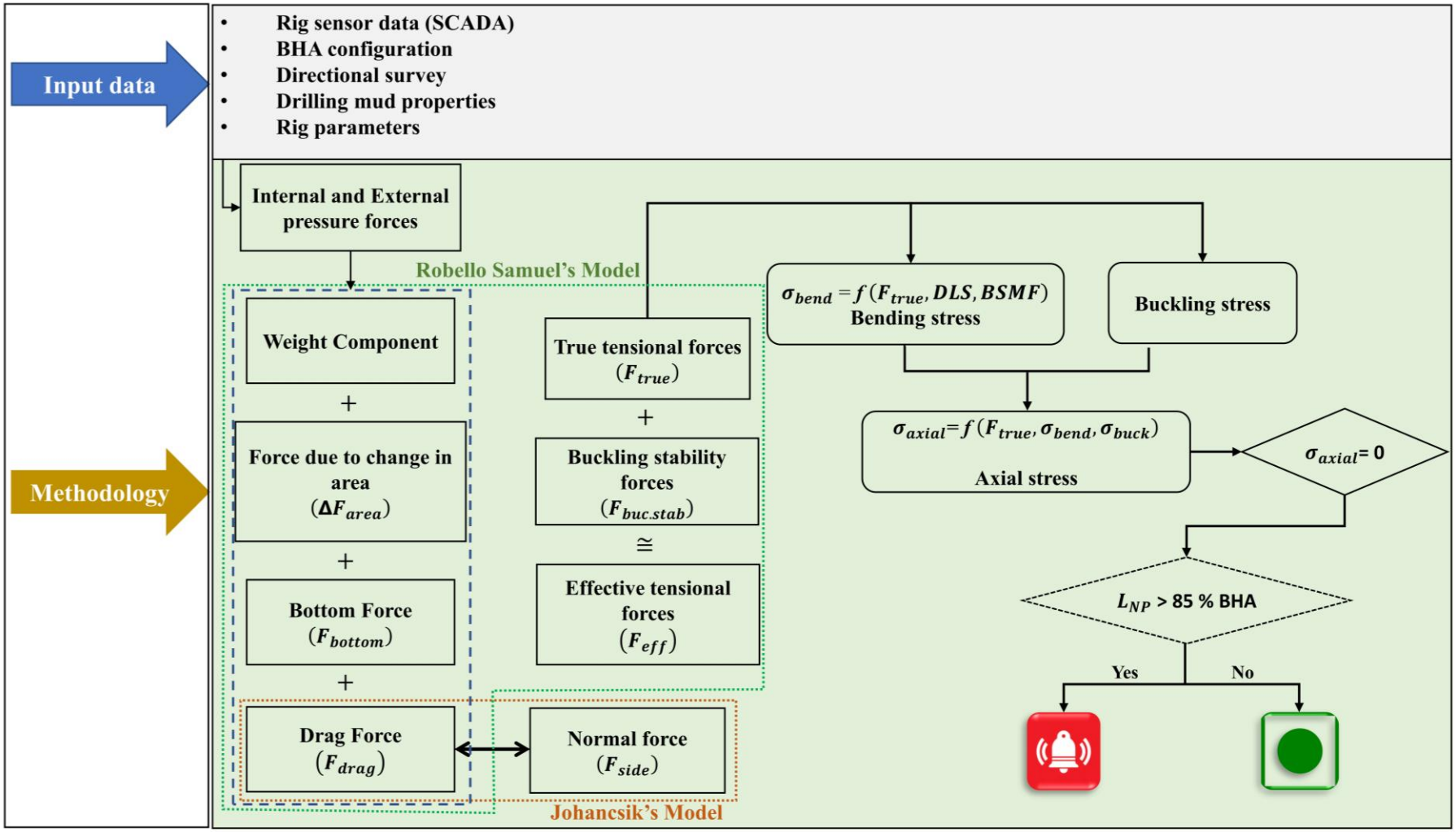

Fig. 4-3. Flow diagram depicting the complete stress analysis chart, hookload estimation, and neutral point monitoring

4.3. Data description

The data input, pre-processing and overall system architecture were briefly discussed in section 3.3.

4.4. Implementation procedure

The overall procedure and computing algorithm for estimation of hookload at the deadline and forces acting at the deadline, neutral point, and forces along the drill string can be illustrated as mentioned below (as given in Fig. 4-4):

1. The streaming rig sensor information is examined for validity, and the history information (latest rig sensor information) is further used for identification of drilling operation section.3.3.2.
2. Once the drilling activity is confirmed, the stress module, which includes both Robello Samuel's and Johancsik's models, is initiated, as depicted in Fig. 4-4.
3. In the stress module, the complete input data is retrieved from the database.
4. The streaming rig sensor data and retrieved information are utilized to estimate the forces acting along the string and neutral point. And this force estimation is entirely dynamic, and the forces are estimated along the length at each time step.
5. Further, the true tension and effective tension model is used to estimate the load acting at the deadline. The RUC factor enhances the load force acting at the deadline by incorporating various uncertainties associated with the rig.
6. The above-estimated forces, neutral point, and hookload are further utilized for thorough analysis, like key seating identification, buckling determination, hazardous drilling when the neutral point crosses the threshold, i.e., into the drill pipe zone, irregular deviation in hookload, and many more. These abnormal behaviours in the load patterns can signify any downhole inference like drill string parting, severe buckling, stuck up, and cuttings accumulation.

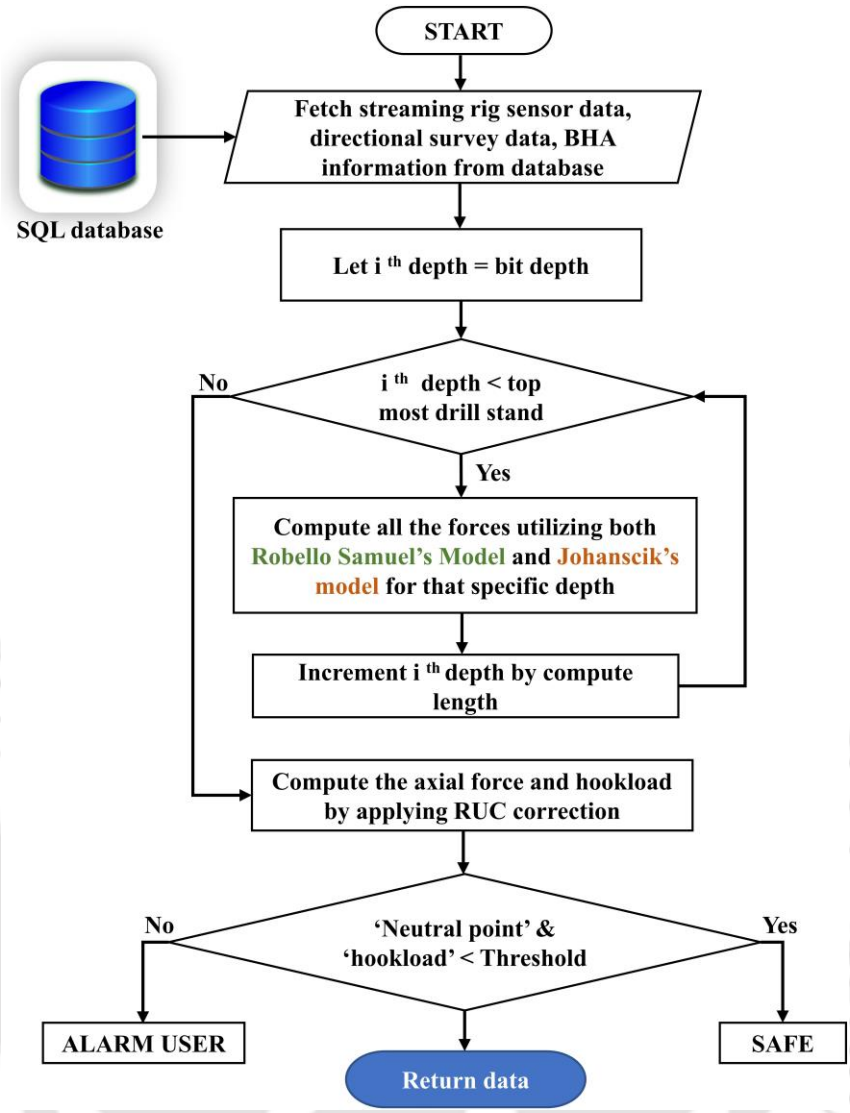

Fig. 4-4. Workflow depicting forces estimation along the drill string

4.5. Results and discussions

4.5.1. Case study – Real-time validation in directional well

Model acceptance mainly depends on the illustration of adequate validation. Therefore, to verify the model accuracy and compare the theory presented in this work, simulations were carried out and compared against the real-time drilling data. The directional well shown in Fig. 3-12 (Galeky field, ONGC, Assam Asset, India) with an overall target depth of 3752 m was used to validate the proposed model. The 12 ¼" section had sustained stiff dogleg at 2410.79 m, and the 8 ½" wellbore section was planned to drill from 2800 m to 3256 m with nominal doglegs. Water-based drilling fluid is used, and the mud weight is maintained at 10.495 ppg. The complete assembly of the bottom hole

assembly (BHA) configuration is illustrated in Table 3-6. The overall wellbore information and BHA details are briefly discussed in section 3.5.2.

4.5.1.1. Evaluation using the hookload at the deadline

The developed model was calibrated to incorporate the uncertainties associated with the borehole and the rig by tuning the model parameters using the drilling data collected for one complete stand of drilling activity for the depth range of 3053 m – 3082 m. The calibration is accomplished by reducing the average residuals between the measured hookload at the deadline and the estimated hookload as given in Eq.3.13. The average residuals (%) were estimated to be 2.66 % after model calibration. Due to wellbore tortuosity and severe dogleg, the global friction factor was found to be 0.39 for the section selected.

The tuned parameters are further utilized for model validation for another two hours of drilling activity (3082 m - 3088.7 m), as shown in Fig. 4-5. The average residuals for the validation section were estimated to be 0.97 %. The tuned model may deviate from the actual hookload measurements during downhole complications and abnormal drilling conditions, which were not captured in the model equation. The hook load deviation between the measured and model-estimated hookload is less than 2.5 tonnes for tuned model parameters, approximately equivalent to about 1% of maximum hookload. Therefore, the deviation in hookload greater than 2.5 tonnes may signify the abnormality in the wellbore. This can be used to trigger alarms for the operator to act on before complications get aggravated.

In the presented case, in zone A, the operator experienced marginally experienced a steady deviation in hookload from the normal, as shown in Fig. 4-5. As the well is entirely tortuous, severe drag was observed in deep sections. The operator tried to focus on crucial rig sensor parameters to recheck for a probable anomaly for having the well under control, but none of them showed significant variation. As per the standard operating procedure, the tripping out operation was held to inspect the whole BHA and drill bit section. And after appropriate gauging of the whole BHA, the drill string was lowered to the total depth to resume drilling. After that, many perturbations in hookload were observed discretely, and gradual gain in load was observed as portrayed in zone B. And immediately, the pressure drop of 51.3 kgf/cm^2 (729.65 psi) was observed at a uniform flow rate, ROP

dropped down to zero, and 9.09 tonnes reduction in load was detected, which indicates the drill string parting (refer to Fig. 3-14, Tracks 1-5).

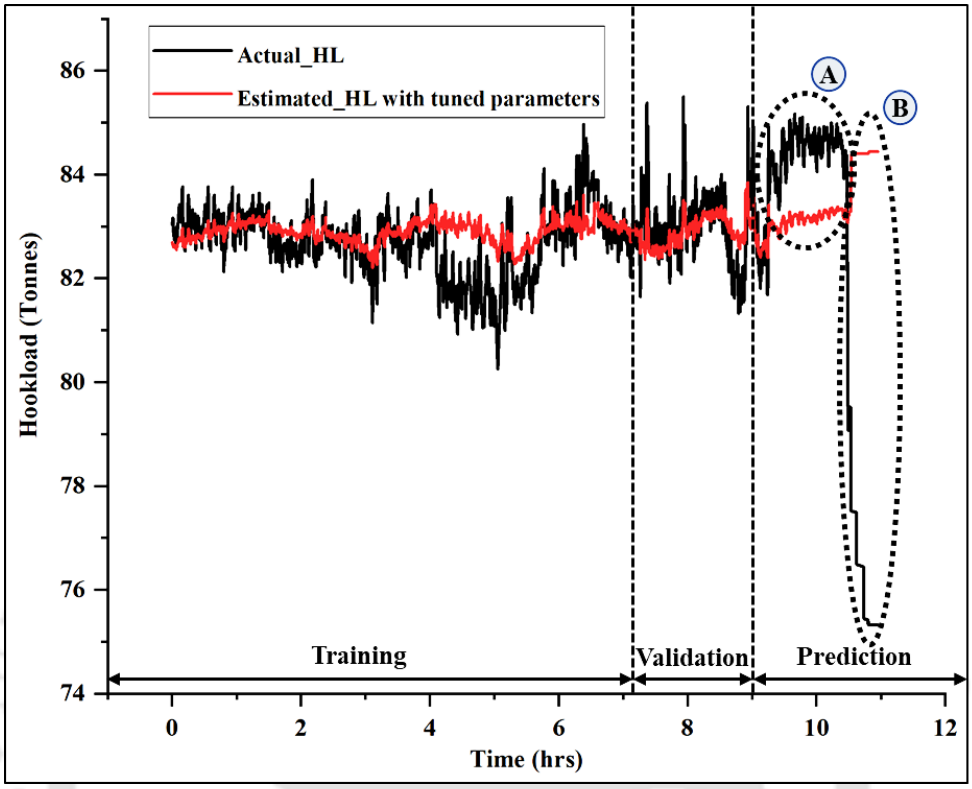

Fig. 4-5. Hookload variation during training, validation, and prediction phases

The hookload measurements can indicate whether the drill string has been parted off or not (Selvaraju et al., 2019). To confirm the anomaly, the operator pulled out the drill string and found string shear from the pin side of HWDP. In many instances, deviations in hookload were observed due to tight hole conditions, just before the string got parted entirely off. Monitoring these load variations would allow the operator to detect the anomalies and take necessary action before the situation worsens. From this analysis, the model can predict the abnormal behaviour of hookload compared to the actual measurement and signifies the wellbore's irregularity.

4.5.1.2. Evaluation of forces along the drill string

During drilling in tortuous wells, the drill string tends to have a high impact on the casing walls and open-hole sections. The rotating tool joints of larger diameter will gradually form a groove in the wellbore and develops crescent-shaped wear. In Fig. 4-6, the normal force acting on the drill string is monitored in real-time drilling activity to prevent key-seating conditions, which might, in turn, lead to mechanical stuck-ups. The 8 ½" section

was carefully monitored such that the normal force doesn't cross the limiting force of 2000 lbs. But, in the previous cased sections, the normal force has crossed its limit in two instances. And such incidents can be used for identifying the entry of drill string into the key-seating region.

As shown in Fig. 4-7, the tensile force and the critical buckling force are plotted to determine the drill string stability regions and buckling tendency zones. Throughout the length of the drill string, $F_{eff} > -F_c$ indicating that the drill string is stable and there is no buckling tendency. The negative force indicates the compressive force, depicting the total weight imparted on the drill bit. And having this information to operator in real-time may enable to take preventive measures in case of any downhole complications.

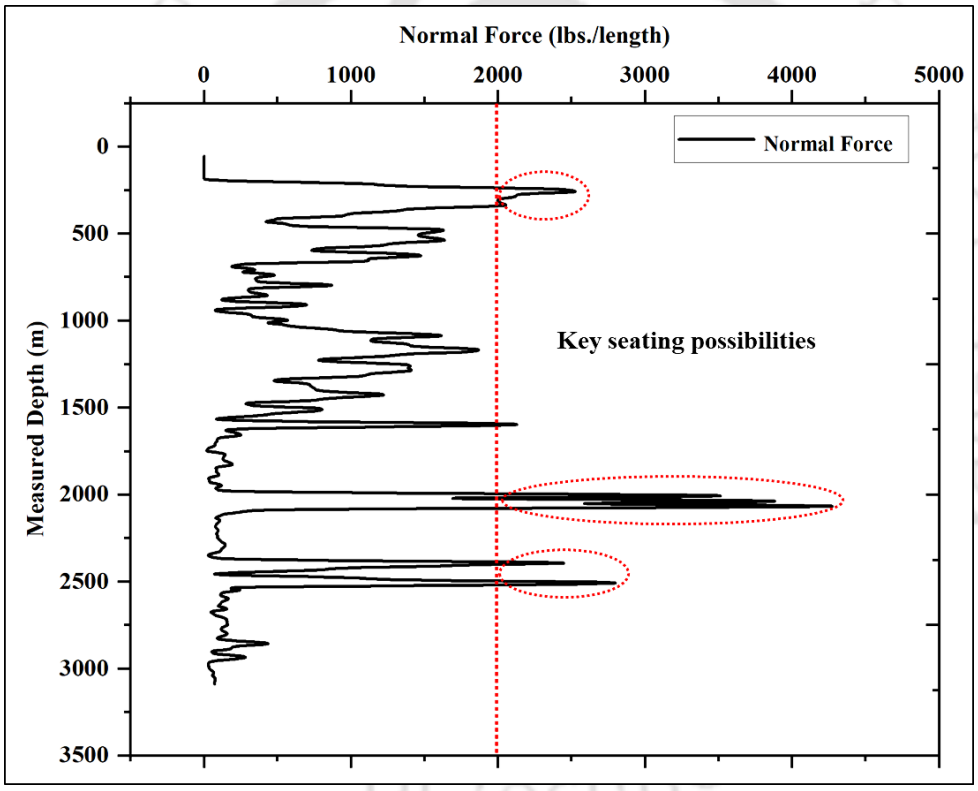

Fig. 4-6. Depiction of the possibility of key-seating

In addition, Fig. 4-8 depicts the neutral point variation along the drill string with the change in depth. It would be a tedious task for the operator to estimate these forces in the actual field conditions. The neutral point position is compared with the total BHA length and 15% of the total BHA length for warning the operator in case of any complications. Suppose the operator is unaware of the position of the neutral point. In that case, it may

eventually shift into the drill pipe region and cause severe buckling, which ultimately leads to complete parting.

The detailed analysis of forces along the length of a drill string with each time step could provide insights into the presented case study. The failure might have occurred due to the higher normal force imparted by the drill string on the wellbore wall and casing section. And due to this, the drill string might have undergone severe fatigue while working in the key-seating and tortuous zones. These complications can only be identified through the hookload analysis at the deadline and force analysis along the drill string. Further, the evaluation of secondary forces aids in conforming to the downhole anomaly in real-time.

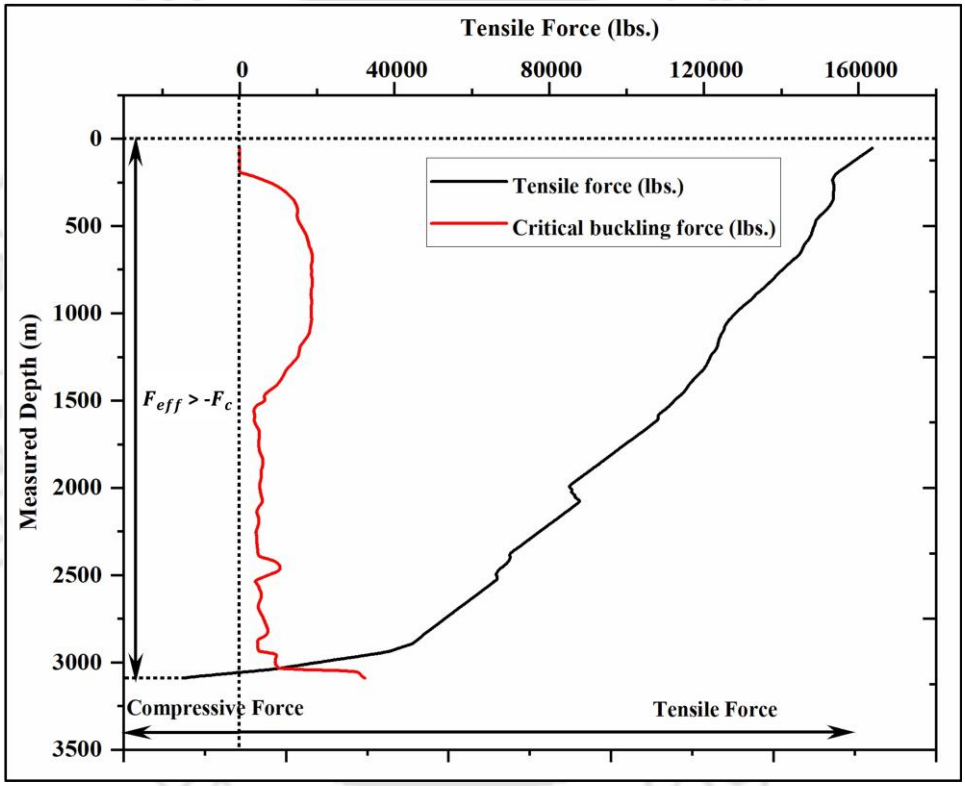

Fig. 4-7. Variation of tensile force with critical buckling force along the drill string

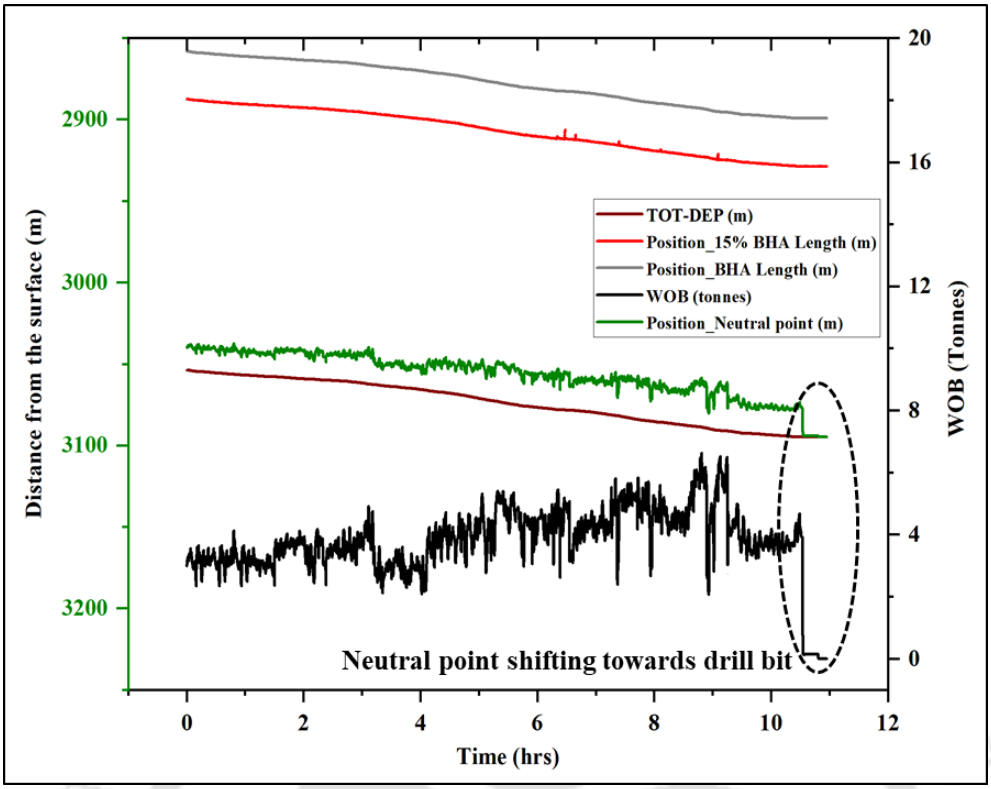

Fig. 4-8. Monitoring of neutral point variation with change in total depth during rotary drilling

4.6. Challenges in real-time implementation

1. **Historical information**: Due to the lack of historical drill string information, it's obvious that the estimated values from the model cannot be used in extreme rugged drilling conditions. In severe fatigue, access to prior drill string running information would help the operator take proactive measures.
2. **Static data requirement**: The mud properties and directional survey must be fed manually to the model to have accurate predictions. Mud properties tend to change rapidly with the change in total depth, and calibrated sensors need to be utilized to have precise measurements. And even the directional survey is measured and fed to the model every 30 meters, as in the hookload model.
3. **Literature selection**: Limited research has been conducted on studies pertaining to the application of true tension and effective tension forces in the drilling industry.

4.7. Summary

The evaluation of structural integrity of tubular under the influence of the hydraulics during actual drilling conditions is carried out in this chapter. The true tension and effective tension model (Robello Samuel Model) and Johanscik Model are utilized to determine the overall stresses acting along the length of the drill string, neutral point, and hookload acting at the deadline. The determined forces are further utilized to identify the upcoming complications before the situation gets worsens. A case study of a directional wellbore was presented with working limits for all the influencing forces. The model could able to identify the complication in the form of drill string parting and alarm the operator.

Chapter

5

CHAPTER 5
Optimization of Drilling Parameters Using Improved Play-back Methodology

Parts of this chapter are published in the research article:

- Viswanth Ramba, Senthil Selvaraju, Senthilmurugan Subbiah, Muthukumar Palanisamy, Aman Srivastava, "Optimization of Drilling Parameters Using Improved Play-back Methodology", *Journal of Petroleum Science and Engineering*, P.P 108991- [2021], https://doi.org/10.1016/j.petrol.2021.108991

5.1. Problem background

Wellbore economics is directly proportional to the total non-productive time (NPT). The NPT accounts for one-third of the total rig operational expenditure (Webb et al., 2016), and this percentage may increase with respect to the complexity of the wellbore. To drill a well successfully and to achieve a better rate of penetration (ROP), the following three drilling process parameters have to be maintained at their optimal value: as weight on bit (WOB), rotations per minute (RPM), mudflow in terms of strokes per minute (SPM). Similarly, other drilling parameters such as torque, standpipe pressure (SPP), mud weight, and mud rheological properties also play a critical role in achieving optimal ROP. However, these parameters cannot be manipulated in real-time since they are a function of formation type, lithology, temperature, etc. (Alali et al., 2021). The drilling without real-time monitoring and optimization may lead to sub-optimal drilling, i.e., high drilling costs with reduced ROP. Also, applying excessive WOB to achieve maximum ROP can eventually result in higher torques and further lead to drill string snapping off, buckling, severe stick-slip, and other downhole complications. To overcome this hindrance, this chapter presents the method to apply a play-back methodology similar to drill-off test (DOT) in real-time for calculating optimum drilling parameters. The method involves identification of optimum drilling parameters from an exploratory well and then implementing these optimal conditions in development wells for a similar lithology. The benefit of applying the optimal drilling parameters derived from play-back methodology is established by calculating drilling specific energy (DSE), mechanical specific energy (MSE) and hydraulic drilling impact (HDI) for all operating conditions. The importance of monitoring the HDI is evaluated in this chapter, and it is observed to provide a more reliable assessment to the operator when compared to other drilling performance evaluation techniques based on MSE and DSE alone ((F. E. Dupriest, 2006), (Abbott, 2015)) and act as a powerful quantifier for monitoring drilling efficiency. The proposed concept is demonstrated using drilling data collected from an 8 ½″ section of a directional wellbore drilled in North-Eastern parts of India.

5.2. Model development

5.2.1. Drill-off Test (DOT)

The drill-off test methodology was developed in the 1950's to curtail the time to determine its performance at various WOB's. It is basically a step-by-step process of varying the drilling parameters to maximize the rate of penetration and determining the "Founder Point." The founder point is defined as the point at which ROP stops responding linearly with an increase in WOB and RPM. In another aspect, the founder point is also the optimal ROP with respect to WOB and RPM. This test is proven to work with roller cone bits at moderate to low drilling rates, but it tends to be less effective with polycrystalline diamond compact (PDC) bit due to its sensitivity (IADC Drilling Manual EBook Version, 2014). Therefore, while employing the PDC bits on the field, the drill-off test is conducted more frequently to improve the drilling performance. Also, the PDC bits were found to give optimal drilling for soft formations in comparison to hard formations or soft formations with stringers. Even though better penetration rates are possible in hard formations using PDC bits, its cutters may accelerate wear. And this is mainly due to severe axial vibrations. These axial vibrations can cause bit bounce, resulting in loss of contact between the drill bit cutter and the rock formation (Sodbury et al., 2001).

Further, the drill-off tests are conducted in active and passive mode (Guerrero, 2007). The best operating range for achieving optimal ROP is established in passive mode, and in the active mode, the founder point (optimum ROP) is derived. The detailed steps involved in both passive and active are presented below.

Passive Drill-off Test:

Step -1: Lock the brake such that the drill string is not allowed to progress forward.

Step -2: Fix the maximum WOB allowed for a given drill string configuration (say 25 kips).

Step -3: Rotate the drill string at maximum RPM that can be achieved for a given rig (for example, 100 RPM) and maintain sufficient circulation.

Step -4: Count down the time required for the WOB to reach 0. For example, as given in Table 5-1, the test sheet for a fixed RPM is given.

Step -5: Repeat steps 1-4 for different RPM (maximum to minimum RPM).

Step -6: Similar to Table 5-1, multiple tables are generated for each RPM. Then, find out the RPM at which the minimum time is taken to reduce the WOB from maximum to zero.

Table 5-1. Sample Test Sheet

Test Case	WOB	Time elapsed
1	25 kips – 20 kips	15 s
2	20 kips - 15 kips	10 s
3	15 kips - 10 kips	13 s
4	10 kips - 5 kips	15 s
5	5 kips - 0 kips	25 s

Active Drill-off test:

Step -1: Find out the optimal range of RPM derived from the passive drill-off test
Step -2: Fix the RPM either at low or high and low WOB from the range derived in step-1 and maintain sufficient circulation.
Step -3: Increase the WOB from low to a maximum in steps of 2000 lbs. for a fixed RPM, the ROP increases and then reaches the founder point and then decreases.
Step -4: Repeat step-3 for multiple RPM by maintaining sufficient mud circulation.
Step -5: Find out the optimal RPM and WOB at which the maximum ROP is achieved.
The above described passive and active DOT requires detailed off-line analysis by the operator to determine the optimal drilling conditions. Therefore, this chapter proposed a new methodology for the drill-off test to calculate the optimal drilling condition in real-time.

5.2.2. Reverse engineering: Play-back methodology

Surface drilling mechanics parameters during rotary drilling operation for a specific section are chosen from an exploratory well. The parameters include RPM, ROP, WOB, and SPM. Utilizing these specific parameters in the actual field condition, the operator will visualize a drill rate test curve. Steps in achieving this drill-rate test curves are as follows: (i) First level segregation in historical drilling data for a given lithology with respect to RPM with an interval of 5 RPM for constant mudflow (ii) Then, second-level segregation of data within 5 RPM interval data with respect to WOB with an interval of

1 tonne (iii) The drill rate test curve for each RPM range is derived (refer to Fig. 5-1). Besides, to drill rate test curves, the model performs a comprehensive analysis of energy in the mechanical drilling system as it is imperative for performance improvement and drilling energy management (W. Chen et al., 2019).

5.2.3. Mathematical model for drilling

5.2.3.1. Model for ROP calculation

As shown in Fig. 5-1 (Dupriest et al., 2005), the ROP is observed to be a function of both WOB and RPM on the drill bit for a given type of rock, and the corresponding bit's performance can be studied through the drill-off curve. In region I, the performance was hindered by inadequate depth-of-cut due to lower WOB. The relationship between the WOB/RPM and ROP tends to be linear if the drill bit can cut the ground efficiently (region II) and the drill bit eventually approaches its peak efficiency. ROP vs. WOB slope for fixed RPM is relatively constant for a given bit type and formation. The curve behaves nonlinearly in the transition zone (regions II and III) due to bit balling, stick-slip, and other bit dysfunctions (Nascimento et al., 2017). This non-linear behavior can be modeled by using quadratic functions. Therefore, the optimum WOB and RPM to achieve maximum ROP can be estimated by using conventional optimization techniques.

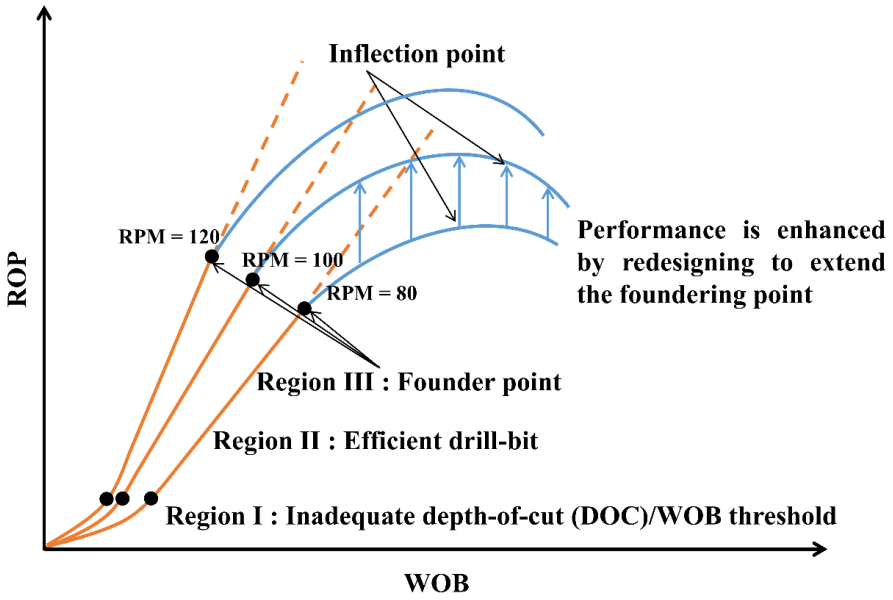

Fig. 5-1. Representation of three regions of efficiency during drilling

5.2.3.2. Model for Specific Energy Calculation

The model to determine the amount of specific energy required to excavate and lift the cuttings until the surface is briefly discussed.

Mechanical Specific Energy (MSE)

The mechanical work expended to remove a unit volume of rock is defined as mechanical specific energy (Armenta, 2008). The cutting of the rock is achieved by applying thrust and rotational forces. It can be defined as given by Eq.5.1, wherein the WOB, RPM, Torque, and ROP are measured at the surface.

$$MSE = \frac{WOB}{A_B} + \frac{120\pi \times RPM \times Torque}{A_B \times ROP} \tag{5.1}$$

where the first and second term represents the weight and torque component respectively. The mechanical rotating system comprises a rotary or top-drive, which transmits the power through the drill string from the surface to the drill-bit (refer to Fig. 5-2). There would be numerous parasitic losses while transferring the power, such as axial drag forces, frictional torque forces, contact forces, and severe bit rock interaction. Therefore, the actual MSE required for a given ROP will be higher than the ideal MSE. The graphical display of an 8 ½" section of a wellbore drilled with a top-drive system is shown in Fig. B-1.

The product $ROP \times MSE$ determines the area-specific mechanical energy power (MPSI). It is defined as the ratio of total available power without losses in the wellbore (P) and the wellbore cross-sectional area (A_B).

$$MPSI = \frac{ROP \times MSE}{1.98 \times 10^6} = \frac{\left(\frac{P}{A_B}\right)}{1.98 \times 10^6} \tag{5.2}$$

where the constant 1.98×10^6 is used to convert ft-lb/hr to HP

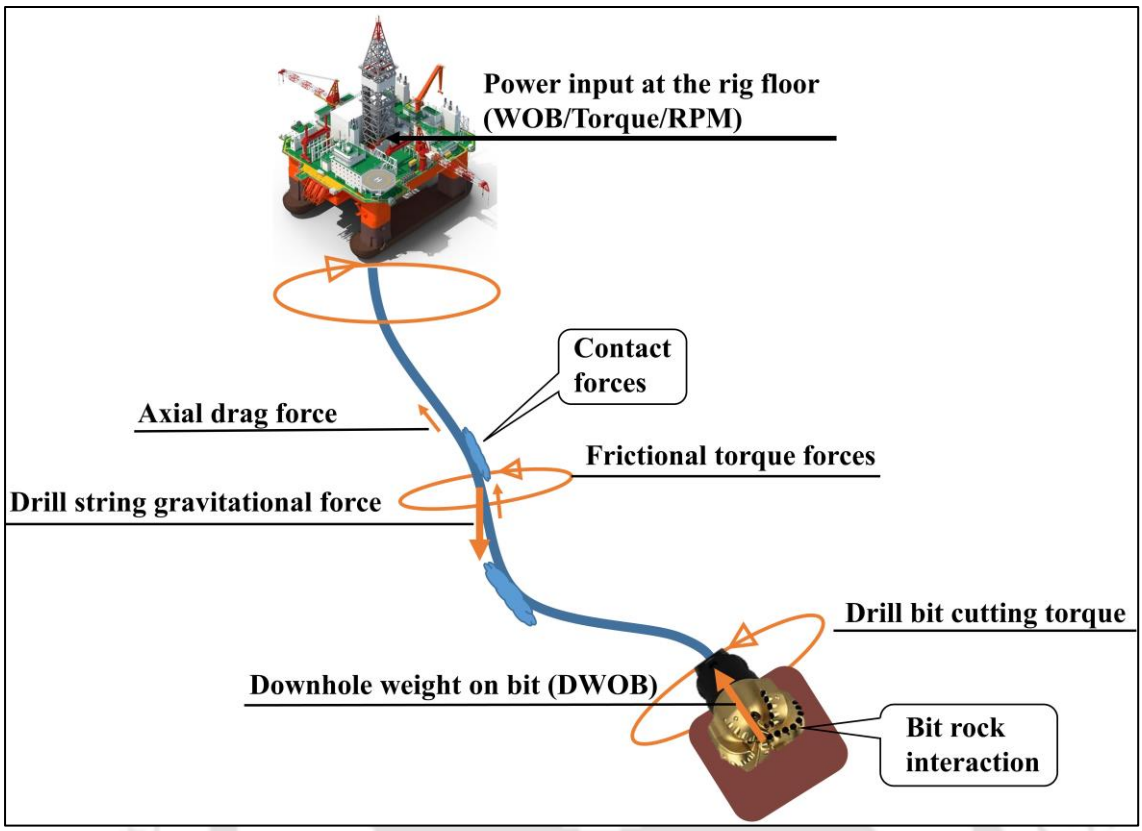

Fig. 5-2. Schematic of the mechanical drilling system

From Eq.5.3, the total available power can be calculated for a given ROP, MSE, and drill bit cross-sectional area.

$$P = MPSI \times A_B \tag{5.3}$$

when the input power remains constant with respect to depth, then the power available at the bit will be varying with respect to depth, well path, lithology, type of drill bit, and other physical aspects. Therefore, to maintain optimal ROP, the operator will vary the power available at the surface. Otherwise, both MSE and ROP vary such that the power is constant. The constant power curve between MSE, ROP can be drawn by using Eq.5.3. The combined plot between MSE, ROP, and constant power curve is called a power-graph. The power-graph can help the operator interpret the optimal ROP zone wherein MSE is minimum and ROP is maximum for constantly available power.

Drilling Specific Energy (DSE)

The DSE is defined as the amount of energy spent on cutting and lifting rock per unit volume. The concept of MSE and its original equation was laid down by (Teale, 1965),

and later it was modified by Armenta, (2008) by including the bit-hydraulic related term as given in Eq.5.4.

$$DSE = \frac{WOB}{A_B} + \frac{120\pi \times RPM \times Torque}{A_B \times ROP} - \frac{1{,}980{,}000 \times \lambda \times BHHP}{A_B \times ROP} \tag{5.4}$$

where the first two terms of the right-hand side of the Eq. 5.4 are derived from Teale's original equation, and the third term represents the bit hydraulic associated term, where the constant 19,80,000 is the unit conversion factor. The parameter **λ** is a function of bit hydraulic factor and bit diameter, as shown in Fig. B-2.

The bit hydraulic horsepower (BHHP) is a measure of the energy per unit time that is expended across the drill bit nozzles. It is estimated using Eq. 5.5.

$$BHHP = HHP_s - HHP_c \tag{5.5}$$

$$BHHP = \frac{P_s Q}{1714} - \frac{kQ^{n+1}}{1714} \tag{5.6}$$

$$HSI = \frac{BHHP}{A_B} \tag{5.7}$$

where k represents the consistency index, n indicates the index for the degree of turbulence in the circulating system. P_s and Q determine the surface pressure and circulating pressure, respectively. The constant 1714 is a conversion factor to yield hydraulic power in hydraulic horsepower (HHP). And the ratio of the BHHP to the bit cross-sectional area determines the bit HSI (bit hydraulic horsepower per area of the drill bit). The bit manufacturers recommend maintaining 2.0 to 7.0 HHP for optimized fluid hydraulics energy across the bit and ensuring adequate bit tooth and hole cleaning (minimum HHP). And maximum HHP is maintained across the bit to avoid the premature erosion of itself (Schlumberger Limited, 2021).

5.2.3.3. Model for Hydraulic Drilling Impact (HDI) Calculation

The PDC drill bits have been instrumental in achieving a higher rate of penetration when compared to roller cone bits and were inherently efficient (Alsubaih et al., 2018). The power utilization to shear the formation was relatively higher in PDC bits, and eventually, higher torque is generated, resulting in the variance of torsional oscillations. And these oscillations, along with drill string parasitic energy losses and downhole stick-slip, would

hinder the transfer of energy to the drill bit and result in a low penetration rate. Due to poor bit hydraulics, the particles may not be lifted by mud, settling at the bottom hole and then regrinding. These phenomena may limit the penetration rate. Therefore, incorporating the dependency of ROP on bit hydraulics can provide better insights into overall drilling efficiency. The new metric, Hydraulic Drilling Impact (HDI), is introduced to incorporate the impact of bit hydraulics on ROP. The HDI is defined as the ratio of ROP and bit hydraulic contribution given by Eq. 5.8.

$$\text{HDI} = \text{ROP} / \text{Bit hydraulic contribution} \tag{5.8}$$

wherein bit hydraulic contribution is calculated by Eq. 5.9

$$\text{Bit hydraulic contribution} = \text{MSE} - \text{DSE} \tag{5.9}$$

In the absence of downhole tools such as measurement while drilling (MWD) and strain gauges, the HDI will act as a powerful quantifier for the operator to monitor the wellbore health, bit performance, and rate of penetration. HDI can further be utilized to investigate the changes in the formations or detection of dynamic dysfunctions. Higher HDI indicates better drilling performance and whereas lower HDI indicates hindrance to drilling rates due to wellbore complications like improper hole cleaning, poor hydraulics, or harder formations.

5.3. Data description

From the available drilling parameters, only four parameters are considered to be the vital features for the model, namely: weight on bit (WOB), revolutions per minute (RPM), mudflow rate (TOT-SPM), and rate of penetration (ROP). Out of which, WOB, RPM, and TOT-SPM can be controlled by the operator in real-time. A total of 73,288 raw data points was retrieved from the database for this particular section of the wellbore, and the data is observed at a frequency of 7.2 s/ data sample (0.138 Hz). The outliers from the above-retrieved raw data samples are removed using the interquartile range (IQR) technique. After eliminating outliers as per rules tabulated in section 3.3.2, a total of 55641 data points was available to study improved playback methodology. The statistical information of the filtered drilling data is described in Table 5-2. For representation purposes, Fig. B-1 depicts the streaming drilling information with respect to depth.

Table 5-2. Statistical properties of the complete data set

	Minimum	Maximum	Mean	Standard deviation	Median
ROP (ft/hr)	0.1	60	16.37	10.929	12.071
WOB (Tonnes)	0.5	18	10.56	2.407	11.4
RPM	80	110	99.85	8.668	100
TOT-SPM	128	134	132.53	1.414	133.032

Fig. 5-3 illustrates the distribution of ROP, WOB, RPM, and TOT-SPM, indicating sub-optimal drilling parameters are chosen to drill the wellbore where most drilling rates fluctuate between 0.1 ft/hr – 25 ft/hr. For achieving these low drilling rates, higher WOB ranging from 6 – 13 tonnes and over 100 RPM are chosen, resulting in BHA fatigue and higher energy input. The mud circulation rate tends to be constant and varies slightly between 128-134 SPM.

For uncertainty estimation in the overall specific energy, which is multivariate, the following approach is followed as given in Eq.5.11. In this case, the uncertainty estimated in MSE and DSE is 7.036 kpsi and 6.457 kpsi, respectively.

$$\Delta y = \sqrt[2]{\left(\frac{\partial y}{\partial x_1}\times\Delta x_1\right)^2+\left(\frac{\partial y}{\partial x_2}\times\Delta x_2\right)^2} \tag{5.11}$$

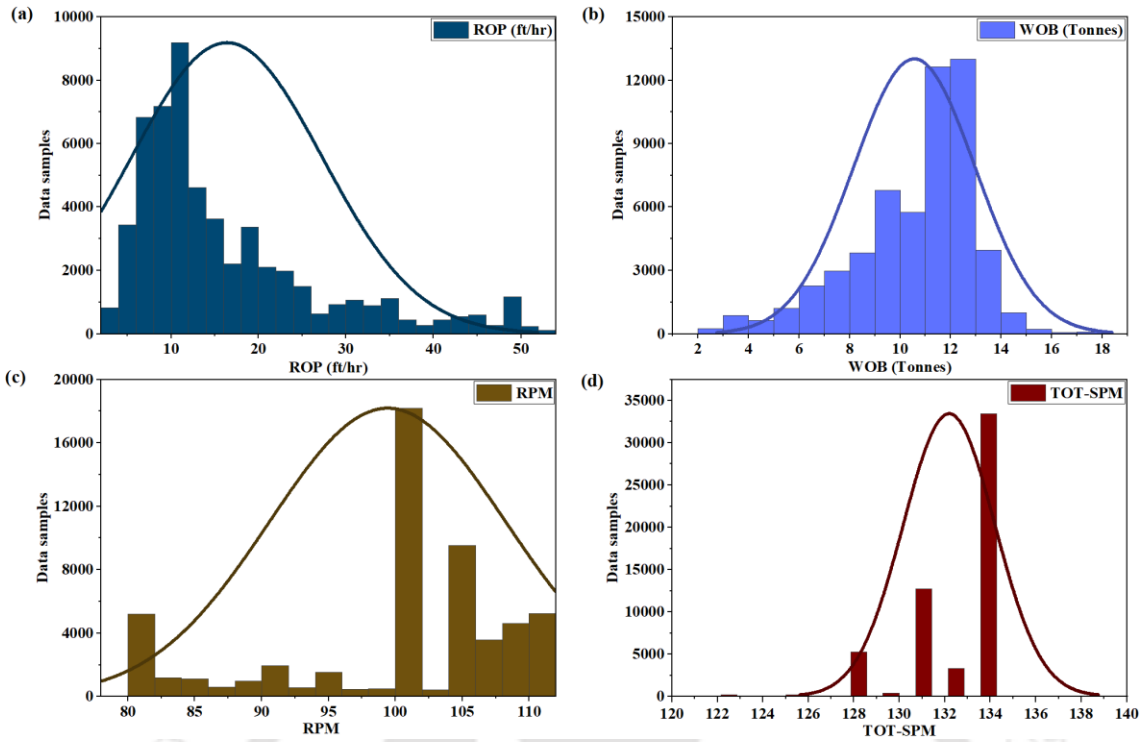

Fig. 5-3. Distribution of complete data set utilized for model development

5.4. Implementation procedure

As shown in Fig. 5-4, this work proposes a new integrated approach to optimize ROP and energy efficiency. The same can be summarized as follows:

- The drilling data comprises drill-string configuration, online sensor data from SCADA, mud parameters, and directional survey information. All this data belongs to an exploratory well is initially stored in a centralized SQL database.
- Later, the historical data is retrieved from the database, and the rotary drilling activity data alone was filtered based on the rules framed, as discussed in section 3.3.2.
- At the first level in the data segregation module, the rotary drilling data is segregated with respect to RPM for every 5 RPM interval from 80 -110 RPM.
- The second level of data segregation was done based on WOB for an interval of 1 tonne (2200 lbs).
- After two-level segregation, the ROP is plotted with respect to averaged WOB for each RPM range.

- The optimal WOB for each RPM range of an exploratory well was determined, and all the results were stored in the centralized database.
- During the development well drilling operation, the live drilling parameter from the sensor captured through SCADA will be classified to find current activity based on rules stated in section 3.3.2.
- The optimal WOB for a given RPM range, formation, and total vertical depth is retrieved from a database that was established from previous well historical data.
- The retrieved optimal WOB for the best RPM range is taken as reference value; the operator can add or subtract additional weight on the bit (WOB_{res}) to find fine-tuned optimal WOB ($WOB_{optimal}$), thereby avoiding the actual drill-off tests as given in Eq.5.12.

$$WOB_{optimal} = WOB_{SCADA} \pm WOB_{res} \quad (5.12)$$

- The new WOB and RPM combination for the optimal ROP will be stored back in the database so that it can be used for the Input Energy Module.
- In the Input Energy Module, the MSE, DSE, and HDI were estimated and are plotted against ROP and the measured depth (MD).
- Based on the play-back methodology's interpretation, the operator can be intimated about the efficient and inefficient zones and suggest appropriate actions.

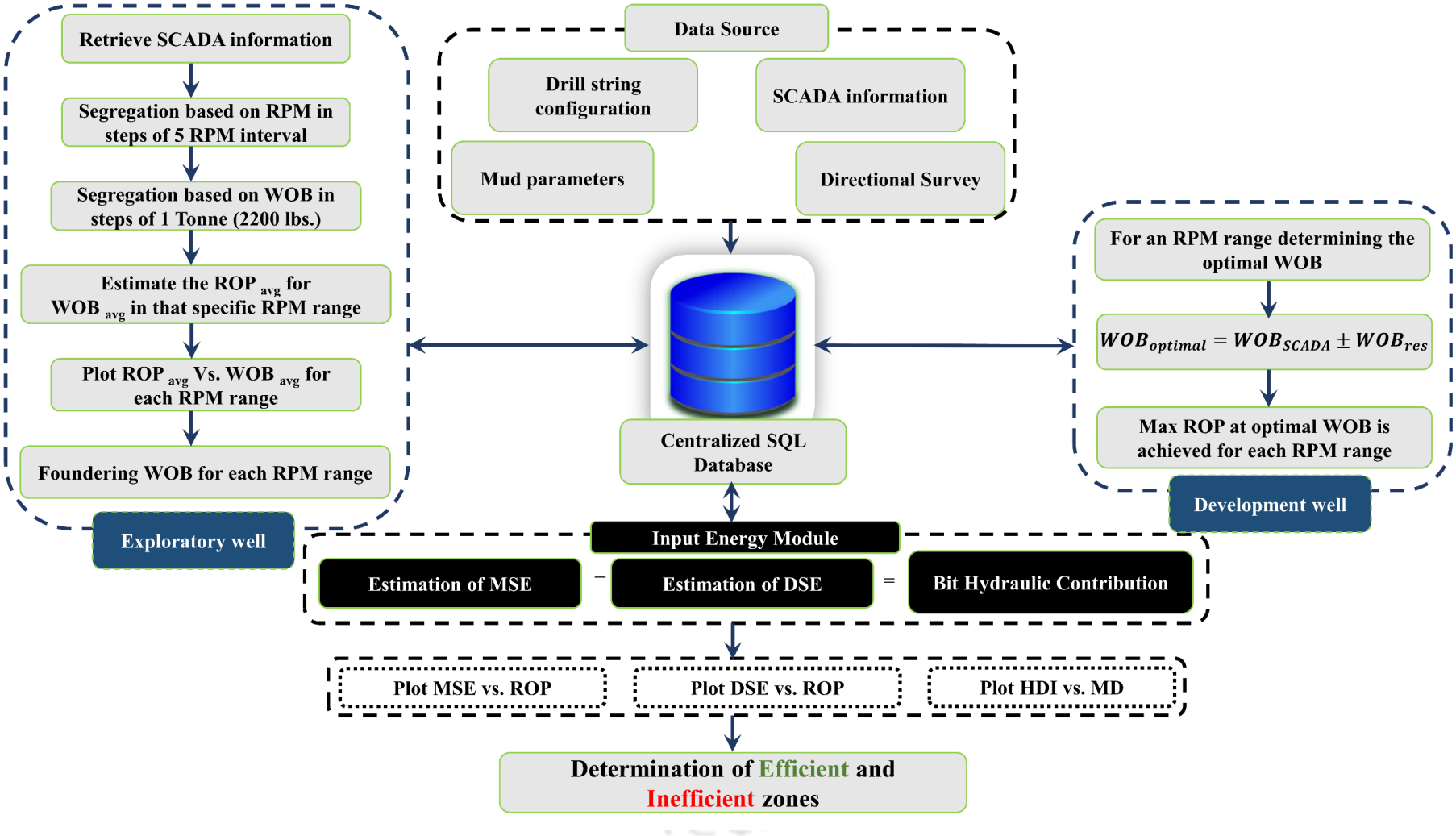

Fig. 5-4. Overall implementation methodology in exploratory and development well

5.5. Results and discussions

The above-described mathematical model is used to calculate the drilling process performance for two different wells drilled in the same geographical location in Assam by ONGC Ltd, India. The results of those well analysis are presented in this section. The design specifications of Well-A and Well-B are illustrated in Fig. 5-5.

The drilling activity planned for Well A are summarized below:

- The Well-A has to reach a target depth of 3930 m, and the 8 ½" section was planned to drill from 3460 m – 3930 m (470 m). And the lithology of the reservoir at this depth was found to be "sandstone with shale interbedded with coal and minor claystone with siltstone."
- Therefore, to combat reactive shales or clays, it is decided to adopt the KCL-Polymer PHPA (Partially Hydrolysed Poly Acrylamide) mud system. The K+ ion works powerfully, and the size of the ion fits the shale/clay pore once it arrives on the surface of clay or shale. The combination of KCL with the polymer will improve its effectiveness in concern with combating the shale. The PHPA helps encapsulate the clays/shale surface with a shielding film. This block or acts like a hindrance for base exchange and hydration, but the mud's main demerit is poor solid control. Quantities of high solid content available in the mud are always perceived as an essential factor affecting operational efficiency. Eventually, the operator won't be able to achieve optimized ROP's even when the WOB is increased to higher levels.

The daily progress report as per actual drilling is summarized based on the Drilling progress report (DPR).

- Day 1: Running in up-to the casing shoe and then followed by mud circulation, followed by running in hole to bottom till 3590 m. Later, while lifting the string, the operator has observed over pull, further to reduce the same Well-A was conditioned with mud circulation. Therefore, the operator has not observed over-pull during the next pull out. Drilling progressed to 3649 m, and then the operator observed a severe pressure drop due to blockage in the strainer. After cleaning the pump strainer, drilling progressed further.

- Day 2: While reaching depth 3690 m, again operator observed pressure drop and abnormal sound from mud pump. Also, leakage from the internal blowout preventer (IBOP) was identified. Then both the mud pump strainer was cleaned, and the leakage in the IBOP was arrested by welding. The drilling continued till 3697 m.
- Day 3: The drilling continued with the previous day established mud conditioning and circulation, and the operator has observed high torque and drag in the string. Irrespective of high torque fluctuations, the operator has attempted to drill further from 3697 m to 3739 m. Later, to reduce the risk of string stuck, the operator continued mud conditioning and improved circulation to minimize torque, and with that, drilling continued to 3746 m. However, during string reciprocation, the operator has observed severe tight pull. The operator started with mud conditioning and circulation intermittently to reduce the tight pull string and stalling. Even then, the tight pull was observed quite frequently. With no further option, the operator has increased the pull force in steps of 5 tonnes. Finally, the string got released with 30 tonnes over pull, and the string is secured with established rotation and circulation.
- Day 4: Operator has observed mud cut in the wear plate of mud pump-2. Therefore, the mud circulation was continued with mud pump-1. Then string pull out up-to-the-casing shoe. After repairing the mud pump-1 and drilling continued up to 3746m with appropriate mud conditioning and circulation and string pulled out as a part of the standard operating procedure.
- Day 5: While tripping the drill string, the operator observed high torque, string stalling, tight pull, and sticking tendency at 3624 m. Further to reduce the tight pull, the back reaming was performed up-to-the-casing shoe. Since the manifold got burst, the mud hose was changed. The back reaming and reciprocation continued further. Again, drilling progressed up to 3780 m without much trouble.
- Day 6: While drilling, the operator observed the hydraulic oil leak from the iron roughneck, and then the leak was arrested. Therefore, decided to pull out up-to casing shoe for wiper trip and lowered it to the bottom for further trouble-free drilling and finally well drilled up to 3820 m.

From the DPR summary, it can be observed that wellbore health had been deteriorated due to cuttings accumulation and poor mud hydraulics. Therefore, the wellbore had

been loaded with cuttings followed by string stalling with severe torque was experienced. Besides, the suboptimal drilling resulted in more energy consumption and non-productive time. Further to demonstrate the same, the above-proposed methodology in section.5.2.2 is used to analyse the drilling efficiency.

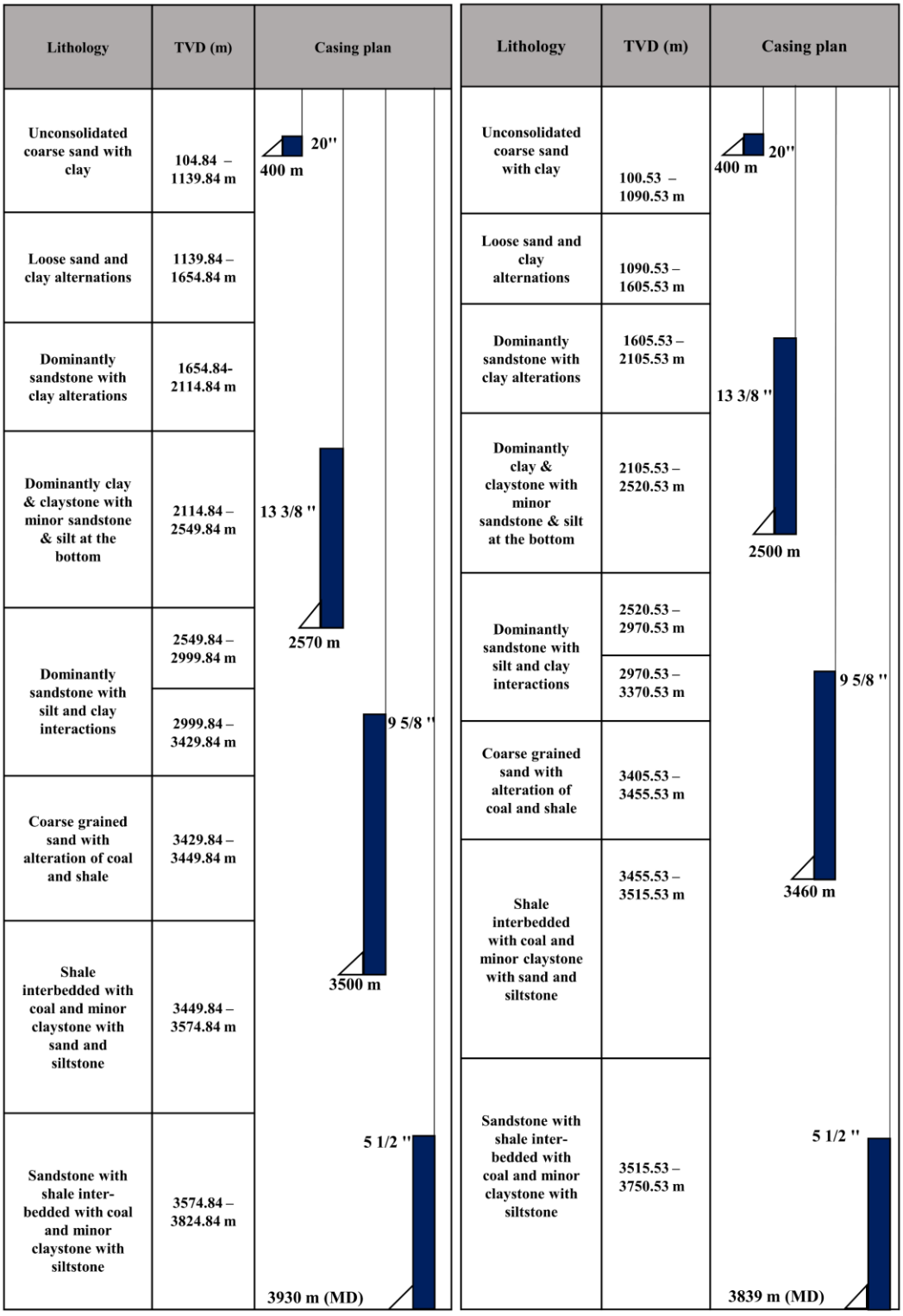

Fig. 5-5. Well plan and casing plan of Well-A and Well-B

5.5.1. Drilling ROP optimization using the play-back methodology

The complete drilling data was segregated into six groups based on RPM ranges. Further, the second level of segregation was done on WOB in steps of 1 tonne (2200 lbs.), yielding 15 data points per rpm range, which were then modelled to fit with a quadratic function (refer to Table 5-3). The plot between WOB and ROP for different RPM ranges can be used for estimating optimal ROP. If this analysis is done to drill the remaining section of the same geological conditions, it is called play-back methodology. Fig. 5-6 illustrates the plots of the play-back methodology for Well-A. A quadratic curve fit was more suitable for ROP vs. WOB data for all RPM ranges. However, in 105-110 rpm data, the trend of actual drilling points was more suitable for higher-order fit, which may be due to noise present in raw data during high RPM and WOB. Further, considering lateral complexity while using higher-order curve fit in playback methodology, quadratic curve fit is adopted for all the RPM range. In group no-1, at low RPM ranges, the maximum ROP is obtained at a foundering WOB of 8.4187 tonnes (18521.14 lbs.). With an increase in ROP, the foundering WOB started to reduce in group no-2 and group no-3 and stands at 7.1533 tonnes (15737.26 lbs.) and 7.3096 tonnes (16081.12 lbs.). And the foundering WOB further reduced in group no-4 to 5.4233 tonnes (11931.26 lbs.) and group no-5 to 2.1526 tonnes (4735.72 lbs.) and group no-6 to 5.6064 tonnes (12334.08 lbs.) respectively. From the above analysis, it can be observed that the top-drive RPM greater than 95 RPM is not helpful to improve ROP's at lower WOB.

Further, the higher RPM's may lead to higher torques, and eventually, the total input mechanical specific energy increases. Therefore, maintaining top-drive RPM less than 95 RPM could be an optimized drilling approach while comparing it with similar ROP at higher RPM conditions. Thus, the energy-based analysis is fundamental to optimize drilling ROP, presented in the below sections. In addition to RPM and WOB, variables such as drilling fluid properties and its flow rates are also significant while optimizing drilling ROP. Under suboptimal drilling conditions, the cutting may accumulate and release as drilling progress, resulting in fluctuation in the top-drive torque, as shown in Fig. 5-8 (a).

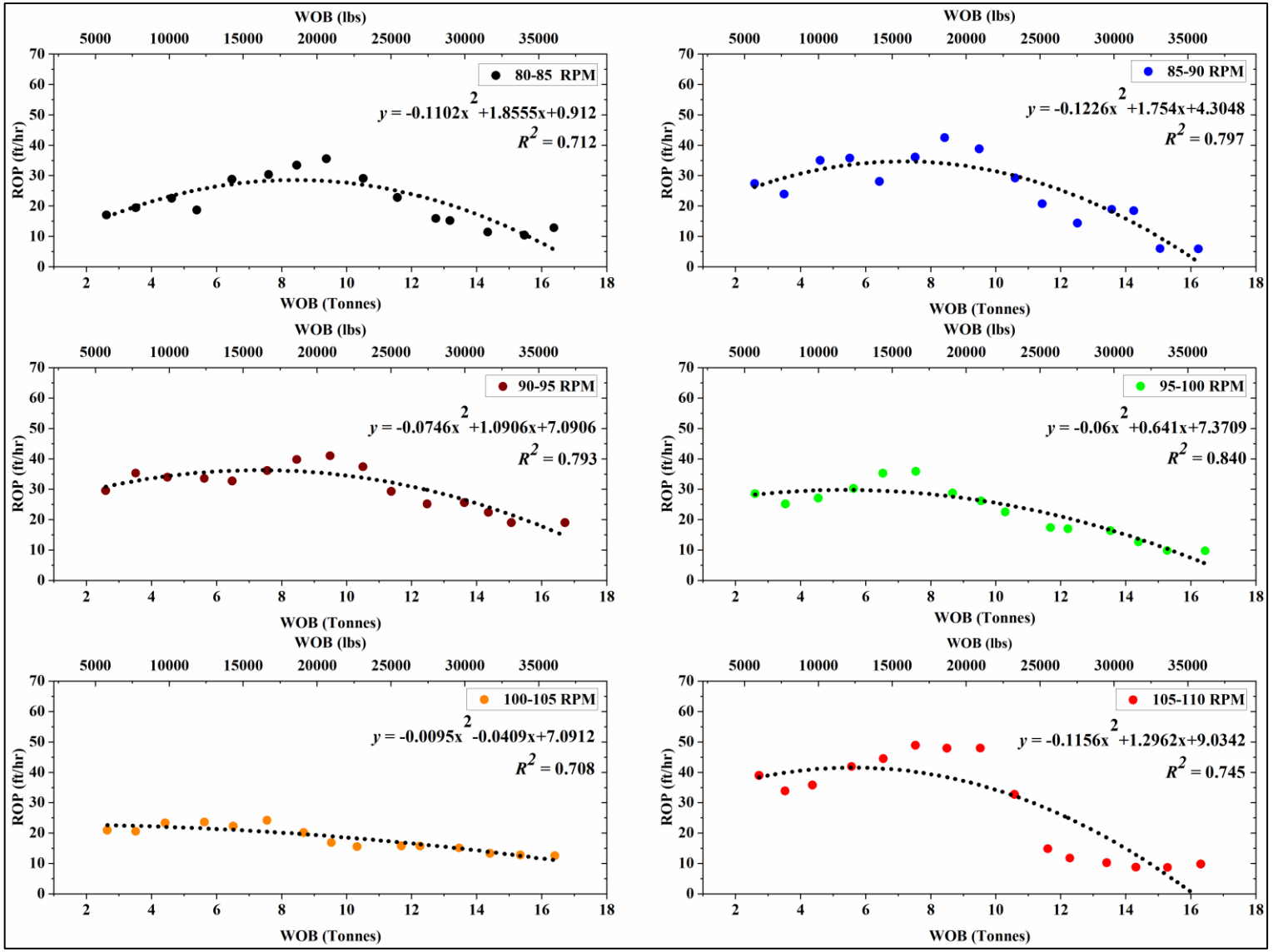

Fig. 5-6. Depiction of the play-back methodology based on drill string RPM for Well-A

Table 5-3. Drill rate test results for Well-A

	No. 1: 80-85 RPM		**No. 2: 85-90 RPM**		**No. 3: 90-95 RPM**		**No. 4: 95-100 RPM**		**No. 5: 100-105 RPM**		**No. 6: 105-110 RPM**	
	WOB	ROP	WOB	ROP	WOB	ROP	WOB	ROP	WOB	ROP	WOB	ROP
01	2.61	5.22	2.58	8.36	2.59	9.01	2.6	8.71	2.64	6.38	2.72	11.88
02	3.52	5.93	3.49	7.29	3.51	10.77	3.53	7.67	3.51	6.27	3.52	10.34
03	4.62	6.89	4.6	10.67	4.49	10.35	4.54	8.26	4.42	7.11	4.36	10.92
04	5.39	7.71	5.51	10.91	5.62	10.23	5.63	9.23	5.63	7.26	5.56	12.77
05	6.47	8.78	6.42	8.57	6.48	9.97	6.53	10.74	6.51	6.78	6.54	13.58
06	7.6	9.28	7.52	11.01	7.56	11.04	7.54	10.95	7.55	7.36	7.53	14.91
07	8.46	10.21	8.43	12.95	8.46	12.14	8.67	8.78	8.68	6.15	8.5	14.61
08	9.38	10.84	9.49	11.84	9.49	12.52	9.55	7.98	9.52	5.13	9.52	14.61
09	10.51	8.87	10.59	8.92	10.5	11.42	10.29	6.87	10.32	4.75	10.57	9.97
10	11.56	6.98	11.43	6.33	11.37	8.93	11.68	5.31	11.68	4.82	11.60	4.54
11	12.74	4.87	12.51	4.41	12.47	7.67	12.22	5.19	12.26	4.79	12.28	3.59
12	13.18	4.65	13.57	5.78	13.62	7.82	13.52	4.99	13.46	4.61	13.41	3.13
13	14.34	3.49	14.24	5.63	14.36	6.83	14.39	3.88	14.41	4.05	14.31	2.68
14	15.47	3.18	15.05	1.83	15.06	5.8	15.27	3.01	15.34	3.89	15.28	2.65
15	16.37	3.91	16.23	1.81	16.71	5.80	16.44	2.98	16.4	3.82	16.3	2.99
Foundering WOB (Tonnes)	**8.4187**		**7.1533**		**7.3096**		**5.4233**		**2.1526**		**5.6064**	

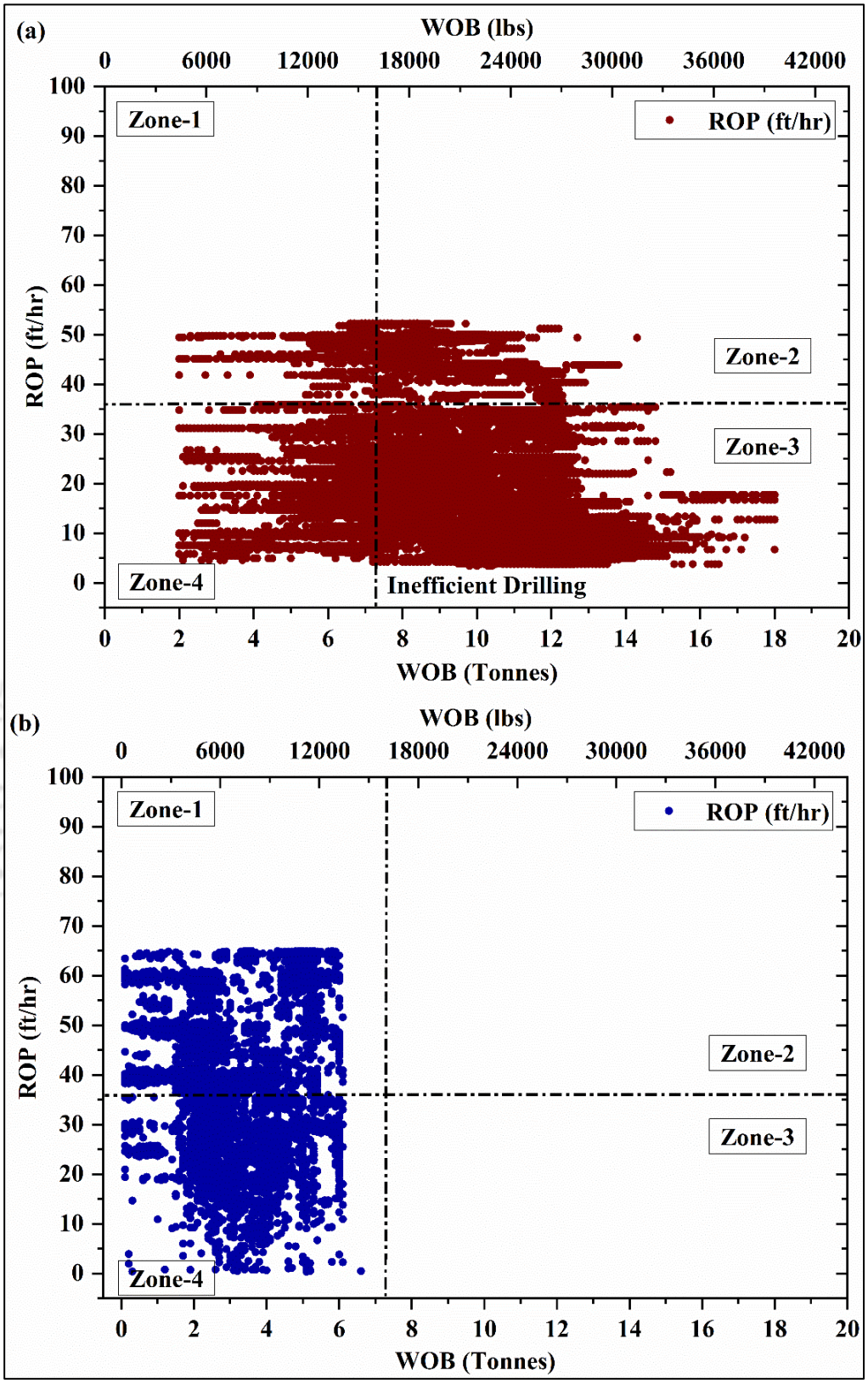

Fig. 5-7. (a) Depiction of ROP with increase in WOB for 8 ½ " section in Well-A, (b) Monitoring of ROP with an increase in WOB for Well-B

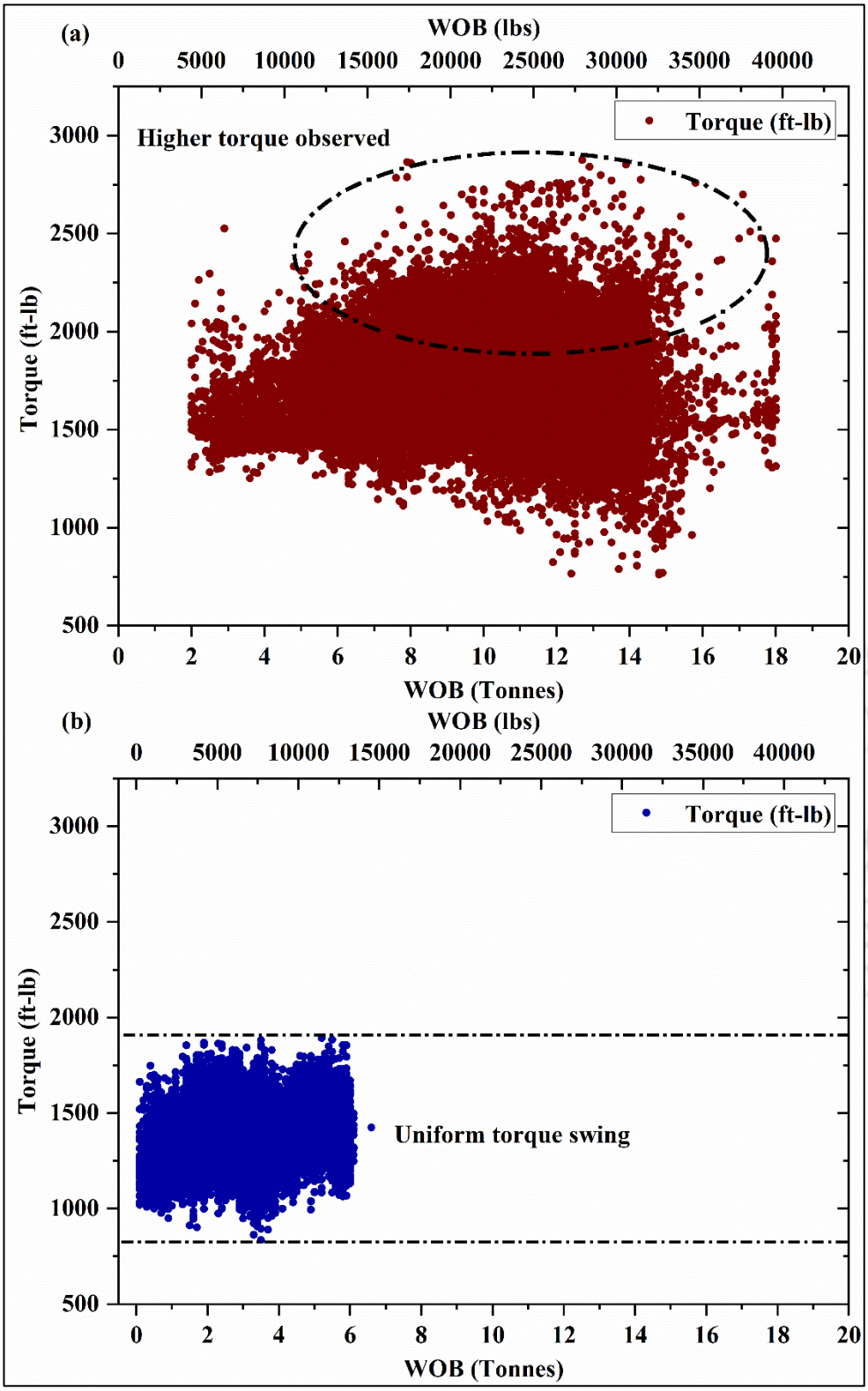

Fig. 5-8. (a) Variation of torque with an increase in WOB for Well-A indicating severe torque, (b) illustration of uniform torque fluctuations with a change in WOB in Well-B

The variation of ROP with the WOB change for Well-A is shown in Fig. 5-7 (a) for the selected depth. The data presented in Fig. 5-7 can be grouped under the zone of drilling

operation with respect to its operating efficiency by using quadratic model equations obtained from the play-back methodology (refer to Fig. 5-6). Zone-1 represents an efficient drilling zone with maximum ROP and minimum WOB. Zone-2 and zone-4 depict moderately efficient drilling zones. And zone-3 represents the inefficient drilling zone where most of the drilling was performed wherein the operator could not achieve higher ROP even with higher WOB. This may be because Well-A is an exploratory well, and the operator couldn't optimize the operational parameters on the field and resulted in more time in drilling at the expense of more input energy.

Further, the optimized drilling parameters such as WOB_{opt} = 7.30 ± 1 tonne, RPM_{opt} = 80 to 95, and mud flowrate = 128 – 134 SPM, obtained from the post-drilling analysis of Well-A are utilized for optimization of development well (Well-B) drilled in the same geographical zone and lithology. The Well-B is a directional well planned with a target depth of 3839 m. The drilling of the 8 ½" section was started from 3552 – 3839 m (287 m). The drilling optimization results for depth from 3590 m to 3820 m are demonstrated in this work, wherein lithology and formation were demonstrated similar for Well-A and Well-B at this particular depth.

Due to heavy cuttings accumulation and improper solid control in Well-A, heavy torque, string stalling, and drag were observed in several regions, as explained in Fig. 5-8 (a). Therefore, after discussing with the mud crew and drilling experts, it was suggested to drill the Well-B with LTSOBM (low toxic synthetic oil-based mud). The LTSOBM drilling fluid was chosen as it is non-reactive towards shale formations and helps achieve better ROP. It also provides better lubricity, thereby minimizing the friction between the drill pipe and the wellbore wall and lowering the possibility of stuck-pipe, torque and drag, and total input energy.

Fig. 5-8 (b) depicts the uniform variation of torque along the 8 ½" section of Well-B with WOB change. There is always a strong interdependence between the input torque and applied WOB. It was observed that the torque fluctuated between 950 ft-lb to 1900 ft-lb as WOB was chosen less than the optimal WOB of 7.309 tonnes. The operator was advised to maintain WOB close to 7.309 tonnes from the play-back method and, in any case, not more than the optimal value to avoid excess energy loss.

Further, to analyse the drilling rates, ROP variation with WOB less than 7.309 tonnes (optimal WOB for Well-A) was chosen and found to give appreciably better ROP

throughout the depth (refer to Fig. 5-7 (b)). It indicates that maximum ROP can be obtained even at lower WOB. Lower WOB eventually results in lower torque and further reduces the input energy consumption and the well cost.

5.5.2. Analysis of optimized drilling process data

5.5.2.1. Mechanical specific energy (Power-Graph) approach

MSE comprises both the energy spent for imparting WOB (weight term) and energy spent in rotational movement (torque term). The calculated MSE from WOB and torque for Well-A are presented in Fig. 5-9. The contribution to MSE by WOB is observed to be in the range of 1-2 % of total MSE, and this concludes that MSE is contributed by torque.

The complete graphical illustration of ROP Vs. MSE is divided into four quartiles to analyse the efficient and inefficient zones. Based on the optimal results obtained from the play-back methodology, ROP greater than 36.33 ft/hr is able to provide excellent drilling performance (refer to Fig. 5-9). This benchmark value varies with respect to formation and the type of drill bit utilized. Further, in terms of MSE values, a value lower than 31.579 kpsi indicated better drilling efficiency. The Well-B was drilled by applying the optimal values derived from the play-back methodology. The post-analysis of non-optimal drilling data of Well-A is presented in Fig. 5-9. Zone-1 signifies the efficient drilling zone where the operator can observe maximum ROP (greater than 36.33 ft/hr) with minimum expenditure of MSE (lower than 31.579 kpsi).

Zone-2 and zone-4 are considered moderately efficient drilling zones, and zone-3 represents an inefficient drilling zone as more energy is being consumed to achieve low drilling rates. And most of the drilling has taken place in zone-3 for Well-A, as the operator is not aware of the optimal drilling conditions in exploratory wells. As shown in Fig. 5-9, the power-graph is utilized to analyse the relationship between ROP, MSE, and power where the actual field data of Well-A is used. It was observed that with an increase in RPM, the input power at the top drive system increases. Sometimes, the power input needs to be increased to compensate for the parasitic losses in the directional wells and transfer enough power to the drill bit to achieve better drilling efficiency. However, most of the time, it is being misinterpreted and leads to suboptimal drilling conditions. One such case is reported in Fig. 5-9, where the operator tried to increase the energy input to make up for the excessive torque and drag and ended up suboptimal drilling.

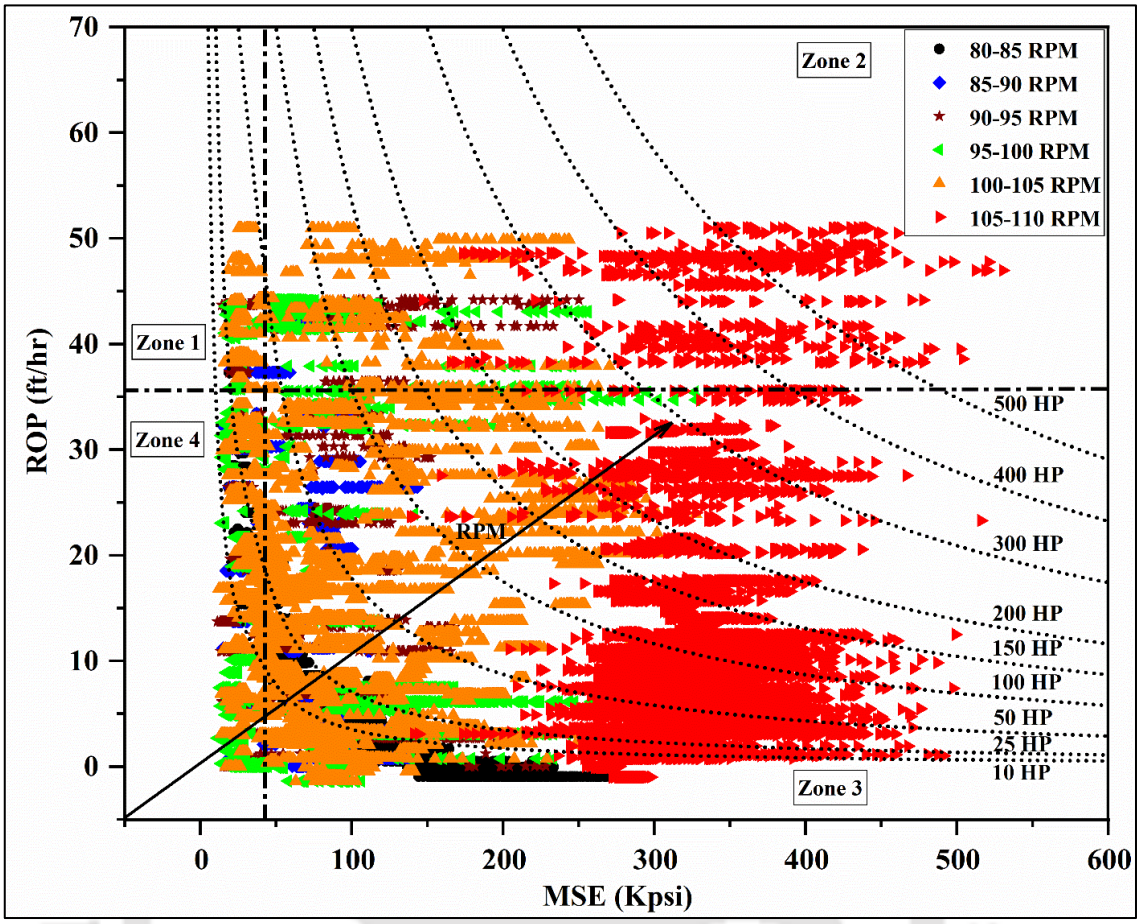

Fig. 5-9. Depiction of MSE and ROP with an increase in drill string RPM in Well-A

The input power crossed the maximum mark of 500 HP as RPM was increased, where the optimum lies around just 10 HP. It can be observed that 10 HP - 125 HP is sufficient to drill quite efficiently in the 8 ½" section of Well-A. Therefore, to effectively reduce drilling time and energy consumption, the optimal drilling parameters obtained from the play-back methodology were utilized to drill the complete section of Well-B, as shown in Fig. 5-10. The RPM ranges 80-95 were only used to drill the complete 8 ½" section, and eventually, maximum ROP was attained with much lesser input power (i.e., less than 50 HP). Comparatively, the horsepower expended in Well-B was found to be approximately 75% less than the overall horsepower spent in Well-A. The operator could efficiently avoid getting into zone-3 (i.e., in-efficient drilling zone) so that most of the operating points lie under the 50 HP curve.

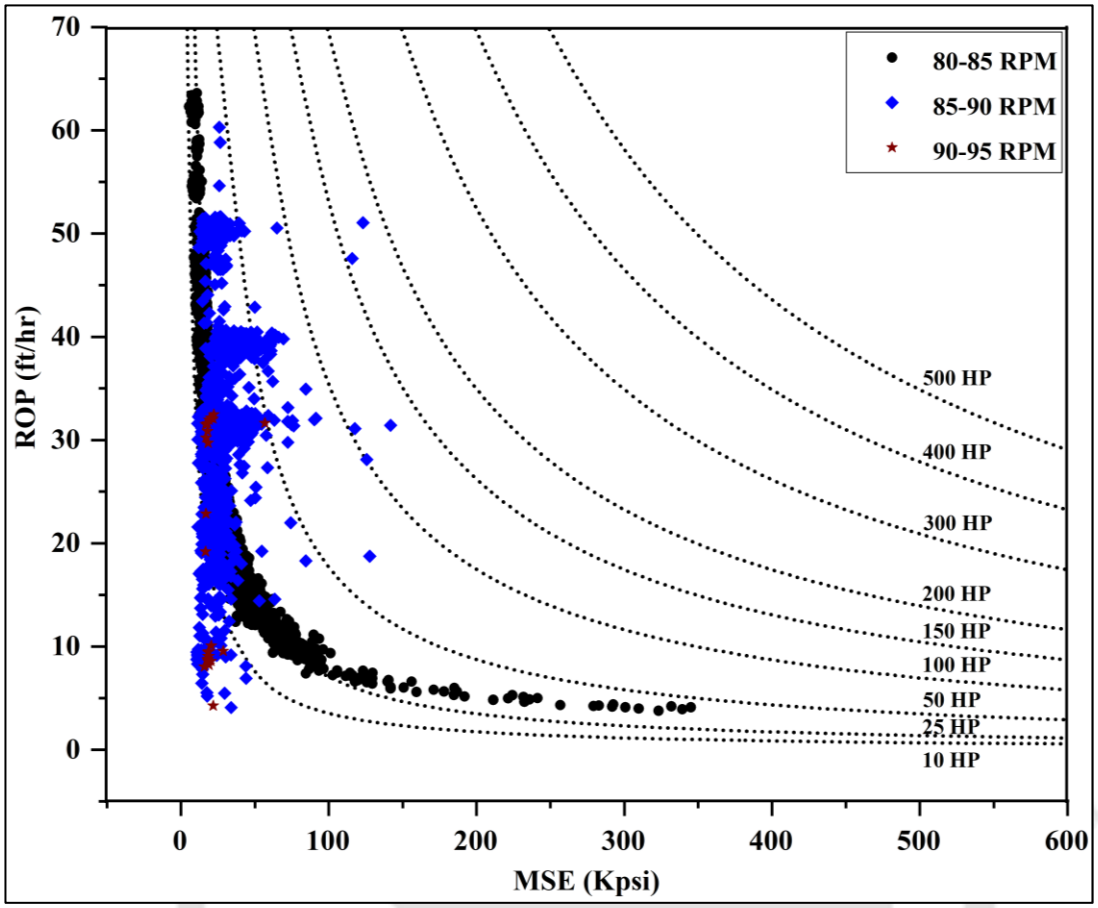

Fig. 5-10. Monitoring of MSE and ROP with an increase in drill string RPM in Well-B

5.5.2.2. Drilling specific energy (DSE) approach

Like MSE, DSE is also calculated and analysed to observe the benefit of implementing the optimized drilling condition for Well-B. As described above, the analysis of MSE can help the operator finalize the optimum WOB and RPM derived from the play-back methodology. Further, the required mud flow rate for efficient evacuation in the drill bit and transportation in the annulus can be calculated by calculating the DSE.

It's common practice in the oil industry to keep HSI in the range of 2.0 – 7.0 HP/in^2 for drilling operations (Armenta, 2008). As described in Eq.5.7, the bit hydraulic contribution reduces with an increase in weight on the bit for a fixed HSI. For example, the operator can identify an efficient drilling zone by estimating the DSE using MSE and bit hydraulic contribution. When HSI falls below the threshold value, the drilling becomes more inefficient. Therefore, the operator always aims to operate the rig above the threshold value by manipulating the mudflow rate.

The reduction of bit hydraulic contribution could explain that the HSI lower than 2 HP/in^2 falls in the inefficient drilling zone (i.e., higher DSE and lower ROP). In Fig. 5-11, the DSE was plotted against the ROP for the complete 8 ½" section of Well-A to find the efficient and inefficient zones. It was observed that with an increase in RPM, the DSE curve shifts towards the right with high HSI, and that shows the lower DSE is spent for excavating and transportation of the cuttings to the top. On the other hand, at lower ROP, the operator observed low HSI and high DSE, which indicates the inefficient drilling zone. All the drilling data that falls in the region greater than 2 HP/in^2 fits in an efficient drilling zone; this is where the maximum ROP can be obtained with minimum specific energy consumption. Therefore, the operator can adjust the operating conditions according to the region the DSE falls in and make drilling more efficient.

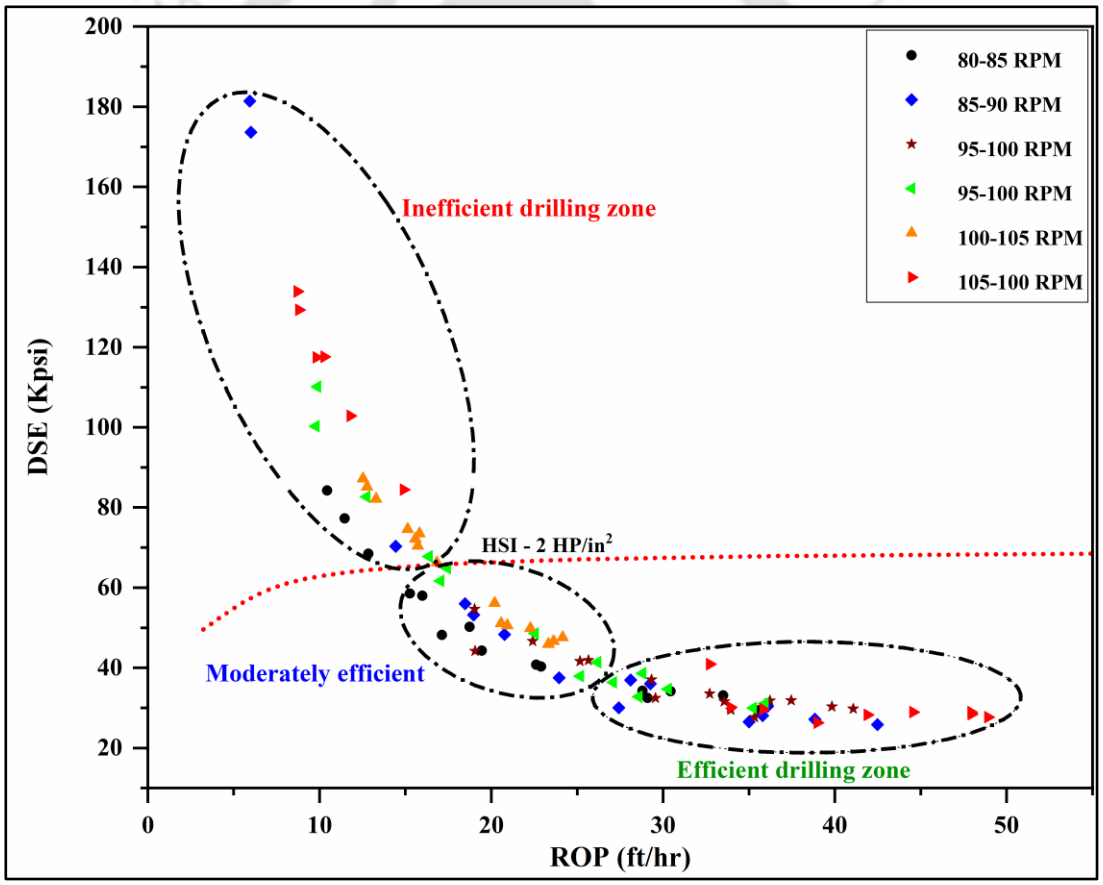

Fig. 5-11. Representation of DSE vs. ROP with field data grouped according to RPM ranges in Well-A

Additionally, it can be stated that with an increase in HSI, the drill bit's actual downhole condition can be monitored. Especially in PDC drill bits, the bit surface area can be cleaned much more efficiently and faster to remove cuttings between the bit and rock

interface and the junk slot area. With an increase in HSI, the bit balling can be prevented, lowering the ROP specifically in the regions of claystone of shale, as the cutters are entirely covered with the cuttings.

5.5.2.3. MSE and DSE combined - HDI approach

As described in section 5.2.3.3, it is obligatory to excavate the cuttings underneath a bit for efficient drilling. The ratio between ROP and the bit hydraulic contribution (a function of MSE and DSE) is termed as HDI. By calculating HDI, the operator can understand the contribution of drill bit hydraulics while maximizing the ROP. For example, the HDI equals 10 ft/hr/kpsi, signifying that the bit alone will expend one kpsi power to drill at 10 feet per hour rate for the particular WOB and RPM. Therefore, low HDI indicates that more energy is spent in the bit to drill that particular formation. It also shows the significance of cuttings accumulation in the annulus and beneath the bit, bit wear, formidable impermeable formations. Accordingly, the operator can change the type of drill bit or adjust flow conditions to maximize penetration rate at minimum consumed energy. Higher HDI values indicate efficient drilling with better wellbore conditions (i.e., proper cuttings transportation, no caving deposition, no downhole complications, and other positive signs) and soft to medium formation, bit health. The results indicate that bit hydraulic horsepower significantly influenced the drilling rate for the range of drilling conditions and rocks examined. The degree to which the drilling rate was affected by bit hydraulic horsepower depended on the rock/drilling-fluid combination.

Fig. 5-12 (a.1) illustrates the change in HDI along with the depth for the 8 ½" section in Well-A. From 3590 – 3630 m, the HDI was around 50 ft/hr/kpsi, indicating better ROP with efficient cuttings transportation. After crossing the 3630 m, the HDI value had dropped down to around 10 ft/hr/kpsi, depicting insufficient drilling operational parameters and inefficient hydraulics. Later, the HDI fluctuated approximately 50 ft/hr/kpsi for a short time and collapsed to below 5 ft/hr/kpsi soon after 3700m depth. It is evident from the data that poor ROP was achieved for the remaining depth. Eventually, drilling hours increased, and hence the total energy input too. Besides, Fig. 5-12 (a.2) represents the variation of HDI with ROP. The optimal ROP is achieved from the play-back study at HDI 27.01 ft/hr/kpsi, which is not enough to clean the bore well and eventually encountered many downhole problems like high torque (refer to Fig. 5-8 (a)) and tight pulls. HDI above 47 ft/hr/kpsi is recommended for the formation and section

considered. Maintaining HDI above the optimal value is essential to achieve better hole cleaning to avoid downhole complications.

Further, to validate the concept of HDI, the calculated HDI at optimal drilling conditions for Well-B is shown in Fig. 5-12 (b.1). Except for the depth range of 3660 – 3685 m (i.e., around 25 ft/hr/kpsi), the HDI was found to be above 47 ft/hr/kpsi, indicating better-operating conditions and hydraulics. Monitoring this metric during real-time drilling activity would help the operator find inefficient drilling zones and maintain improved hydraulics to achieve the target depth in the stipulated time. Fig. 5-12 (b.2) illustrates the variation of HDI with an increase in ROP. In Well-B, most of the drilling is observed at higher HDI indicating proper wellbore health and efficient cuttings transportation.

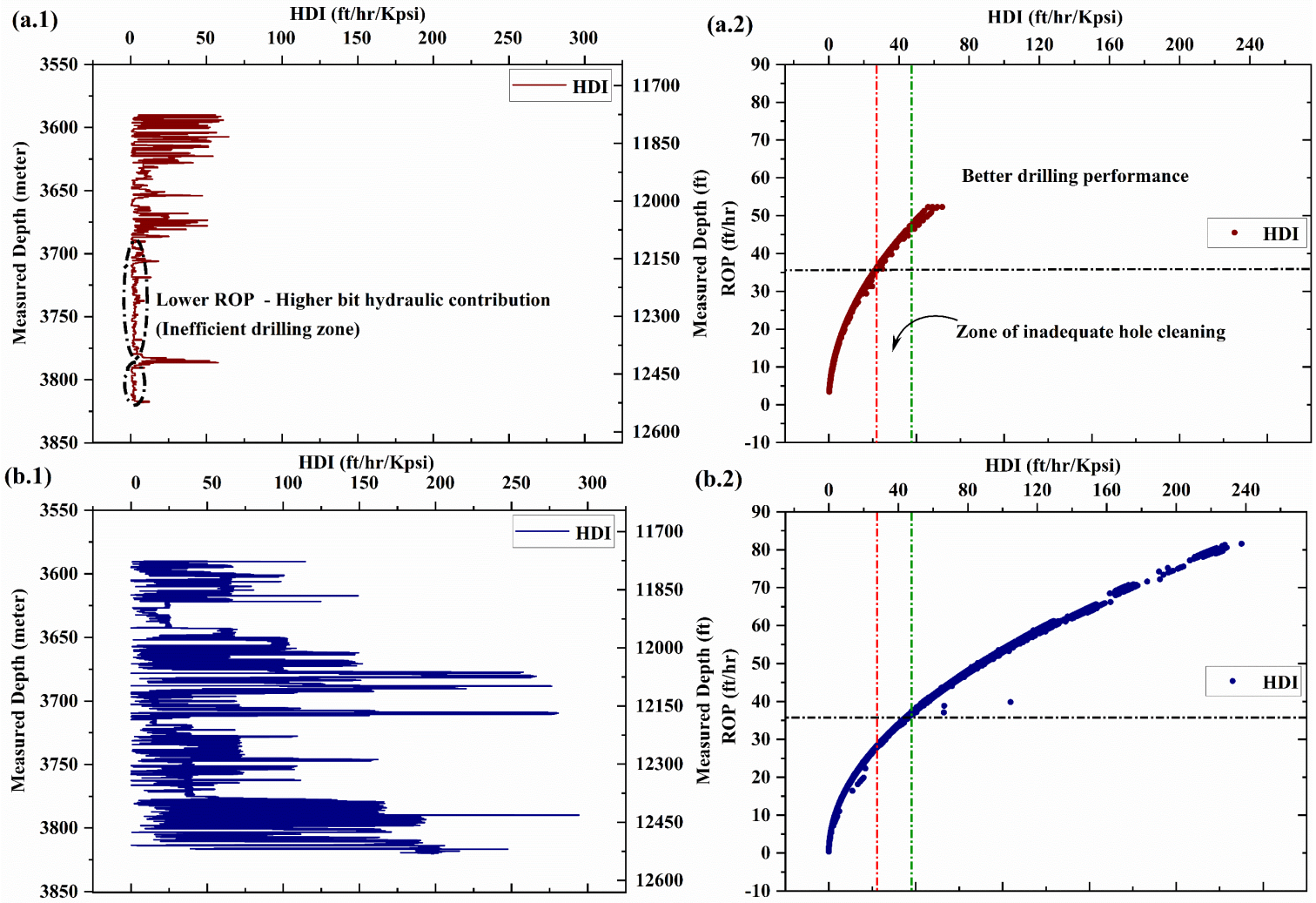

Fig. 5-12. (a.1) Depiction of HDI with an increase in depth for 8 1/2 " section in Well-A, (a.2) Variation of HDI with ROP in Well-A, (b.1) Monitoring the HDI with depth for 8 ½" section in Well-B during real-time drilling activity, (b.2) Variation of HDI with ROP in Well-B

5.6. Challenges in real-time implementation

1. **Data aggregation**: Accumulation of exploratory data from the field database of the sponsoring agency (Oil and Natural Gas Corporation, India) for the preliminary analysis has been difficult due to sensitivity and security reasons. Further, while implementing the field trial, problems associated with the rig-server, collection of the geotechnical order (GTO), daily drilling progress reports, mud reports, and discussions with on-field experts are time-consuming.
2. **Data segregation**: During the preliminary analysis, various methodologies were tested for the selection of optimum drilling parameters. The data segregation rules vary from method to method, which consumes a lot of time.
3. **Literature selection**: Most of the works published in recent times have completely shifted towards AI/ML techniques, which rely on a huge quality of information. And very few research works have reported the utilization of minimal available information for model implementation. Henceforth, the identification of suitable literature for the current study is really challenging.

5.7. Summary

A comprehensive investigation on the selection of optimal drilling parameters using improved playback methodology is presented in this chapter. The selected optimal parameters are further utilized to drill an offset well (development well). By adopting this methodology, the total specific energy input expended is minimized. A new concept for monitoring the ROP with bit hydraulic contribution is introduced and is labelled as Hydraulic Drilling Impact (HDI). An actual case study of a directional well drilled in North-Eastern India is presented and discussed in brief.

Chapter

6

CHAPTER 6

Conclusions and Future Work

6.1. Foreword

This chapter outlines this thesis's significant contributions to develop hybrid models to prevent downhole complications and select optimal drilling parameters. The critical observations made from the field study conducted in directional wellbores drilled in North-Eastern parts of India are presented.

6.2. Anomaly detection using predicted hookload and neutral-point

The work is focused on a detailed investigation of the development and utilization of a hookload model to detect the upcoming downhole complications in both vertical and directional wellbores. Aadnoy's 3-Dimensional frictional model is modified to determine the total load acting at the deadline. A bottom-up approach is employed where the real-time weight on the bit is fed to the model. The model was integrated with a Decision Support System (DSS) and deployed during real-time drilling conditions in a directional wellbore. The following conclusions are made from the study:

- The Rig Uncertainty Compensation (RUC) factor considered all the uncertainties that arise from various sources, namely: drill lines weight, stick-slip in rotating sheaves, tilting of traveling block, and uncertainties from unaccounted sources have helped in determining an accurate hookload at the deadline.
- The deviation of the actual hookload from the estimated hookload provided preliminary information to the operator about the upcoming complication through necessary signatures.
- Any hookload deviation greater than ±2.5 tonnes, which is 1% of the total rig capacity, is considered a zone of anomaly.
- Analysis-based hookload alone might have given wrong interpretations for operator in the case of identifying complications. Monitoring secondary key drilling parameters in real-time helped the operator take appropriate action for vertical and directional wellbores:
    - In the study conducted on vertical wellbores, cuttings accumulation in the wellbore section is recognized by the reduction in RPM at non-negative WOB, drop down in ROP, and gradual SPP shoot-up. Further, gradual loss of weight (load at the deadline) indicated an under-gauged wellbore with slow cuttings accumulation.

- In directional wellbores, the shearing of the drill string is identified by the variation in hookload, sudden drop in ROP with increasing WOB, and loss in SPP at a constant flow rate. The post-drilling investigation revealed that the drill string got sheared at the pin section, as the pin joints take up more stress when compared to the total body.

- The neutral point monitoring along the drill string helped the operator take preventive measures and control the operating parameters such that it doesn't enter the drill pipe region. The neutral point is compared with the total BHA length and 15% BHA length, alerting the operator if it shifts into the danger zone.

Although the modified hookload model is a feasible option to detect the downhole complications, there is a need to account for the effect of hydraulics on the true loads and evaluate the overall stresses acting on the drill string to determine the root cause. This motivated the research work to further extend towards evaluating the structural integrity of tubular using true tension and effective tension model. The key findings of the study are presented in the next section.

6.3. Evaluation of structural integrity of tubulars in directional wellbores

The current study focuses on evaluating the structural integrity of the tubular in directional wellbores using a true tension and effective tension model. In addition, Johancsik's model was included in determining the overall stresses acting along the length of the drill string. All these determined forces are further utilized to determine the hookload at the deadline and neutral point. The developed model was implemented in the directional wellbore and modified Aadnoy's 3-Dimensional frictional model to help detect the downhole complications and identify the root cause of the upcoming problem. The real-time implementation of the overall stress model in the directional wellbore had drawn some significant conclusions as follows.

- Incorporating the RUC factor in the true tension and effective tension model helped in the inclusion of hydraulic effects and the rig and wellbore uncertainties for hookload determination.
- The proposed model can estimate the hookload at the deadline with an average residual error of 0.97 % for regular drilling operations in directional wellbores. Moreover, monitoring of actual hookload with measured hookload helps in the identification of downhole complications. And to confirm the anomaly and root

cause identification, the other key rig sensor parameters are monitored with an increase in total depth.

- The inclusion of the bending stress magnification factor (BSMF) in the bending stress calculations will help determine actual fatigue stresses that the drill string experience in actual drilling conditions.
- Monitoring of the normal forces has helped the operator in the identification of the key-seating zones. Any force more significant than 2000 lbs. is marked as crucial operating zones, and appropriate action is taken instantly.
- The tensional forces along the drill string are compared to the critical buckling force at each time step and helped prevent buckling, eventually leading to severe fatigue. Upon repetitive application of loads, the extreme fatigue section of the drill string would part off entirely and will cause an increase in NPT.
- The outcomes from the current study signify that the developed model can evaluate all the forces during rotary drilling activity. However, utilization of these methodologies can only prevent upcoming complications. Further applying optimal drilling parameters may prevent complications and minimize the total energy expended. Therefore, the study was extended to determine the optimal drilling parameters using an improved playback methodology presented in the next section.

6.4. Optimization of drilling parameters using improved playback methodology

The ROP optimization by using play-back methodology is demonstrated to improve drilling efficiency. The proposed method utilized historical data of the exploratory Well-A data and applied it to develop Well-B located in the same geographical zone in real-time (3590 m – 3820 m). The validation of the play-back methodology is presented by calculating and analysing MSE, DSE, and HDI. While developing and demonstrating the play-back methodology, the following essential observations are concluded.

- The drill-off test is one of the critical requirements to apply playback methodology for ROP optimization. The optimized drilling operating conditions such as WOB_{opt} = 7.30 tonne, RPM_{opt} = 80 to 95, and mud flow rate = 128 – 134 SPM are obtained from the post drilling analysis.
- By monitoring the power graphs plotted between the MSE and ROP, the efficient and inefficient drilling zones can be identified and can rectify the malfunctions in

real-time. The optimal results from the play-back methodology aided in the segregation of the zones, where ROP greater than 36.33 ft/hr and MSE lesser than 31.579 kpsi is designated as efficient drilling zone.

- Similarly, by monitoring the DSE, the required optimal mud flow rate can be calculated in real-time.
- The cutting transport efficiency and wellbore health can be monitored by plotting HDI with changes in depth and ROP. The HDI profile helps adjust the flow rate and mud weight and even implicates the rock-drilling mud interaction. And in the studied lithological section, HDI greater than 47 ft/hr/kpsi indicates better operating conditions and hydraulics selection.

6.5. Recommendation for future research

The work carried out for this thesis offers better prospects to improve and enhance the research work on the prediction and prevention of downhole complications. It is crucial to the outcome that more improvements should be carried out during the commercialization of the DSS tool. From the research conducted and facts reported in this thesis, some additional work can be performed which were not covered in this thesis and may be appropriate for future progress:

- The developed analytical models can be extended to advanced top-drive systems or rotary table drive systems with different rig horsepower and mud hose systems to consider all the physical rig uncertainties pertained to specific rig and wellbore.
- Instead of measuring the hookload at the deadline, the TTS sub can be installed onto the top drive in all modern rigs, avoiding many uncertainties. Eventually, the analytical hookload model need not consider all the rig and wellbore uncertainties. This would minimize the total computational load and provide better accuracy in determining the downhole complications such as high MSE, stick-slip, excessive hole drag, and stuck pipe. In addition, the TSS sub can also be fortified with additional sensing capabilities for the determination of shear and bending stress to diagnose complications that arise due to top drive alignments.
- In the wells where the top drive system and the positive displacement motor (PDM) give the essential power input, the developed model needs to be modified considering the downhole bit RPM and effective WOB transferred to the drill bit.

- Determining wellbore pressures during drilling activity would help the operator take proactive measures by altering the mud properties or flow rate. This would prevent downhole complications such as differential sticking, lost circulation, and kick. And can be achieved by utilizing a downhole sensor or developing an ML technique to estimate the formation pressures based on the offset well information.
- The utilization of additional MWD sensors helps determine formation data, which would aid in the early detection of downhole complications.
- A multi-objective optimization technique implemented in real-time drilling activity would aid the operator in determining optimal drilling parameters. The drilling optimization technique should consider the downhole BHA lateral and torsional vibrations to maximize the ROP and achieve trouble-free drilling.
- A profound investigation using the play-back methodology can be extended for horizontal wells where hole-cleaning and achieving optimized ROP is a daunting task. It can be further improvised with the downhole MWD tool information in subsequent enhancements as it is considered more accurate. Additionally, depending on drill bit type, while utilizing the specific energy concept, the input hydraulic mechanical specific energy (HMSE) should be considered instead of MSE. The HMSE considers all the bit and mud-related factors that improve the accuracy in the estimation of overall specific energy calculations.
- The developed techniques can also be fortified, and necessary changes should also be made for all drilling tools and equipment to sustain high-temperature reservoirs and hard formations in geothermal well drilling. The study can also be extended to drilling planetary bodies like the moon and mars, where water is considered as precious as oil. Designing customized drilling rigs and the application of drilling engineering concepts would reduce the cost of space exploration and helps in the building of human colonies in planetary bodies.
- Application of AI/ML techniques by utilizing vast offset wellbore information and prior knowledge of the field and lithological information would be helpful for early prediction of downhole complications, ROP maximization and eventually helps in reducing the overall well economics and time.

REFERENCES

Aadnoy, B. S. (2010). *Modern well design*. CRC press.

Aadnøy, B. S., & Andersen, K. (2001). Design of oil wells using analytical friction models. *Journal of petroleum Science and Engineering*, *32*(1), 53-71.

Aadnoy, B. S., Fazaelizadeh, M., & Hareland, G. (2010). A 3D analytical model for wellbore friction. *Journal of Canadian Petroleum Technology*, *49*(10), 25-36.

Abbott, A. (2015, September). The MSE ratio: the new diagnostic tool to optimize drilling performance in real-time for under-reaming operations. In *SPE Annual Technical Conference and Exhibition*. OnePetro.

Agbaji, A. L. (2009). Development of an algorithm to analyze the interrelationship among five elements involved in the planning, design and drilling of extended reach and complex wells.

Agbaji, A. L. (2011, May). Optimizing The Planning, Design And Drilling Of Extended Reach And Complex Wells. In *SPE/DGS Saudi Arabia Section Technical Symposium and Exhibition*. OnePetro.

Al-AbdulJabbar, A., Elkatatny, S., Mahmoud, M., Abdelgawad, K., & Al-Majed, A. (2019). A robust rate of penetration model for carbonate formation. *Journal of Energy Resources Technology*, *141*(4).

Alali, A. M., Abughaban, M. F., Aman, B. M., & Ravela, S. (2021). Hybrid data driven drilling and rate of penetration optimization. *Journal of Petroleum Science and Engineering*, *200*, 108075.

Al-Ansari, A. A., & Kilani, M. H. (2009, October). Specially Formulated Drilling Fluid Prevents Differential Sticking, Mud Losses, and Wellbore Instability in Oil and Gas Wells in Saudi Arabia. In *Middle East Drilling Technology Conference & Exhibition*. OnePetro.

Al-Baiyat, I., & Heinze, L. (2012, December). Implementing artificial neural networks and support vector machines in stuck pipe prediction. In *SPE Kuwait International Petroleum Conference and Exhibition*. OnePetro.

Alhamed, H., Alshaarawi, A., Albadran, M., & Alshalan, M. (2020, January). Stuck Pipe Mitigating During Drill Pipe Connection Using Rotation Continuous Circulation Tool. In *International Petroleum Technology Conference*. OnePetro.

Allen, F., Tooms, P., Conran, G., Lesso, B., & Van de Slijke, P. (1997). Extended-reach drilling: breaking the 10-km barrier. *Oilfield Review*, *9*(4), 32-47.

Al Gharbi, S., Ahmed, M., & ElKatatny, S. (2018, November). Use metaheuristics to improve the quality of drilling real-time data for advance artificial intelligent and machine learning modeling. Case study: cleanse hook-load real-time data. In *Abu Dhabi International Petroleum Exhibition & Conference*. OnePetro.

Al-Qasim, A. S., Al-Arfaj, M., & Kokal, S. (2020). *U.S. Patent No. 10,669,798*. Washington, DC: U.S. Patent and Trademark Office.

Al-Rubaii, M. M., Gajbhiye, R., Al-Yami, A., Haq, B., Glatz, G., & Al-Awami, M. (2020, October). An Engineering Approach to Optimise Rate of Penetration through Drilling Specific Energy. In *Offshore Technology Conference Asia*. OnePetro.

Alshaikh, A. A., & Amanullah, M. (2018, April). A Comprehensive Review of Differential Sticking, Spotting Fluids, and the Current Testing and Evaluation Methods. In *SPE Kingdom of Saudi Arabia Annual Technical Symposium and Exhibition*. OnePetro.

Alsubaih, A., Albadran, F., & Alkanaani, N. (2018, January). Mechanical specific energy and statistical techniques to maximizing the drilling rates for production section of mishrif wells in southern Iraq fields. In *SPE/IADC Middle East Drilling Technology Conference and Exhibition*. OnePetro.

Amadi, K., & Iyalla, I. (2012, June). Application of mechanical specific energy techniques in reducing drilling cost in deepwater development. In *SPE deepwater drilling and completions conference*. OnePetro.

Armenta, M. (2008, September). Identifying inefficient drilling conditions using drilling-specific energy. In *SPE Annual Technical Conference and Exhibition*. OnePetro.

Azar, J. J. (2004). Oil and Natural Gas Drilling. In Cutler J. Cleveland (Ed.). *Encyclopaedia of Energy* (pp. 521– 534). Elsevier.

Ben, Y., James, C., & Cao, D. (2019, July). Development and application of a real-time drilling state classification algorithm with machine learning. In *SPE/AAPG/SEG Unconventional Resources Technology Conference*. OnePetro.

Bible, M. J., Hedayati, Z., & Choo, D. K. (1991, March). State-of-the-art Trip Monitor. In *SPE/IADC Drilling Conference*. OnePetro.

Biegler, M. W., & Kuhn, G. R. (1994, February). Advances in prediction of stuck pipe using multivariate statistical analysis. In *IADC/SPE Drilling Conference*. OnePetro.

Bourgoyne, A. T., & Young, F. S. (1974). A multiple regression approach to optimal drilling and abnormal pressure detection. *Society of Petroleum Engineers Journal*, *14*(04), 371-384.

Brady, P. V., Freeze, G. A., Kuhlman, K. L., Hardin, E. L., Sassani, D. C., & MacKinnon, R. J. (2017). Deep borehole disposal of nuclear waste: US perspective. In *Geological Repository Systems for Safe Disposal of Spent Nuclear Fuels and Radioactive Waste* (pp. 89-112). Woodhead Publishing.

Bzdok, D., Altman, N., & Krzywinski, M. (2018). Points of significance: statistics versus machine learning. *Nature Methods 2018a*, 1-7.

Cayeux, E., & Daireaux, B. (2009, March). Early detection of drilling conditions deterioration using real-time calibration of computer models: field example from North Sea drilling operations. In *SPE/IADC Drilling Conference and Exhibition*. OnePetro.

Chatar, C., Suresha, S., Shao, L., Gupta, S., & Roychoudhury, I. (2021, March). Determining Rig State from Computer Vision Analytics. In *SPE/IADC International Drilling Conference and Exhibition*. OnePetro.

Chen, W., Shen, Y., Zhang, Z., Bogath, C., & Harmer, R. (2019, September). Understand Drilling System Energy Beyond MSE. In *SPE Annual Technical Conference and Exhibition*. OnePetro.

Chen, W. C. (1990). Drillstring fatigue performance. *SPE drilling engineering*, *5*(02), 129-134.

Chen, X., Fan, H., Guo, B., Gao, D., Wei, H., & Ye, Z. (2014). Real-time prediction and optimization of drilling performance based on a new mechanical specific energy model. Arabian Journal for Science and Engineering, 39(11), 8221-8231.

Chen, X., Yang, J., & Gao, D. (2018). *Drilling performance optimization based on mechanical specific energy technologies* (Vol. 1, pp. 133-162). London, UK: Intechopen Limited.

Coelho, M. (2018, March 8). *Causes of kicks*. LinkedIn. Retrieved December 1, 2021, from https://www.linkedin.com/pulse/causes-kicks-mariana-coelho.

Collins, T., & Vaghi, F. (2002, February). Analysis of the fatigue resistance of rotary shouldered connections. In *IADC/SPE Drilling Conference*. OnePetro.

Courteille, J. M., & Zurdo, C. (1985, September). A new approach to differential sticking. In *SPE Annual Technical Conference and Exhibition*. OnePetro.

Dangerfield, J. W. (1987). Analysis improves accuracy of weight indicator reading. *Oil Gas J.;(United States)*, *85*(32).

Daireaux, B., Ambrus, A., Carlsen, L. A., Mihai, R., Gjerstad, K., & Balov, M. (2021, March). Development, Testing and Validation of an Adaptive Drilling Optimization System. In *SPE/IADC International Drilling Conference and Exhibition*. OnePetro.

DeGeare, J. P. (2014). *The guide to oilwell fishing operations: tools, techniques, and rules of thumb*. Gulf Professional Publishing.

DrillScan. (2013). Torque & Drag & Buckling/Soft-string vs Stiff-string Models

Dunlop, J., Lesso, W., Aldred, W., Meehan, R., Orton, M. R., & Fitzgerald, W. J. (2006). *U.S. Patent No. 7,128,167*. Washington, DC: U.S. Patent and Trademark Office.

Dupriest, F. E. (2006, September). Comprehensive Drill Rate Management Process To Maximize ROP. In *SPE Annual Technical Conference and Exhibition*. OnePetro.

Dupriest, F. E., & Koederitz, W. L. (2005, February). Maximizing drill rates with real-time surveillance of mechanical specific energy. In *SPE/IADC drilling conference*. OnePetro.

Dupriest, F. E., Witt, J. W., & Remmert, S. M. (2005, November). Maximizing ROP with real-time analysis of digital data and MSE. In *International petroleum technology conference*. OnePetro.

Elgibaly, A. A., Farhat, M. S., Trant, E. W., & Kelany, M. (2017). A study of friction factor model for directional wells. *Egyptian journal of petroleum*, *26*(2), 489-504.

Eren, T., & Ozbayoglu, M. E. (2010, January). Real time optimization of drilling parameters during drilling operations. In *SPE oil and gas India conference and exhibition*. OnePetro.

Eric, C., Skadsem, H. J., & Kluge, R. (2015, March). Accuracy and correction of hook load measurements during drilling operations. In *SPE/IADC Drilling Conference and Exhibition*. OnePetro.

Etesami, D., G Shirangi, M., & Zhang, W. J. (2021). A Semiempirical Model for Rate of Penetration with Application to an Offshore Gas Field. *SPE Drilling & Completion*, *36*(01), 29-46.

Falconer, I. G., Belaskie, J. P., & Variava, F. (1989, February). Applications of a Real Time Wellbore Friction Analysis. In *SPE/IADC Drilling Conference*. OnePetro.

Frafjord, C. (2013). *Friction Factor Model and Interpretation of Real Time Data* (Master's thesis, Institutt for petroleumsteknologi og anvendt geofysikk).

Freithofnig, H. J., Spoerker, H. F., & Thonhauser, G. (2003, October). Analysis of hook load data to optimize ream and wash operations. In *SPE/IADC Middle East Drilling Technology Conference and Exhibition*. OnePetro.

Fruhwirth, R., Arnaout, A., Winter, M., Esmael, B., & Thonhauser, G. (2012). Model-Based Hookload Monitoring and Prediction at Drilling Rigs using Neural Networks and Forward-Selection Algorithm.

Galle, E. M., & Woods, H. B. (1963, January). Best constant weight and rotary speed for rotary rock bits. In *Drilling and production practice*. American Petroleum Institute.

Graham, J. W., & Muench, N. L. (1959, October). Analytical determination of optimum bit weight and rotary speed combinations. In *Fall meeting of the Society of Petroleum Engineers of AIME*. OnePetro.

Guerrero, C. (2007). SPE Drilling Studies Group, Drilling Engineer, Drilling Solutions Team. *Drilling Optimization with Mechanical Specific Energy*.

Guidry, J., Shi, X., Meehan, R., Fang, J., & Lan, L. (2010). *U.S. Patent No. 7,845,429*. Washington, DC: U.S. Patent and Trademark Office.

Hankins, D., Salehi, S., & Karbalaei Saleh, F. (2015). An integrated approach for drilling optimization using advanced drilling optimizer. *Journal of Petroleum Engineering*, *2015*.

Hansford, J. E., & Lubinski, A. (1964). Effects of drilling vessel pitch or roll-on Kelly and drill pipe fatigue. *Journal of petroleum technology*, *16*(01), 77-86.

Hareland, G., & Rampersad, P. R. (1994, April). Drag-bit model including wear. In *SPE Latin America/Caribbean Petroleum Engineering Conference*. OnePetro.

Hegde, C., Daigle, H., & Gray, K. E. (2018). Performance comparison of algorithms for real-time rate-of-penetration optimization in drilling using data-driven models. *Spe Journal*, *23*(05), 1706-1722.

Hegde, C., Daigle, H., Millwater, H., & Gray, K. (2017). Analysis of rate of penetration (ROP) prediction in drilling using physics-based and data-driven models. *Journal of petroleum science and Engineering*, *159*, 295-306.

Hegde, C., & Gray, K. (2018). Evaluation of coupled machine learning models for drilling optimization. *Journal of Natural Gas Science and Engineering*, *56*, 397-407.

Heitmann, N., & Burgos, E. C. (2015, March). Freeing Differential Stuck-Pipe with Nitrogen Reduces Significantly Lost-In-Hole Drill Strings. In *SPE/IADC Drilling Conference and Exhibition*. OnePetro.

Hempkins, W. B., Kingsborough, R. H., Lohec, W. E., & Nini, C. J. (1987). Multivariate statistical analysis of stuck drillpipe situations. *SPE Drilling Engineering*, *2*(03), 237-244.

Hoteit, L., Dunlop, J., Aldred, W., & Meehan, R. (2005). *U.S. Patent No. 6,868,920*. Washington, DC: U.S. Patent and Trademark Office.

Hydraulic_horsepower. *hydraulic horsepower* | Oilfield Glossary. (n.d.). Retrieved December1,2021,from https://glossary.oilfield.slb.com/en/terms/h/hydraulic_horsepower.

Inoue, T., Ozaki, M., Miyazaki, T., Nishigaki, M., & Setta, K. (2008, November). Fatigue strength evaluation of drill pipe constantly bent in strong current. In *The Eighth ISOPE Pacific/Asia Offshore Mechanics Symposium*. OnePetro.

Inteq, B. H. (1995). Drilling engineering workbook. *Baker Hughes INTEQ, Houston, TX, 77073*.

Jain, R., Mahto, V., & Sharma, V. P. (2015). Evaluation of polyacrylamide-grafted-polyethylene glycol/silica nanocomposite as potential additive in water based drilling

mud for reactive shale formation. *Journal of Natural Gas Science and Engineering*, *26*, 526-537.

Jardine, S. I., McCann, D. P., & Barber, S. S. (1992, February). An Advanced System for the Early Detection of Sticking Pipe. In *IADC/SPE Drilling Conference*. OnePetro.

Jarvis, B. P. (2001). *U.S. Patent No. 6,227,044*. Washington, DC: U.S. Patent and Trademark Office.

Javeri, S. M., Haindade, Z. W., & Jere, C. B. (2011, October). Mitigating loss circulation and differential sticking problems using silicon nanoparticles. In *SPE/IADC Middle East Drilling Technology Conference and Exhibition*. OnePetro.

Johancsik, C. A., Friesen, D. B., & Dawson, R. (1984). Torque and drag in directional wells-prediction and measurement. *Journal of Petroleum technology*, *36*(06), 987-992.

Joshi, D. R., Eustes, A. W., Rostami, J., & Dreyer, C. (2021, March). Evaluating Data-Driven Techniques to Optimize Drilling on the Moon. In *SPE/IADC International Drilling Conference and Exhibition*. OnePetro.

Kent, S., Curtis, C., Mark, S., & Khaydar, V. (2016). Stuck-Pipe Prediction Using Automated Real-Time Modeling and Data Analysis.

Kucs, R. J. W., Spoerker, H. F., Thonhauser, G., & Zoellner, P. (2008, March). Automated real-time hookload and torque monitoring. In *IADC/SPE Drilling Conference*. OnePetro.

Lubinski, A. (1961). Maximum permissible dog-legs in rotary boreholes. *Journal of petroleum technology*, *13*(02), 175-194.

Lubinski, A., & Althouse, W. S. (1962). Helical buckling of tubing sealed in packers. *Journal of Petroleum Technology*, *14*(06), 655-670.

Luke, G. R., & Juvkam-Wold, H. C. (1993). The determination of true hook-and-line tension under dynamic conditions. *SPE Drilling & completion*, *8*(04), 259-264.

Mahto, V. (2013). The prevention of differential pipe sticking problems caused by water-based drilling. *Petroleum science and technology*, *31*(21), 2237-2243.

Maidla, E. E., & Ohara, S. (1991). Field verification of drilling models and computerized selection of drill bit, WOB, and drillstring rotation. *SPE Drilling Engineering*, *6*(03), 189-195.

Maidla, E. E., & Wojtanowicz, A. K. (1988). A field method for assessing borehole friction for directional well casing. *Journal of Petroleum Science and Engineering*, *1*(4), 323-333.

Mason, C., & Chen, D. C. (2007, February). Step changes needed to modernise T&D software. In *SPE/IADC Drilling Conference*. OnePetro.

McCormick, J. E., Frilot, M., & Chiu, T. (2011, June). Torque and Drag Software Model Comparison: Impact on Application and Calibration of Field Data. In *Brasil Offshore*. OnePetro.

Megabite. (2018, February 19). *Statoil to drill the world's first automated exploration well on a floating rig:* Sekal. Retrieved December 1, 2021, https://sekal.com/statoil-to-drill-the-worlds-first-automated-exploration-well-on-a-floating-rig/

Menand, S. (2012, June). A new buckling severity index to quantify failure and lock-up risks in highly deviated wells. In *SPE Deepwater Drilling and Completions Conference*. OnePetro.

Moraveji, M. K., & Naderi, M. (2016). Drilling rate of penetration prediction and optimization using response surface methodology and bat algorithm. *Journal of Natural Gas Science and Engineering*, *31*, 829-841.

Motahhari, H. R., Hareland, G., & James, J. A. (2010). Improved drilling efficiency technique using integrated PDM and PDC bit parameters. *Journal of Canadian Petroleum Technology*, *49*(10), 45-52.

Murillo, A., Neuman, J., & Samuel, R. (2009, April). Pipe sticking prediction and avoidance using adaptive fuzzy logic modeling. In *SPE Production and Operations Symposium*. OnePetro.

Nascimento, A., Elmgerbi, A., Roohi, A., Prohaska, M., Thonhauser, G., Gonçalves, J. L., & Mathias, M. H. (2017). Reverse Engineering: A New Well Monitoring and Analysis Methodology Approaching Playing-Back Drill-Rate Tests in Real-Time for Drilling Optimization. *Journal of Energy Resources Technology*, *139*(1).

Nergaard, A. (2015, September). Effective Force; Fiction Or Reality?. In *SPE Annual Technical Conference and Exhibition*. OnePetro.

Newman, K., Kenneth, B., & McSpadden, A. (2003). Basic tubing forces model (tfm) calculation. *Conroe: CTES, LP*.

Newman, K. R., & Procter, R. (2009, March). Analysis of hook load forces during jarring. In *SPE/IADC Drilling Conference and Exhibition*. OnePetro.

New Technologies, innovations. *Oil & Gas Portal.* (n.d.). Retrieved December 1, 2021, from http://www.oil-gasportal.com/drilling/new-technologies-innovations/.

Oketch, B. A. (2014). Analysis of Stuck Pipe Incidents in Menengai. *UNU-GTP, Reykjavik*.

Ouahrani, L., Haris, A. N., Suluru, S., Chiha, A., & Al Fakih, A. (2018, April). Invisible Lost Time measurement and reduction contributes to optimizing total well time by improving ROP and reducing flat time. In *SPE Kingdom of Saudi Arabia Annual Technical Symposium and Exhibition*. OnePetro.

PAŠIĆ, B., GAURINA-MEĐIMUREC, N. E. D. I. L. J. K. A., & MATANOVIĆ, D. (2007). WELLBORE INSTABILITY: CAUSES AND CONSEQUENCES NESTABILNOST KANALA BUŠOTINE: UZROCI I POSLJEDICE. *Rudarskogeolosko-naftni zbornik, 19*, 187-198.

Paslay, P. R., & Cernocky, E. P. (1991, October). Bending stress magnification in constant curvature doglegs with impact on drillstring and casing. In *SPE annual technical conference and exhibition*. OnePetro.

Pessier, R. C., & Fear, M. J. (1992, October). Quantifying common drilling problems with mechanical specific energy and a bit-specific coefficient of sliding friction. In *SPE annual technical conference and exhibition*. OnePetro.

Pink, T., Applewhite, B., Kverneland , H., & Bruce, A. (n.d.). *Automation of downhole, surface components optimizes drilling process: Cover story: Magazine*. Automation Of Downhole, Surface Components Optimizes Drilling Process | Cover Story | Magazine. Retrieved December 2, 2021, from https://www.aogr.com/magazine/cover-story/automation-of-downhole-surface-components-optimizes-drilling-process.

Pinto, C. N., & Lima, A. L. (2016, August). Mechanical specific energy for drilling optimization in deepwater Brazilian salt environments. In *IADC/SPE Asia Pacific Drilling Technology Conference*. OnePetro.

Precise automated drilling system. *Automated Drilling System* | Schlumberger. (n.d.). Retrieved December 1, 2021, from https://www.slb.com/drilling/rigs-and-equipment/rig-equipment/cabins-and-controls/precise-automated-drilling-system.

Price, D. (2021, January 10). *Lost circulation - well control*. Rig Worker. Retrieved December 1, 2021, from https://www.rigworker.com/well-control/lost-circulation.html.

Reid, P. I., Meeten, G. H., Way, P. W., Clark, P., Chambers, B. D., Gilmour, A., & Sanders, M. W. (2000). Differential-sticking mechanisms and a simple wellsite test for monitoring and optimizing drilling mud properties. *SPE Drilling & Completion*, *15*(02), 97-104.

Royal Dutch Shell plc. *Investors Handbook 2007–2011 - Innovative technology*. (2012, May 3). Shell. Retrieved December 1, 2021, from https://reports.shell.com/investors hand book/2011/ projects technology/innovative technology.html

Samuel, R. (2011). *Formulas and calculations for drilling operations* (Vol. 50). John Wiley & Sons.

Samuel, R., & Kumar, A. (2012, March). Effective Force and True Force: What are They?. In *IADC/SPE Drilling Conference and Exhibition*. OnePetro.

Sparks, C. P. (1984). The influence of tension, pressure and weight on pipe and riser deformations and stresses.

Selvaraju, S., Ramba, V., Subbiha, S., Uppaluri, R., Dubey, P. K., & Musale, A. (2019, November). An Innovative System Architecture for Real-Time Monitoring and Alarming for Cutting Transport in Oil Well Drilling. In *Abu Dhabi International Petroleum Exhibition & Conference*. OnePetro.

Sheppard, M. C., Wick, C., & Burgess, T. (1987). Designing well paths to reduce drag and torque. *SPE Drilling engineering*, *2*(04), 344-350.

Shi, X., Liu, G., Gong, X., Zhang, J., Wang, J., & Zhang, H. (2016). An efficient approach for real-time prediction of rate of penetration in offshore drilling. *Mathematical Problems in Engineering*, *2016*.

Silva, N. S., Netto, T. A., Lourenço, M. I., & Plácido, J. C. R. (2009, July). Comparative Study of Multiaxial Fatigue Criteria For Aluminum Drill Pipe Life Prediction. In *The Nineteenth International Offshore and Polar Engineering Conference*. OnePetro.

Siruvuri, C., Nagarakanti, S., & Samuel, R. (2006, February). Stuck pipe prediction and avoidance: A convolutional neural network approach. In *IADC/SPE Drilling Conference*. OnePetro.

Skoczylas, P. (2014, October). Drive string fatigue in PCP applications. In *SPE Artificial Lift Conference & Exhibition-North America*. OnePetro.

Soeiinah, E. (1985). *U.S. Patent No. 4,549,431*. Washington, DC: U.S. Patent and Trademark Office.

Statista. (2021, July 14). *Global primary energy consumption by country 2020*. https://www.statista.com/statistics/263455/primary-energy-consumption-of-selected-countries/

Teale, R. (1965, March). The concept of specific energy in rock drilling. In *International journal of rock mechanics and mining sciences & geomechanics abstracts* (Vol. 2, No. 1, pp. 57-73). Pergamon.

Themig, D. (1996, June). Multilateral Drilling And Completions-Applications In Practice. In *Annual Technical Meeting*. OnePetro.

Training Committee Limited, A. D. I. (Ed.). (2019). The Drilling Manual.

TOTAL. (2021, August 13). *Horizontal drilling, a pillar of our technological identity*. Exploration & Production. Retrieved December 2, 2021, from https://ep.totalenergies.com/en/expertise/drilling-wells/horizontal-drilling-pillar-our-technological-identity.

Tsuchihashi, N., Wada, R., Ozaki, M., Inoue, T., Mopuri, K. R., Bilen, H., ... & Kusanagi, K. (2021). Early Stuck Pipe Sign Detection with Depth-Domain 3D Convolutional Neural Network Using Actual Drilling Data. *SPE Journal*, *26*(02), 551-562.

U.S. Energy Information Administration - EIA - independent statistics and analysis. Short-Term Energy Outlook - U.S. Energy Information Administration (EIA). (n.d.). Retrieved December 1, 2021, from https://www.eia.gov/outlooks/steo/.

Vaisberg, O., Vincke, O., Perrin, G., Sarda, J. P., & Fay, J. B. (2002). Fatigue of drill string: state of the art. *Oil & Gas Science and Technology*, *57*(1), 7-37.

Version, E. (2014). IADC Drilling Manual. *IADC, Houston, USA*.

Vos, B. E., & Reiber, F. (2000, September). The benefits of monitoring torque & drag in real time. In *IADC/SPE Asia Pacific Drilling Technology*. OnePetro.

Wang, J., Ye, J., Yin, H., Feng, E., & Wang, L. (2012). Sensitivity analysis and identification of kinetic parameters in batch fermentation of glycerol. *Journal of Computational and Applied Mathematics*, *236*(9), 2268-2276.

Webb, J., Roze, E., Jarret, C., Le Roux, S., & Mejia, C. (2016, May). Drilling engineering and formation evaluation: an integrated approach to improve real time drilling optimization. In *SPE Western Regional Meeting*. OnePetro.

Wesley, A. (2016). *U.S. Patent No. 072978 A1*. Houston, Texas: U.S. Patent and Trademark Office.

Willersrud, A., Blanke, M., Imsland, L., & Pavlov, A. (2015). Drillstring washout diagnosis using friction estimation and statistical change detection. *IEEE Transactions on Control Systems Technology*, *23*(5), 1886-1900.

World Bank Group. (2021, October 21). *Commodity Markets Outlook October 2021*. World Bank. Retrieved December 1, 2021, from https://www.worldbank.org/en/news/press-release/2021/10/21/soaring-energy-prices-pose-inflation-risks-as-supply-constraints-persist.

World energy needs. CAPP. (2021, October 29). Retrieved December 1, 2021, from https://www.capp.ca/energy/world-energy-needs/.

Wu, J. (1996, October). Drill-pipe bending and fatigue in rotary drilling of horizontal wells. In *SPE Eastern Regional Meeting*. OnePetro.

Wylie, R., Standefer, J., Anderson, J., & Soukup, I. (2013, March). Instrumented Internal Blowout Preventer Improves Measurements for Drilling and Equipment Optimization. In *SPE/IADC Drilling Conference*. OnePetro.

Yi, P., Kumar, A., & Samuel, R. (2015). Realtime rate of penetration optimization using the shuffled frog leaping algorithm. *Journal of Energy Resources Technology*, *137*(3).

Zha, Y., Ramsay, S., & Pham, S. (2018, September). Real time surface data driven wob estimation and control. In *SPE Annual Technical Conference and Exhibition*. OnePetro.

Zoanni, R., Everage, S. D., Wadsworth, T. M., & Cassanelli, J. P. (2009, March). Further Developments in Drill Pipe Fatigue Management: A Case Study. In *SPE/IADC Drilling Conference and Exhibition*. OnePetro.

APPENDIX-A

Demonstration of effective tension and true tension concept in possible wellbore conditions (shown in Fig. A-1). The below-given examples are presented to illustrate the influence of true and effective tensional forces on simple hydro-mechanical systems. In real working scenarios, the drill string will experience severe fluidic and mechanical stresses, and establishing an accurate, effective tensional force illustration will be much more challenging.

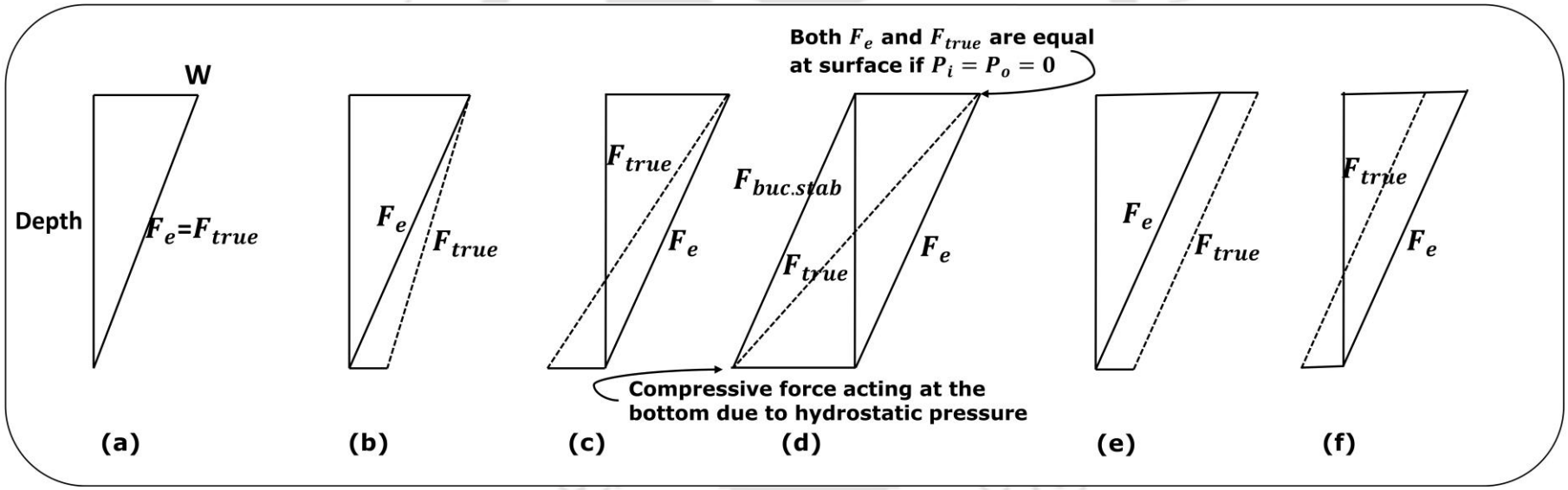

Fig. A-1. Illustration of effective tension and true tension in different wellbore scenarios

Table A- 1. Influence of true tension and effective tension in possible wellbore scenarios.

Case	Description of wellbore scenarios	Set of Equations
a	When there is no drilling fluid in the wellbore, the effective tension and true tension are equal and include true weight.	$F_e = F_{true} = W$
b	In the drill string with internal fluid, the true tension is higher than the effective tension, and the fluid weight is exerted at the bottom of the drill string.	$F_e = F_{true} - P_i A_i$ $F_e = W + P_{ib} A_{ib} - P_i A_i$ $F_e = W + W_{fi}$
c	When the drill string is surrounded by fluid externally, the true tension is lower than the effective tension, and the compressive force acts at the bottom of the drill string.	$F_e = F_{true} + P_e A_e$ $F_e = W - \left(P_{eb} A_{eb} - P_e A_e\right)$ $F_e = W - F_b$
d	Even though two different approaches estimate the axial force, both the forces congregate at the surface when internal and external surface pressures are zero, as shown in case (d). Due to the hydrostatic pressure, the compressive force acts at the drill string bottom and is equivalent to the buckling stability force. Since the surface pressures are assumed to be equal, the buckling stability force acting at the top of the drill string at the surface is zero.	$F_e = F_{true} + \left(P_e A_e - P_i A_i\right)$ $F_e = F_{true} + F_{buc.stab}$ $F_{buc.stab} = \left(P_e A_e - P_i A_i\right)$
e	The true tension shifts to the right when the drill string is exposed to internal pressure, similar to the case (b). The differential pressure (ΔP) will be zero as the complete system is closed. The effective tension remains identical to the true tension force and is not affected due to the internal pressure application.	$F_e = F_{true} - P_i A_i$ $F_e = W + P_{ib} A_{ib} - P_i A_i$ $F_e = W$
f	If the drill string is experiencing only external pressure, the true tensional force is less than the effective force, and as the pressure is externally applied, the string will endure compressive force at the bottom identical to case (c).	$F_e = F_{true} + P_e A_e$ $F_e = W - P_{eb} A_{eb} + P_e A_e$ $F_e = W$

APPENDIX-B

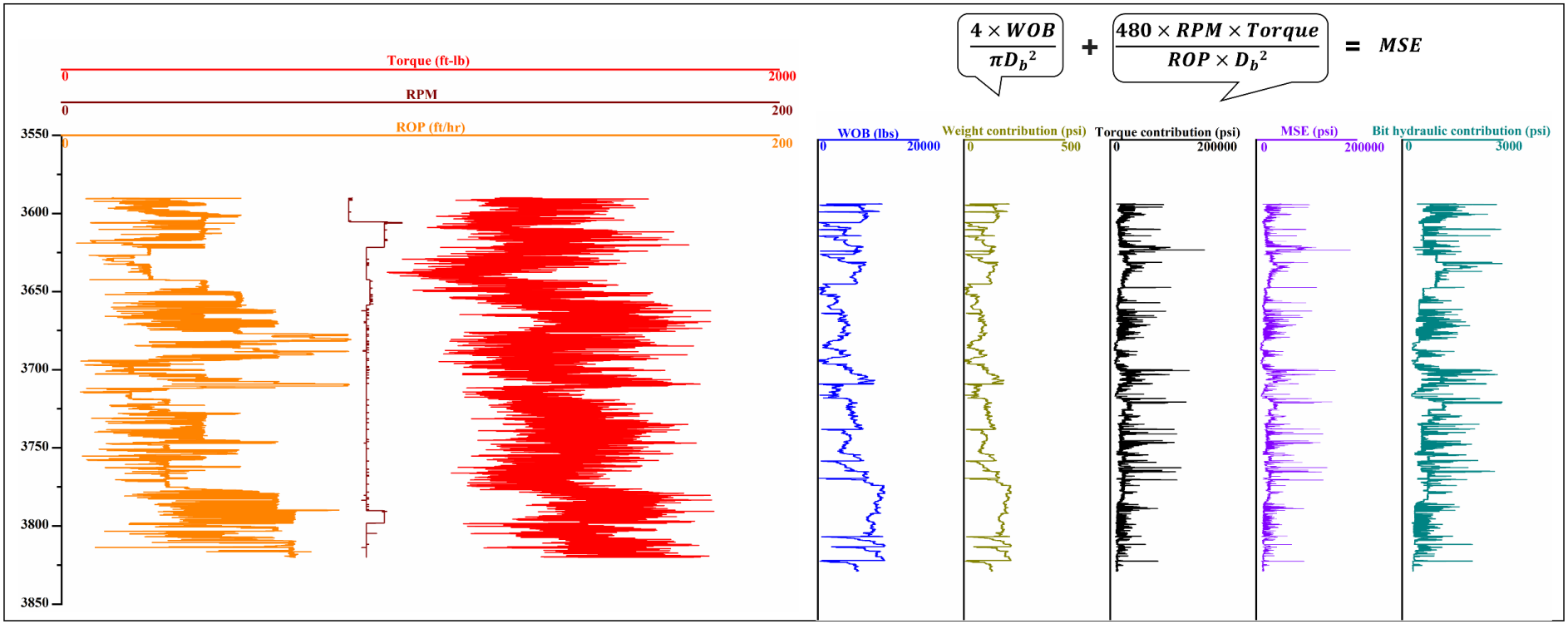

Fig. B-1. Illustration of the significance of weight term, torque term, and bit hydraulic contribution with respect to increasing in depth

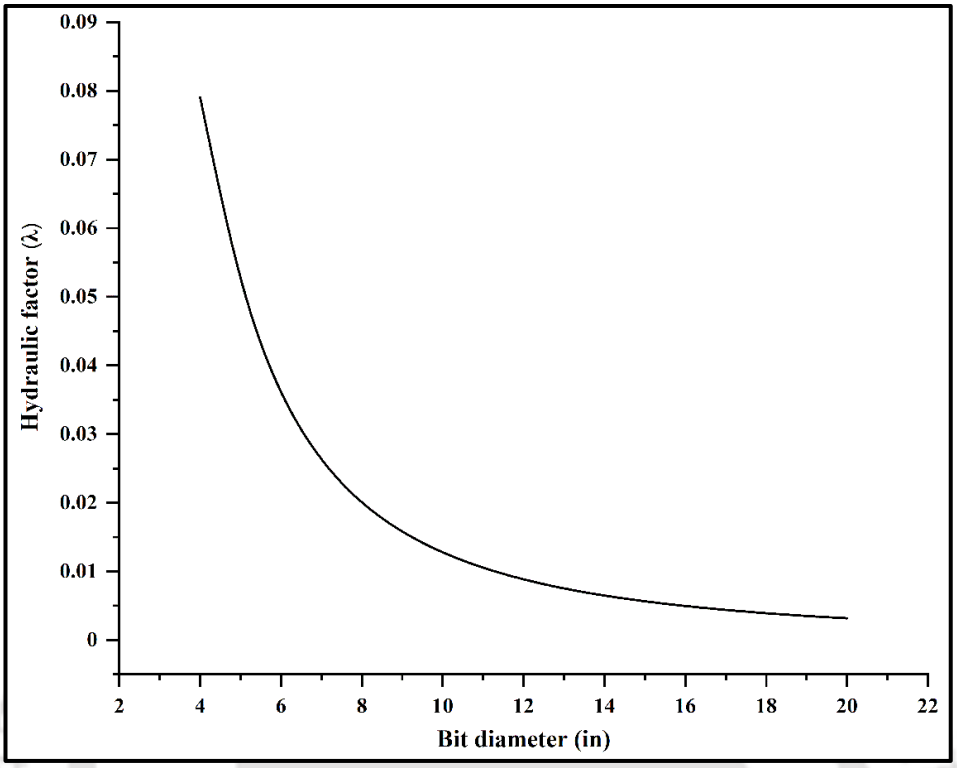

Fig. B-2. Variation of the hydraulic factor with a change in bit diameter

APPENDIX-C

Fundamentals of oil and gas well drilling

The following sequence of steps is universally followed for drilling oil wells.

a) Well planning

Well planning is the one crucial aspect of drilling engineering. It necessitates the integration of engineering principles, corporate philosophies, and experience factors. The main objective was to drill a well that needs to be safe, minimum cost, and usable. And these objectives are governed by the constraints such as geology, temperature, drilling equipment, casing limitations, drilling equipment, hole size, and budget (Watts, 2015).

b) Performing a shallow gas survey

Shallow gas surveys are performed to identify and avoid geo-hazards that would cause wellbore instability and increase NPT (Gherasim et al., 2015).

c) Wellsite preparation

Based on well planning, the site for the drilling rig will be selected for a given oil and gas reservoir. Wellsite preparation may vary for onshore and offshore operations. It also involves the efforts of many expert teams from the O&G operating company. A typical scenario of actions by a specific expert team is as follows (Netwas Group Oil, 2021):

- Geologists will develop a prospect and outline desired well locations.
- Leases are acquired through routine channels such as farm-ins and land departments.
- A surveyor chooses a precise well location on the surface based on a well plan.
- The drilling engineer selects the exact rig, and the contractor describes his rig requirements based on the footing, surface space, and rig weight.

d) Setting up the conductor casing

The conductor casing isolates the unconsolidated formations and water sands and shields against the incursion of shallow gas. The casing is typically installed and cemented to the surface (PetroWiki, 2015).

e) Move-in and Rig-up (MIRU)

Once the conductor casing was in place, the equipment needed to build up a rig was moved through trucks and assembled at the well site. The rigging-up process includes setting up all the power sources, pressuring systems, and testing the systems (Schlumberger Limited, 2021).

f) Well spudding (spudding refers to the commencement of rotary drilling operations)

   a. drilling down to the surface casing depth
   b. run and cement the surface casing
   c. drilling continued till the next casing point
   d. shooting till the total depth is reached

g) Utilization of open-hole logs for well-logging

Open-hole logging denotes logging operations that are performed on a wellbore before casing and cementing. These logs are meant to determine the sub-surface formation properties that would be aiding geologists and engineers for further reservoir interpretations.

h) Well-completion

Well-completion includes installing production casing and equipment to transform the well into production from one or more zones. The following sequence of steps is followed during well-completion.

   a. tubing
   b. gravel packs
   c. packers
   d. sliding sleeves
   e. stimulation
      i. acidize the well
      ii. hydraulically fracturing the well
   f. artificial lift

i) Rig down and move out

Rigging down typically means disconnecting all the power sources, decoupling the pressurized systems, disassembling the complete rig structure, and moving off the rig floor.

Complete rig and drill string configuration

(a) Drilling rig

A drilling rig is shown in Fig. 1-3 and comprises many sub-systems that aid in the smooth drilling process. It mainly helps support the drill string and casing, and its size is determined by the weight that it is considered to lift.

(b) Drill string

The drill string consists of series of stands of drill pipes, drill collars, heavyweight drill pipes (HWDP), and the bottom hole assembly (BHA). The complete drill string is supported by the rig structure installed on the surface by a hoisting device through the draw works.

(c) Drill collars

Drill collars are similar to drill pipes and are thick-walled heavy tubular. These are utilized just above the drill bit to provide additional weight for the bit to proceed further.

(d) Rotary table drive

Drilling a formation includes transferring rotary power from the drill floor to the drill bit through the drill string. The rotary table converts the mechanical energy at the surface to the drill string torque.

(e) Drilling mud

Drilling fluids are formulated to serve out a massive number of operations. The key performance features include; controlling formation pressures, removing cuttings from the wellbore, cooling and lubricating the drill bit, transmitting hydraulic energy to the drill bit and downhole tools, and maintaining wellbore stability (Williamson, 2013). The fluid compositions may vary based on the rig capabilities, wellbore demands, and environmental concerns. Besides, fluids are designed to control the subsurface pressures, minimize the potential for lost circulation, borehole erosion control, and optimize drilling rates and hole cleaning. With an increase in wellbore inclination, specific drilling fluid systems are designed to manage wellbore cleaning and stability problems specific to those wells.

(f) Casing

The drilling is performed in multiple stages, and at each stage, after reaching target depth, the borehole is strengthened by providing support through steel

casing and cementing. The casing provides stabilization and aids in keeping the wellbore sides from caving in on themselves. It also helps the well-stream from mingling with the surrounding contaminants and water reservoirs. The casing is usually run from the top of the rig floor, links casing joint by casing elevators on the travelling block, as shown in Fig. C- 1. It is speared into the previous casing string that has already been used been implanted into the wellbore (Schlumberger, 2021).

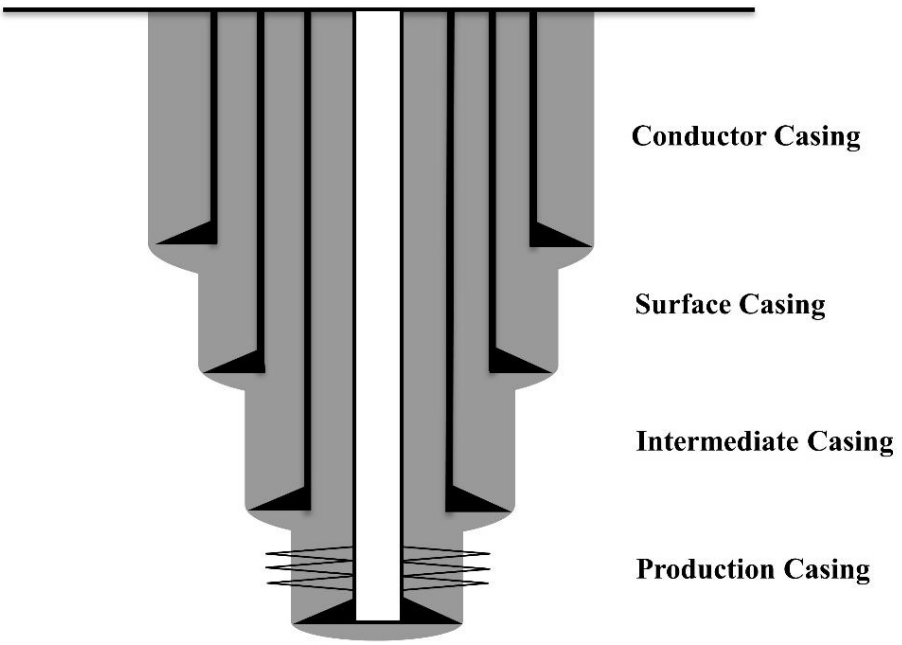

Fig. C- 1. Illustration of casing program

(g) Downhole motors

Downhole mud motors are a substitutive method for developing torque at the drill bit. The drill string is not rotated from the surface in these systems, and the motor rotates the bit placed just above it. The high-pressure mud flow powers the motor. It develops a substantial amount of torque through the rotor to provide power to the drill bit (Ramsey, 2019).

(h) Measurement while drilling

Measurement while drilling (MWD) is the process of measuring essential information in the downhole without interfering in normal drilling operations. The information that can be obtained from these tools are listed below (Inglis, 1987):

- Operational parameters (downhole weight on bit, torque on bit, bit RPM)

- Formation characteristics (gamma-ray, resistivity logs, porosity logs, and other logging tools)
- Directional information (inclination angle, azimuth, tool face)

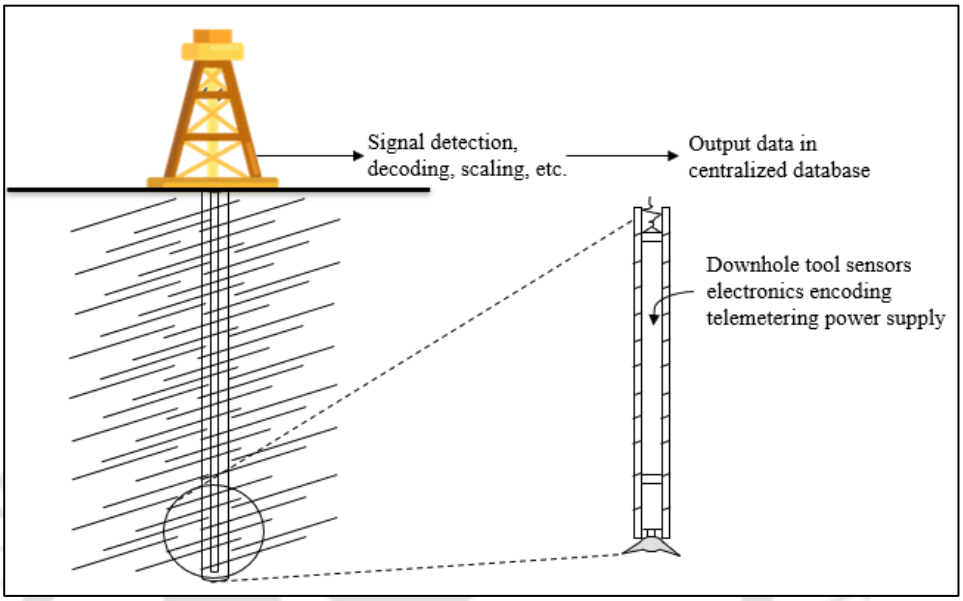

Fig. C- 2. Schematic of measurement while drilling system

The sensors are placed in a tool integral to the bottom hole assembly (BHA), as shown in Fig. C- 2. Also, a transmitter is placed in the tool, which transmits information from the downhole to the surface via a telemetric channel. The mud system is the commonly used telemetric channel for information transfer in the wellbore. The measured signals output on the surface are decoded and processed for the appropriate application.

(i) Logging while drilling

Logging while drilling (LWD) systems are utilized to gather crucial downhole information while drilling without removing the drill string from the wellbore. LWD offers similar functions to wireline logging without comprising coverage, resolution, and data quality (Simpson, 2017). The complete information is transferred to the surface through mud pulse telemetry and is processed by the computers to reconstruct the information. These tools are more significant in extended reach horizontal wellbores. The major difference between the LWD and MWD is that the information recorded in the LWD tools can only be retrieved when the tools reach the surface. And the information recorded in MWD tools is transmitted through mud pulse telemetry during real-time drilling.

List of publications, conferences, and patents

Peer-reviewed Journals

1. **Viswanth Ramba**, Senthil Selvaraju, Senthilmurugan Subbiah, Muthukumar Palanisamy, "A Robust Anomaly Detection Methodology Using Predicted Hookload and Neutral point for Oil Well Drilling," *Journal of Petroleum Science and Engineering*, 195, 107787- [2020], (Impact Factor – 4.346).
2. **Viswanth Ramba**, Senthil Selvaraju, Balakumara Vignesh Muppidathi, Senthilmurugan Subbiah, Muthukumar Palanisamy, "Evaluation of Structural Integrity of Tubulars in Directional Wellbores: A Case Study in North-Eastern Parts of India," *Journal of Petroleum Science and Engineering*, P.P 109067- [2021], (Impact Factor – 4.346).
3. **Viswanth Ramba**, Senthil Selvaraju, Senthilmurugan Subbiah, Muthukumar Palanisamy, Aman Srivastava, "Optimization of Drilling Parameters Using Improved Playback Methodology," *Journal of Petroleum Science and Engineering*, P.P 108991- [2021], (Impact Factor – 4.346).

Peer-reviewed Conferences

1. **Viswanth Ramba**, Senthil Selvaraju, Senthilmurugan Subbiah, Muthukumar Palanisamy, Sanjaykumar Gauba, Suresh Jandial, "Real-Time Evaluation of Structural Integrity of Tubulars in Directional Wellbores," *ASME-OMAE-2020, Virtual Conference*, August 3-7, 2020.
2. **Viswanth Ramba**, Senthil Selvaraju, Senthilmurugan Subbiah, Muthukumar Palanisamy, "Anomaly Detection During Oil Well Drilling Operation in Vertical Wellbores"; *NCUPE 2019*, IIT Guwahati, Assam, India.
3. Senthil Selvaraju, **Viswanth Ramba**, Senthilmurugan Subbiah, Ramgopal Uppaluri, PK Dubey, Amol Musale, "An Innovative System Architecture for Real-Time Monitoring and Alarming for Cutting Transport in Oil Well Drilling"; *Abu Dhabi International Petroleum Exhibition & Conference (ADIPEC 2019)*, Abu Dhabi, UAE, Society of Petroleum Engineers.
4. Senthil Selvaraju, **Viswanth Ramba**, Senthilmurugan Subbiah, Ramgopal Uppaluri, "Prediction and Alarming for Complications during Oil Well Drilling: Case Study with Field Data"; *NCUPE 2019*, IIT Guwahati, Assam, India.

Patent filed

1. Sanjay Kumar Gauba, Pradeep Kumar Dubey, Amol Suresh Musale, Senthilmurugan Subbiah, Rashmi Dutta Baruah, Senthil Selvaraju, **Viswanth Ramba**, Achyut Mani Tripathi, Balakumara Vignesh Muppidathi, "A System and Method for Activity Identification and Problem Prediction During Oil and Gas Well Drilling," *Indian Provisional Patent Application No. 201911040595*, Filing date: October 7, 2019